CSIC
CONSEJO SUPERIOR DE INVESTIGACIONES CIENTÍFICAS

eez
Estación Experimental del Zaidín

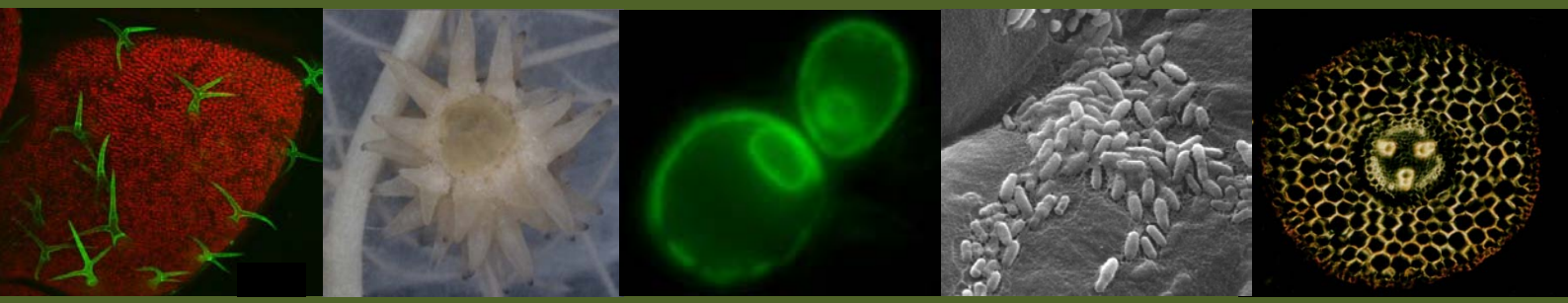

30 years of (e-) microscopy at the EEZ in images

Estación Experimental del Zaidín, CSIC
2013

30 years of (e^-) microscopy at the EEZ in images

Edited by Antonio J. Castro and Juan de Dios Alché

CSIC
Consejo Superior de Investigaciones Científicas

eez
Estación Experimental del Zaidín

30 years of (e^-) microscopy at the EEZ in images

Editors: Antonio Jesús Castro López
Juan de Dios Alché Ramírez

Published by the Plant Reproductive Biology Research Group
Estación Experimental del Zaidín (CSIC)
Profesor Albareda 1
18008 Granada, Spain
E-mail: buzon@eez.csic.es
http://www.eez.csic.es

First published November, 2013
Printed in Granada (Spain)

ISBN 10: 84-616-7277-1
ISBN 13: 978-84-616-7277-6

SPONSORS

Consejo Superior de Investigaciones Científicas

Estación Experimental del Zaidín

Sociedad de Microscopía de España (SME)

Zeiss

Remoa

Izasa

FOREWORD

Knowledge of the surrounding living beings and non-living objects starts when we visualize them for the first time. It is only then when we can ask ourselves questions about their nature and function. Answering these questions is the aim of scientific research. Therefore, observation is the foundation of science. The microscopic world remained hidden for humans till the invention of the early optical instruments. Already in ancient times, men had discovered that the image of an object became augmented when looking through a curved glass. The results of archaeological excavations carried out in Nínive (Syria) over the middle of the XIXth century, and where a lens carved in glass rock coming from the XIth century was found, suggest that magnifying glasses were already known and used in the Arab culture of that time. However, the first compound light microscope was first built at the end of the XVIth century or early at the XVIIth century.

The word "microscope" derives from the Greek "mikrós" (small) and "skopeîn" (observe). There is no consensus about authorship of the first light microscope. Several historians state that the first author was the Dutch builder of lenses Zacharias Jansen in 1590. Others attribute such merit to the Italian astronomer and mathematician Galileo Galilei in 1609. Early scientific publications in the field of microscopy dated from the second half of the XVIIth century. Robert Hooke coined the term "cell" for the first time in his book "Micrographia", published in 1665. A decade later (1974), Anton van Leeuwenhoek observed bacteria and other microorganisms for the first time, and named them in a generalised form as "animalcules". During the XIXth century, and from a technical point of view, it is remarkable the improvement introduced by Abbe in 1877 around immersion microscopy, by replacing water by cedar oil. Over this period, the great discoveries determining the foundations of Cytology and Histology prospered. Some of the most important highlights include: 1) Mathias Shleiden and Theodor Schwann propose the "cell theory" (1838), 2) Albert von Kolliker describes mitochondria in animal cells (1857), 3) Alexander Flemming describes chromosomal behaviour during mitosis in animal cells (1879), 4) Robert Koch identifies bacteria causing tuberculosis and cholera (1882), 5) Santiago Ramón y Cajal develops new staining methods and establishes the basics of microscopical anatomy, and 6) Camillo Golgi describes the apparatus named after him (1898). Both the discovery of the electron at the beginning of the XXth century and the further development of quantum mechanics allowed Max Knoll and Ernst Ruska building the first transmission electron microscope in 1931. A decade later (1942), Manfred von Ardenne built the first scanning electron microscope. The development of electron microscopy and the corresponding sample preparation methods over the second half of the XXth century laid the ground for current Cell Biology. In 1974, the importance of this discipline was recognized, and the Nobel Prize of Medicine was awarded to Christian R. de Duve, Albert Claude and George Palade. The invention of the electron microscope, the scanning tunneling microscope and the atomic force microscope was also awarded with the Nobel Prize of Physics in 1986, endowed to Ernst Ruska, Gerd Binning and Heinrich Roher.

In the 70's decade, microscopy techniques had an enormous diffusion, and were highly appreciated and used routinely in all centres and institutes developing pioneer research. In Spain, a majority of these laboratories were located in Madrid

and Barcelona over these years. Microscopy infrastructure at the EEZ was scarce at the end of the 70's (several stereomicroscopes and light microscopes), apparently because research under progress at the institute in that time did not need of such techniques. However, Prof. Julio López Gorgé foresaw both the enormous advantages offered by the microscopy techniques for biology research, and the need of creating a microscopy platform at the institute. Under his auspice, the first transmission electron microscope (Zeiss) arrived to the EEZ in 1982. In addition to the microscope, a microscopy facility requires additional infrastructure, specialized technical staff and more importantly, service demand by researchers. None of these basics were fulfilled at that time at the EEZ, therefore the initial objective became a little bit more unpretentious: make operative the electron microscope and start training technical and research staff in this field. For this purpose, the needed equipment started to be acquired through projects or special actions, and Matilde Garrido was appointed as the technical staff in charge of handling and servicing the electron microscope. That was how, with plenty of work, disposition and a bit of luck, the laboratory of microscopy of the EEZ began to grow to become later the Plant Cell Biology group (currently Plant Reproductive Biology). The presence today of a Microscopy Facility at the EEZ is the result of the collaboration of many people, of course the support of the current management committee of the institute and the work, effort and devotion of the staff of the Plant Reproductive Biology Group since its beginning to the present days. This book is a little tribute to all of them.

The operation of a Microscopy Facility, once the basics requirements are fulfilled, represents a commitment, which will certainly allow researchers of the institute to progress in the use of the most recent technologies for the preparation and observation of samples, under the best conditions for such use. This will represent undoubtedly a great benefit for our community.

Granada, November 2013

María Isabel Rodríguez García

Professor *ad honorem*

PREFACIO

El conocimiento de los seres vivos y objetos no animados que nos rodean se inicia cuando los visualizamos por primera vez. Sólo entonces podemos hacernos preguntas sobre su naturaleza y función. Dar respuesta a estas preguntas es el objetivo de la investigación científica. Por tanto, la observación es la base de la ciencia. El mundo microscópico permaneció oculto para el ser humano hasta la invención de los primeros instrumentos ópticos. Ya en la antigüedad, el hombre había descubierto que al mirar a través de un cristal curvo se aumentaba la imagen de un objeto. Los resultados de unas excavaciones arqueológicas realizadas a mediados del siglo XIX en Nínive (Siria), en las que se encontró una lente tallada en cristal de roca procedente del siglo XI, sugieren que la lupa era conocida y utilizada en la cultura árabe de aquella época. No obstante, el primer microscopio óptico compuesto no se construyó hasta finales del siglo XVI o principios del XVII.

La palabra "microscopio" deriva del griego "mikrós" (pequeño) y "skopeîn", (observar). No existe unanimidad sobre la autoría en la construcción del primer microscopio óptico. Algunos historiadores afirman que fue el fabricante holandés de lentes Zacharias Jansen en 1590. Otros atribuyen ese mérito al astrónomo y matemático italiano Galileo Galilei en 1609. Las primeras publicaciones científicas en el campo de la microscopía datan de la segunda mitad del siglo XVII. Robert Hooke acuñó por primera vez el término célula en su libro "Micrographia", publicado en 1665. Una década más tarde (1974), Anton van Leeuwenhoek observó por primera vez bacterias y otros microorganismos a los que denominó genéricamente como "animálculos". En el siglo XIX, desde el punto de vista técnico, cabe destacar la mejora introducida por Abbe en 1877 en la microscopía de inmersión al sustituir el agua por aceite de cedro. En este periodo se suceden los grandes descubrimientos que van a sentar las bases de la Citología e Histología. Algunos de los hitos más importantes fueron: 1) Mathias Shleiden y Theodor Schwann proponen "la teoría celular" (1838), 2) Albert von Kolliker describe las mitocondrias en células animales (1857), 3) Alexander Flemming describe el comportamiento de los cromosomas durante la mitosis en células animales (1879), 4) Robert Koch identifica las bacterias que causan la tuberculosis y el cólera (1882), 5) Santiago Ramón y Cajal desarrolla nuevos métodos de tinción y establece los fundamentos de la anatomía microscópica, y 6) Camillo Golgi describe el aparato que lleva su nombre (1898). El descubrimiento del electrón a principios del siglo XX y el posterior desarrollo de la mecánica cuántica permitieron a Max Knoll y Ernst Ruska construir en 1931 el primer microscopio electrónico de transmisión. Una década más tarde (1942), Manfred von Ardenne construyó el primer microscopio electrónico de barrido. El desarrollo de la microscopía electrónica y las técnicas de preparación de muestras durante la segunda mitad del siglo XX sentaron las bases de la Biología Celular actual. En 1974 se reconoció la importancia de esta disciplina, otorgándose el Premio Nobel de Medicina a los investigadores Christian R. de Duve, Albert Claude y George Palade. El invento del microscopio electrónico, el microscopio de efecto túnel y el microscopio de fuerza atómica, también fue galardonado en 1986 con el Premio Nobel de Física, concedido a Ernst Ruska, Gerd Binning y Heinrich Roher.

En la década de los 70, las técnicas de Microscopía tenían una enorme difusión y eran muy valoradas y utilizadas de forma rutinaria en todos aquellos centros e institutos donde se llevaba a cabo una investigación pionera. En España, en aquellos años, la mayoría de estos laboratorios se encontraban en Madrid y Barcelona. La infraestructura en microscopía en la EEZ a finales de los 70 era muy escasa (algunas lupas y microscopios ópticos), debido aparentemente a que la investigación que entonces se desarrollaba en el instituto no lo requería. Fue el Prof. Julio López Gorgé quien intuyó las enormes ventajas que la microscopía ofrecía a la investigación en el campo de la biología, y la necesidad de crear un servicio de microscopía en el instituto. Bajo su auspicio llegó a la EEZ el primer microscopio electrónico (Zeiss) en el año 1982. Además del microscopio, un servicio de microscopía requiere una infraestructura adicional, personal técnico especializado y, lo más importante, demanda del servicio por parte de los investigadores. Ninguna de estas premisas se cumplía en aquel momento en la EEZ, por lo que el objetivo inicial fue más modesto: hacer que el microscopio electrónico estuviera operativo y comenzar a formar personal técnico e investigador en dicho campo. Para ello, se fue adquiriendo todo el equipamiento necesario que fue financiado por proyectos o acciones especiales y Matilde Garrido se incorporó como personal técnico a cargo del manejo y mantenimiento del microscopio electrónico. Y así fue como comenzó con mucho trabajo, ánimo y un poco de suerte a crecer el laboratorio de microscopía de la EEZ, que más tarde se convirtió en el Grupo de Biología Celular de Plantas (actualmente es el Grupo de Biología Reproductiva de Plantas). Si hoy la EEZ cuenta con un Servicio de Microscopía es gracias a la colaboración de muchas personas, y por supuesto al apoyo de la Dirección actual del Instituto, pero sobre todo al trabajo, esfuerzo y dedicación de todos los que desde su inicio hasta la actualidad han formado parte del Grupo de Biología Reproductiva de Plantas. Este libro es un pequeño homenaje a todos ellos.

La existencia de un Servicio de Microscopía, una vez cubiertas esas premisas mínimas, constituye una apuesta que seguramente permitirá avanzar a los investigadores del centro en el uso de las más recientes tecnologías de preparación y observación de muestras, en unas buenas condiciones para su utilización. No cabe duda de que ello representa un gran beneficio para nuestra comunidad.

Granada, Noviembre de 2013

María Isabel Rodríguez García

Profesor *ad honorem*

INDEX

1. ENVIROMENTAL PROTECTION..... 1

1.1. Microscopy for the study of entomology..... 3

1.2. Plant Sociomicrobiology examined through the microscope..... 5

2. BIOCHEMISTRY, CELL AND MOLECULAR BIOLOGY OF PLANTS..... 7

2.1. Peroxisomes and metabolism of reactive oxygen and nitrogen species (ROS and RNS)..... 9

2.2. Microscopy techniques for studying oxidative stress in plants..... 11

2.3. Microscopy to study ion homeostasis and membrane transporters..... 13

2.4. Microscopy to study plant sexual reproduction..... 15

3. SOIL MICROBIOLOGY AND SYMBIOTIC SYSTEMS..... 17

3.1. Microscopy to study PAHs caption by roots inoculated with *R. custos*..... 19

3.2. Observation of the arbuscular mycorrhizal fungal structures in roots by microscopy-based techniques..... 21

3.3. Microscopy to study plant-bacteria interaction..... 23

3.4. Microscopy to study structure, dynamics and function of rhizobacterial genomes..... 25

4. ANIMAL NUTRITION..... 27

4.1. Microscopy use in ruminant nutrition..... 29

4.2. Microscopy in primary culture of porcine hepatocytes and liver histology..... 31

5. ENVIRONMENTAL GEOCHEMISTRY..... 33

5.1. Electron microscopy in mineralogy and material science..... 35

5.2. Observation of the thermal decomposition of calcite by heating and the process of hydration in bentonites by environmental scanning electron microscopy (ESEM)..... 37

CHAPTERS

ENVIRONMENTAL PROTECTION


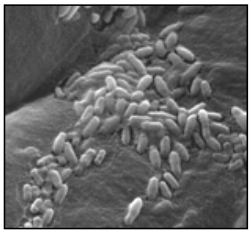

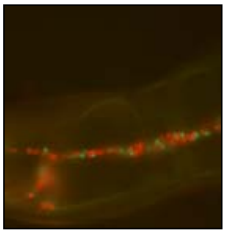

Microscopy for the study of entomology

Daniel Paredes, María Luisa Fernández and Mercedes Campos*

Department of Environmental Protection, Estación Experimental del Zaidín, CSIC, Profesor Albareda 1, 18008 Granada, Spain

*corresponding author: mercedes.campos@eez.csic.es

- **Arthropods taxonomic determination based on morphological traits**

Figure 1. (A-C), Different morphological traits of *Eurytoma ornata* used for its taxonomic determination.

- **Characterization of arthropods' phenological stages**

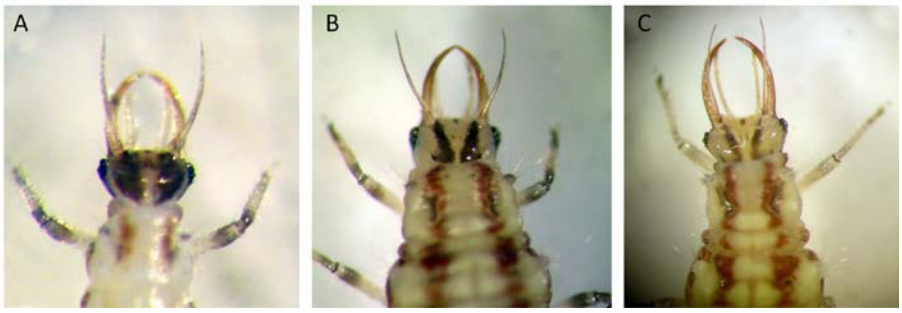

Figure 2. (A) First stage of *Chrysoperla carnea* larva. (B) Second stage of *C. carnea* larva. (C) Third stage of *C. carnea* larva. Note that the black coloration of the head decreases during development.

- **Sexual determination of arthropods**

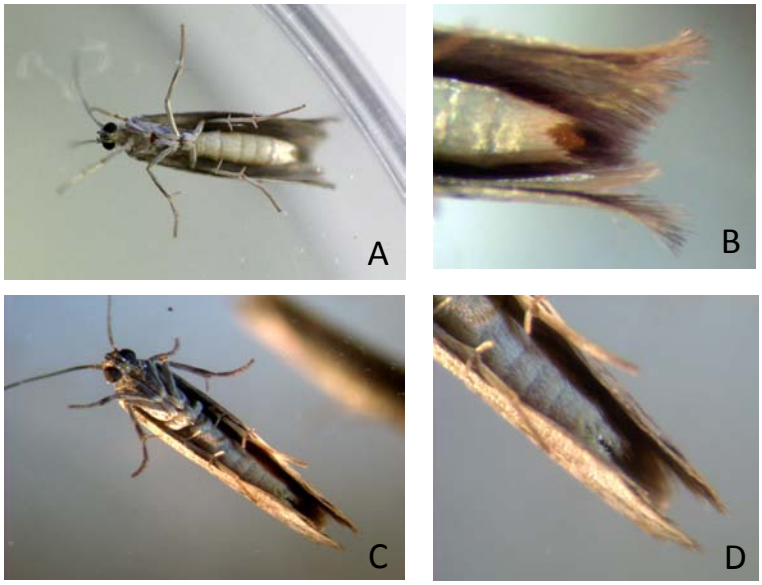

Figure 3. (A) Female of the olive pest *Prays oleae*. (B), Detail, at the end of the abdomen, for female determination. (C), Male of the olive pest *Prays oleae*. (D), Detail, at the end of the abdomen, for male determination.

- **Analyses of trophic interactions between arthropods**

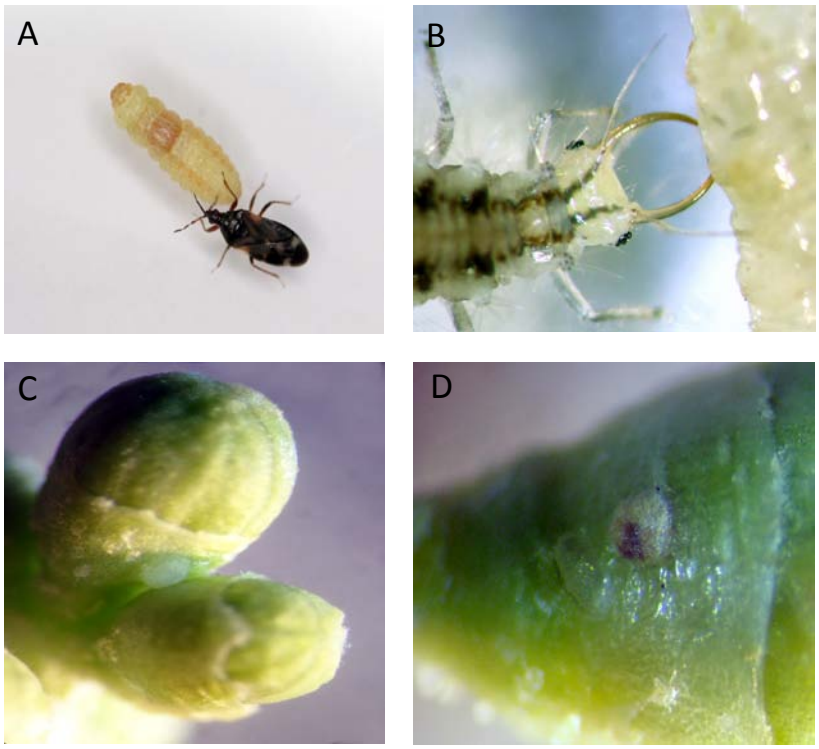

Figure 4. (A) *Anthocoris nemoralis* feeding on *Prays oleae* larva. (B) *Chrysoperla carnea* preying on *Bactrocera oleae* larva. (C) Egg of *Prays oleae* on a flower bud of *Olea europaea*. (D) Parasitized egg of *Prays oleae.*

- **Determination of pollen associated with bees**

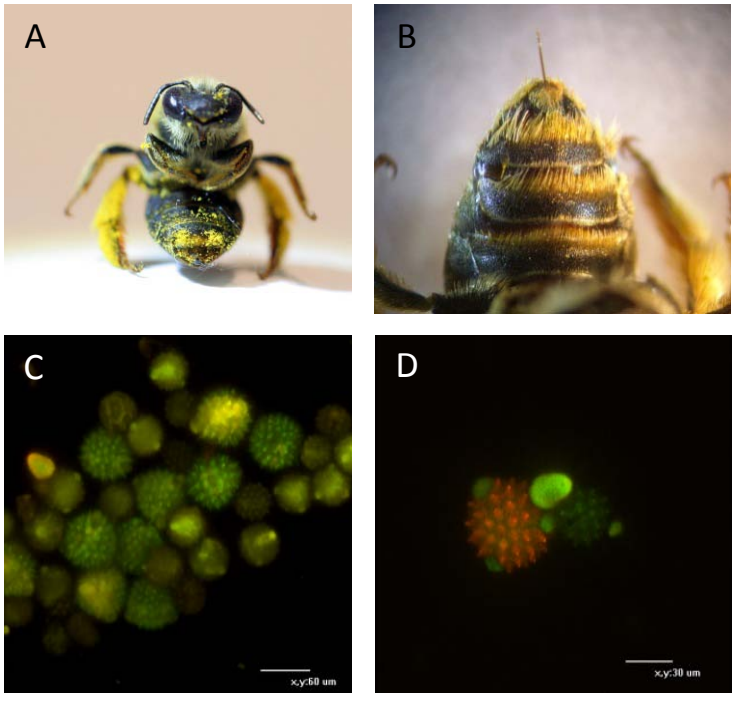

Figure 4. (A) Bee, belonging to family Megachilidae, with pollen in its abdomen and legs. (B) Detail of the abdomen hair, where the pollen is gathered. (C-D) Photomicrographs of pollen grains collected from the body of the bee.

Acknowledgements. This work has been supported by numerous research projects: P07-AGR-0274 (Junta de Andalucía), Biosuelo (Syngenta Agro S.A.) and Operación Polinizador (Syngenta Agro, S.A.).

Plant Sociomicrobiology examined through the microscope

María Isabel Ramos-González, Fátima Yousef-Coronado, Marta Martínez-Gil, Saray Santamaría-Hernando, Miguel A. Matilla-Vázquez, Regina Fernández-Piñar, José Miguel Quesada, María L. Travieso, María Isabel Soriano, Óscar Huertas and Manuel Espinosa-Urgel*

Department of Environmental Protection, Estación Experimental del Zaidín, CSIC, Profesor Albareda 1, 18008 Granada, Spain

*corresponding author: manuel.espinosa@eez.csic.es

In nature, bacteria commonly live as multicellular communities colonizing solid surfaces. The development of these communities, called biofilms, is influenced by environmental and genetic factors, as well as by the exchange of chemical signals between cells. This has given rise to the concept of "Sociomicrobiology". Our group studies colonization of plant root surfaces by beneficial bacteria, comparing this process with biofilm formation on abiotic surfaces.

- **Colonization of plant roots by the plant beneficial bacterium *Pseudomonas putida* KT2440 visualized with fluorescence and scanning electron microscopy**

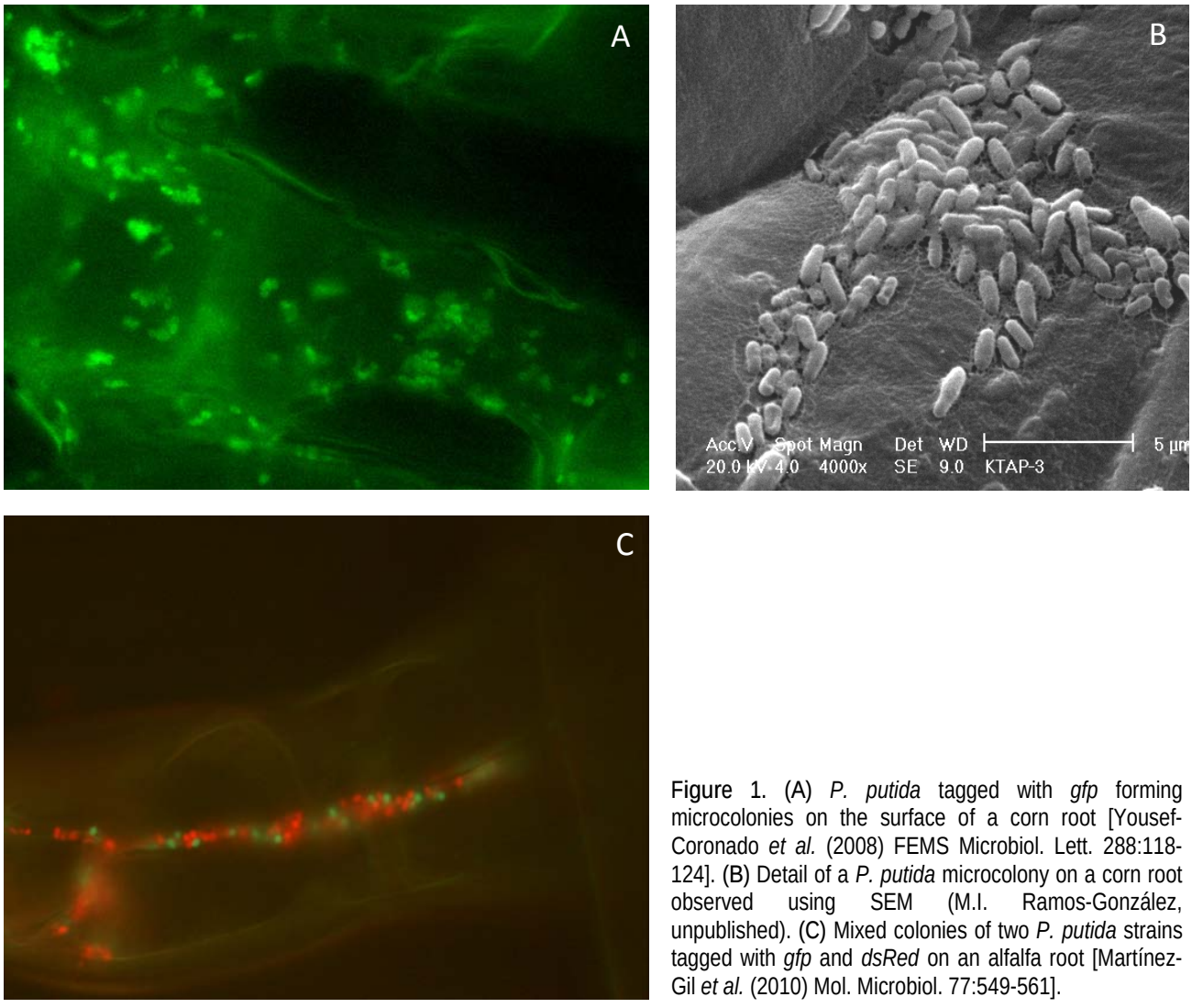

Figure 1. (A) *P. putida* tagged with *gfp* forming microcolonies on the surface of a corn root [Yousef-Coronado *et al.* (2008) FEMS Microbiol. Lett. 288:118-124]. (B) Detail of a *P. putida* microcolony on a corn root observed using SEM (M.I. Ramos-González, unpublished). (C) Mixed colonies of two *P. putida* strains tagged with *gfp* and *dsRed* on an alfalfa root [Martínez-Gil *et al.* (2010) Mol. Microbiol. 77:549-561].

- **Analyzing the physiological state of bacterial cells in a biofilm**

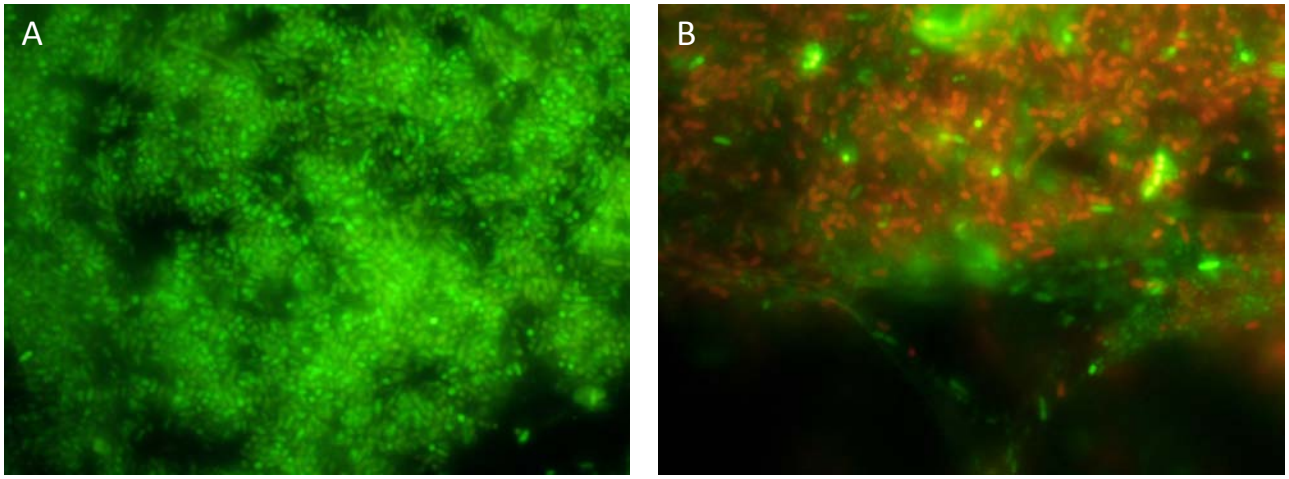

Figure 2. The LIVE/DEAD® *Bac*Light™ Bacterial Viability Kit allows determining the membrane integrity and physiological state of bacterial cells, by a combination of two fluorescent nucleic acid dyes, green-fluorescent SYTO9 and red-fluorescent propidium iodide. Bacteria with intact cell membranes fluoresce green (A), whereas bacteria with damaged membranes allow the incorporation of propidium iodide, causing significantly less green fluorescence and usually red fluorescence (B). This is useful to determine the state of cells in different parts of a biofilm, or to analyze the effect of stressors on the population.

- **Confocal laser scanning microscopy: reconstructing three-dimensional images of biofilms**

Figure 3. 3-D reconstruction of the biofilm formed by a *P. putida* strain growing on a glass surface under laminar flow conditions. The combination of CLSM data with the COMSTAT software allows a detailed characterization of biofilm parameters such as surface coverage, biomass, thickness, etc.

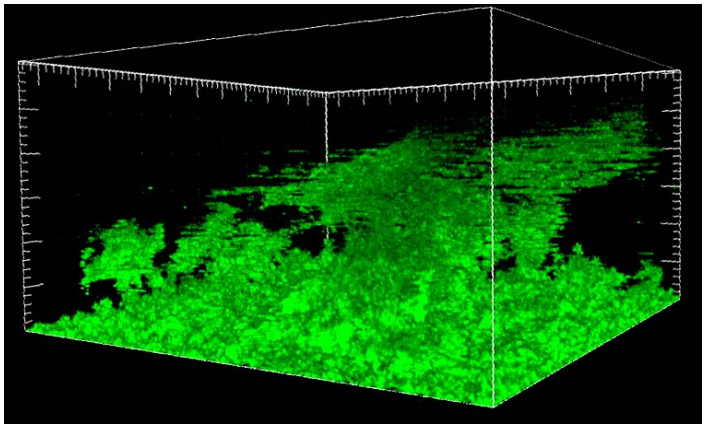

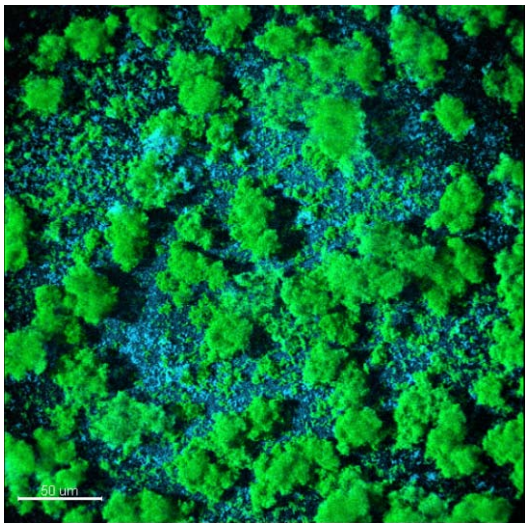

Figure 4. 3-D reconstruction (top view) of a mixed bacterial biofilm. Cells tagged with *gfp* (green) correspond to a *P. putida* mutant with increased biofilm formation capacity and cells tagged with *bfp* (blue) correspond to the wild type strain. The mutant tends to cluster and form isolated microcolonies, while the wild type forms a more flat and uniform biofilm covering most of the surface.

Acknowledgements. Research currently supported by grants BFU2010-17946 from Plan Nacional de I+D+i and P08-CVI-03869 from Junta de Andalucía, and FEDER funds.

BIOCHEMISTRY, CELL AND MOLECULAR BIOLOGY OF PLANTS

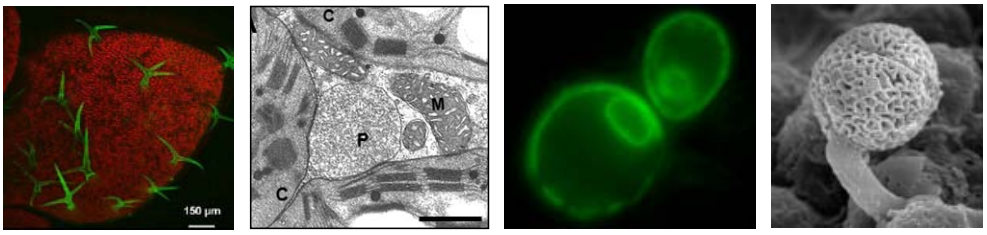

Peroxisomes and metabolism of reactive oxygen and nitrogen species (ROS and RNS)

José Manuel Palma*, Francisco Javier Corpas, Eduardo López-Huertas and Luis Alfonso del Río

Department of Biochemistry, Cell and Molecular Biology of Plants, Estación Experimental del Zaidín, CSIC, Profesor Albareda 1, 18008 Granada, Spain

*corresponding author: josemanuel.palma@eez.csic.es

- **Detection of catalase from peroxisomes of pea leaves: this was the first report in the EEZ on the use of DAB staining to detect catalase in order to use it as a marker for visualization of peroxisomes from plant origin**

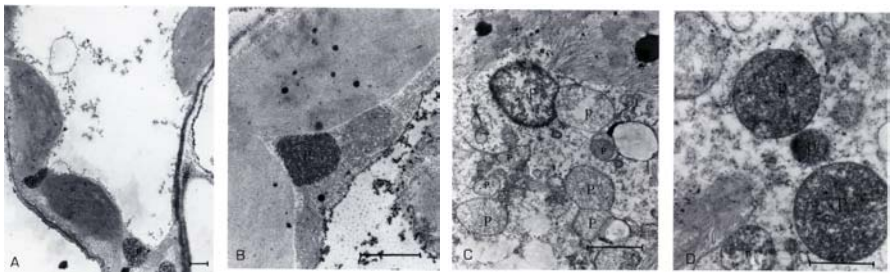

Figure 1. Electron micrographs of leaves from control and clofibrate-treated plants incubated with DAB for cytochemical localization of catalase. (A-B) Control plants. (C-D) Clofibrate-treated plants. P, peroxisomes. [Reprinted from Palma *et al.* (1991) Arch. Biochem. Biophys. 287: 68-74].

- **Organelles from pepper fruits. Isn't it amazing? Is the perfection of the fruit due of this spectacular architecture?**

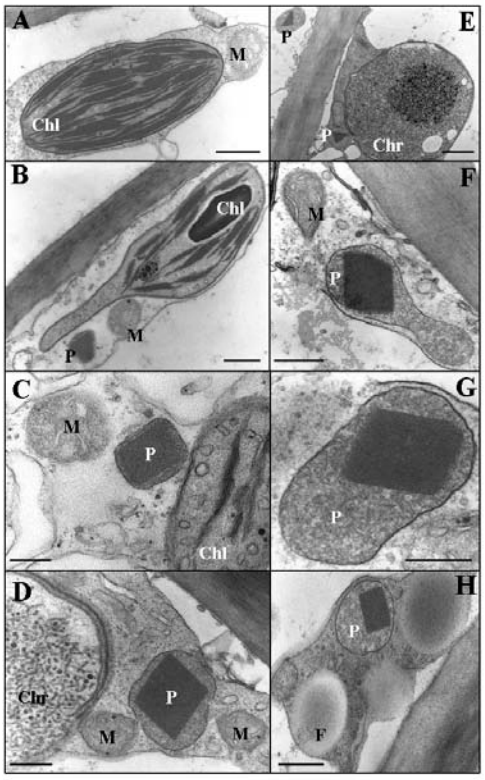

Figure 2. Electron microscopy of ultrathin sections from green (A-C) and red (D-H) peppers. Chl, chloroplasts; M, mitochondria; P, peroxisomes; Chr, chromoplasts; F, fatty bodies. [Reprinted from Mateos *et al.* (2003) J. Plant Physiol. 160: 1507-1516].

- **Pioneer immunolocalization of Mn-SOD in plant peroxisomes**

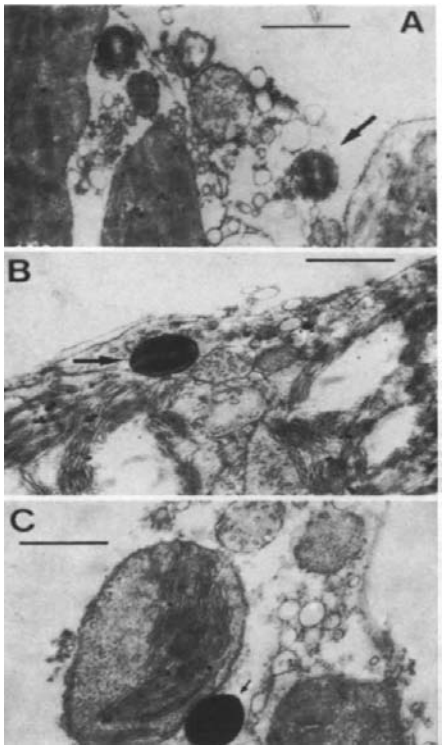

Figure 3. Immunolocalization of Mn-SOD in pea protoplasts by the unlabeled antibody peroxidase-antiperoxidase procedure. (A) Pre-immune serum. (B-C) Incubation with antibody against Mn-SOD from pea leaves [Reprinted from del Río *et al.* (1983) Planta 158: 216-224].

- **Nitric oxide (NO) localization in plant organs**

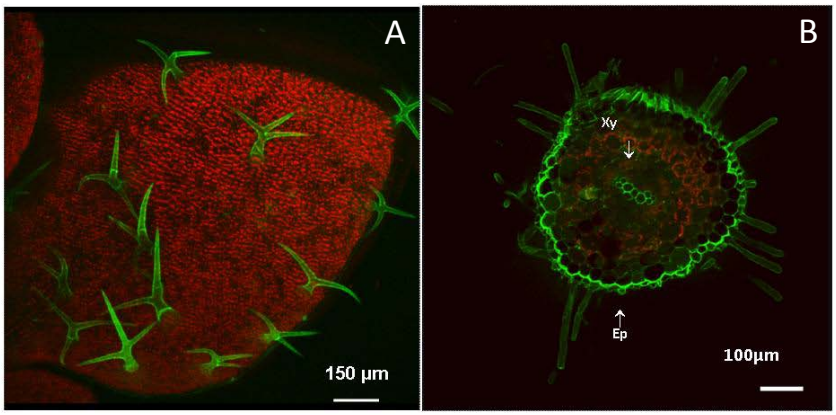

Figure 4. Confocal laser scanning microscopy (CLSM) detection of endogenous NO (green colour) in *Arabidopsis* cotyledons (A) and pepper roots (B). Ep, epidermis; Xy, xylem. [Reprinted from Corpas *et al*. (2009) Plant Physiology 151: 2083-2094, and Airaki (2012) Ph. D. Thesis, University of Granada].

- **NO localization into *Arabidopsis* peroxisomal roots**

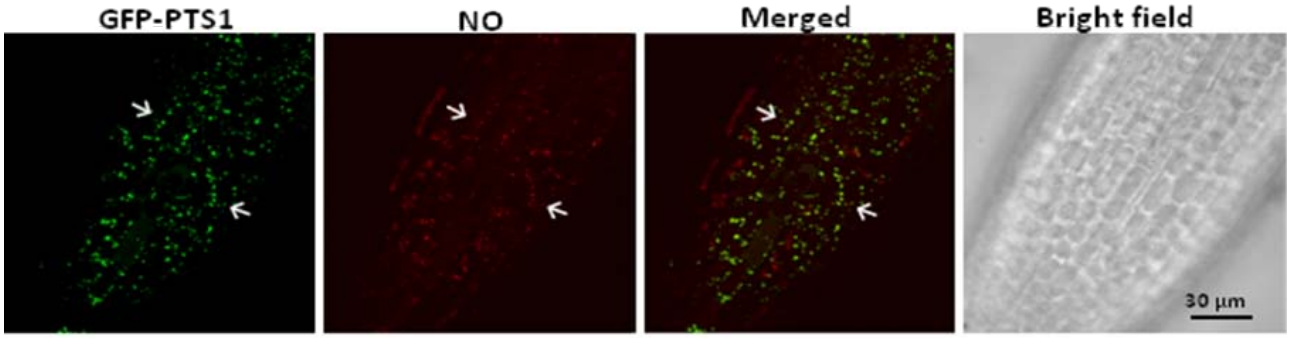

Figure 5. CLSM *in vivo* detection of NO (red colour) and peroxisomes (green colour) in primary roots of *Arabidopsis* roots expressing GFP-PTS1 (green colour) [Reprinted from Corpas *et al*. (2009) Plant Physiology 151: 2083-2094].

- **NO localization in pea leaves**

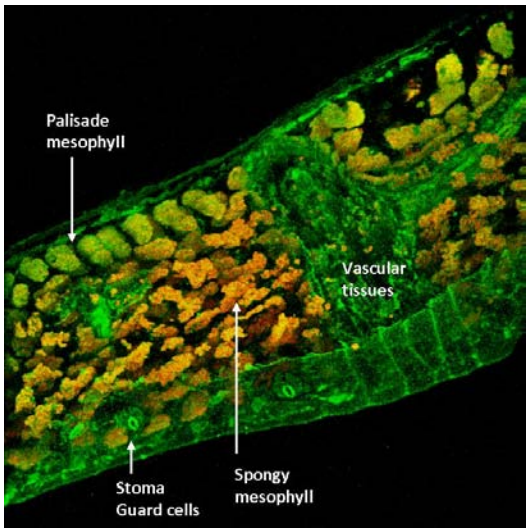

Figure 6. Three-dimensional composition showing the cellular localization of NO (green color) in pea leaves by CLSM. The orange-yellow color corresponds to the chlorophyll autofluorescence [Reprinted from Corpas *et al*. (2004) Plant Physiology 136: 2722-2733].

Acknowledgements. This work has been supported by research ERDF co-funded grants 1FD97-0889-02, PB98-0493-01, BIO2006–14949, AGL2008-00834, BIO2009-12003 and AGL2011-26044 from the Spanish Government, and P06–CVI–1820 from Junta de Andalucía, Spain.

Microscopy techniques for studying oxidative stress in plants

Luisa M. Sandalio*, María C. Romero-Puertas, María Rodríguez-Serrano, Diana M. Pazmiño, Adela Olmedilla, Irene Serrano, Katiuska Cárdenas and María Sanz

Department of Biochemistry, Cell and Molecular Biology of Plants, Estación Experimental del Zaidín, CSIC, Profesor Albareda 1, 18008, Granada, Spain

*corresponding author: luisamaria.sandalio@eez.csic.es

- **Cell ultrastructure and organelle identification**

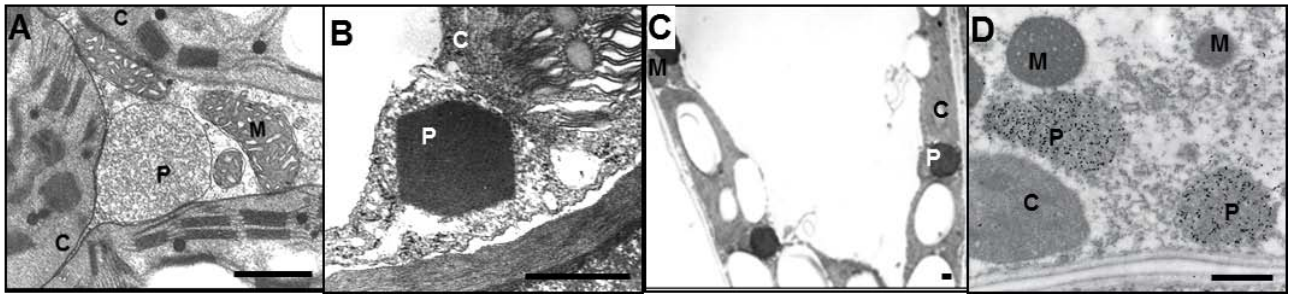

Figure 1. (A-B) Transmission electron microscopy (TEM) micrographs of pea (A) and pepper (B) leaves. (C-D) Peroxisome identification by cytochemistry with DAB (C) and immunocytochemistry of marker proteins (catalase) (D). P, peroxisome; M, mitochondria; C, chloroplasts [Sandalio *et al*. (2013) In: Peroxisomes and their key role in cellular signalling and metabolism, del Río LA (Ed.) Springer].

- ***In vivo* imaging of cell organelles**

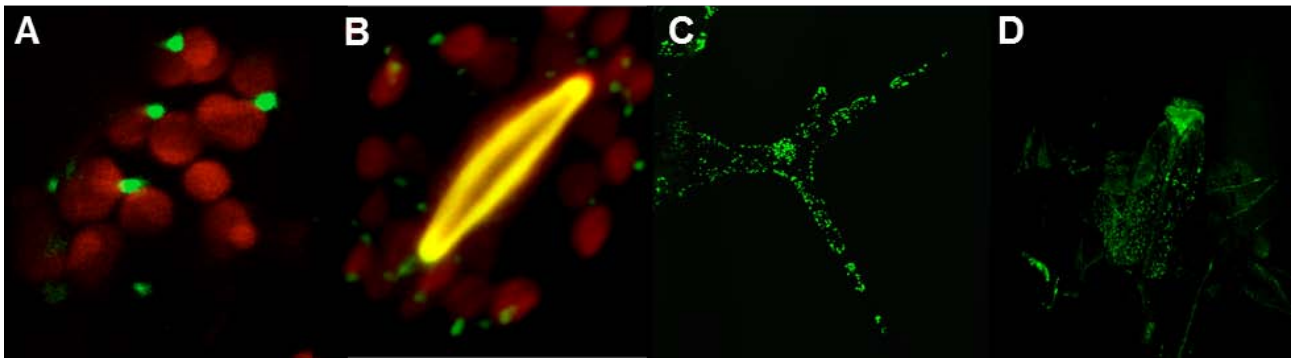

Figure 2. (A-D) Imaging of peroxisomes in *Arabidopsis* lines expressing GFP-SKL (green) by confocal laser scanning microscopy (CLSM). Peroxisomes in mesophyl cells (A), stomata (B), trichomes (C) and flowers (D). Red colour shows chlorophyll autofluorescence [Rodríguez-Serrano *et al*. (2009) Free Rad. Biol. Med. 47: 1632-1639].

- **Imaging of NO and peroxynitrite *in vivo***

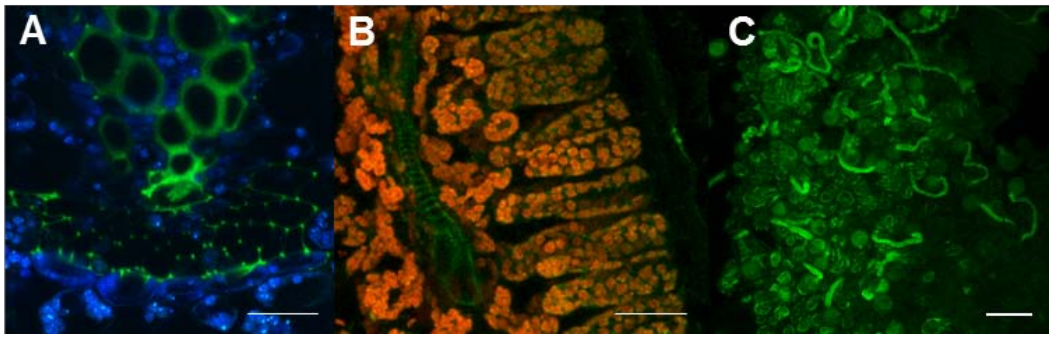

Figure 3. Imaging of NO and $ONOO^-$ under confocal microscope using DAF-2DA and HKGreen-2, respectively. (A-B) Co-localization of NO (green) and chlorophyll (blue in A, red in B) in vascular tissue (A) and mesophyll cells (B). (C) $ONOO^-$ production in pollinated olive stigma [Rodríguez-Serrano *et al*. (2009) Plant Physiol. 150: 229-243; Serrano *et al*. (2012) J. Exp. Bot. 63: 1479-1493].

- **ROS imaging by cytochemistry and TEM**

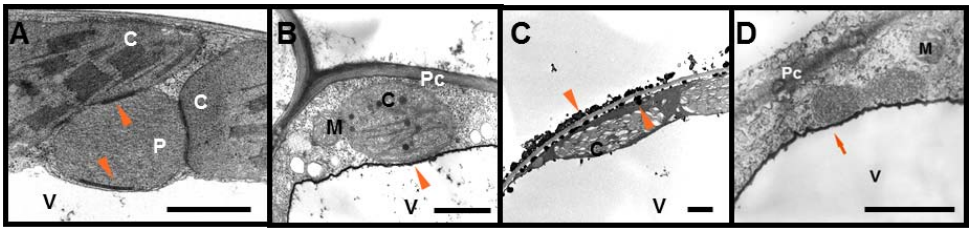

Figure 4. TEM micro-graphs from pea leaves treated with Cd. (A-B) H_2O_2 detection with $CeCl_3$. (C-D) O_2^- detection using Mn/DAB [Romero-Puertas *et al*. (2004) Plant Cell Environ. 27:1122-1134].

- **ROS imaging by histochemistry and LC-M**

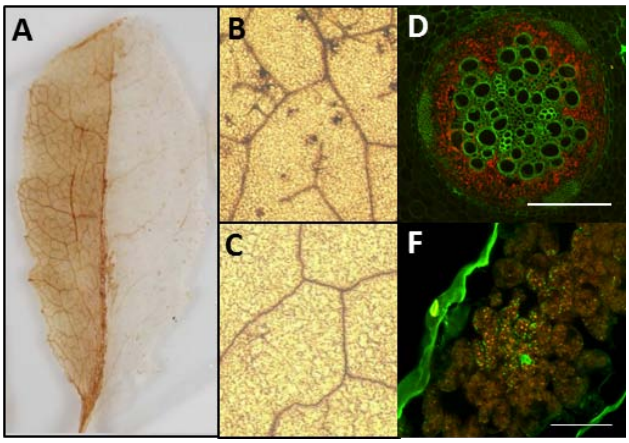

Figure 5. (A) Detection of H_2O_2 accumulation with DAB in pea leaves after *Pseudomonas* infection. (B-C) Stereo microscope pictures of infected (B) and uninfected (C) areas [Romero-Puertas *et al*. (2007) Plant Cell, 19: 4120-4130]. (D-F) Co-localization of H_2O_2/O_2^- (green) and chlorophyll (red) in pea plants using DCF (H_2O_2, D) and DHE (O_2^-, F) in roots (D) and leaves (F) [Rodríguez-Serrano *et al*. (2006) Plant Cell Environ. 29: 1449-1459; Pazmiño DM (2009) PhD thesis].

- **Organelles and cytoskeleton dynamics using LC-M**

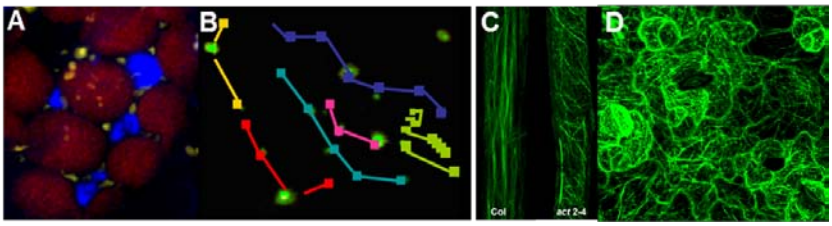

Figure . Organelle cross-talk. (A) Chloroplasts (red), mitochondria (YFP, yellow) and peroxisomes (CFP, blue). Peroxisome (B) and actin cytoskeleton (C-D) dynamic analysis [Rodríguez-Se-rrano *et al*. (2009) Free Rad. Biol. Med. 47: 1632-1639; Lanza *et al*. (2012) Dev. Cell 22: 1275-1285; Pazmiño DM (2009) PhD thesis].

- **Other applications**

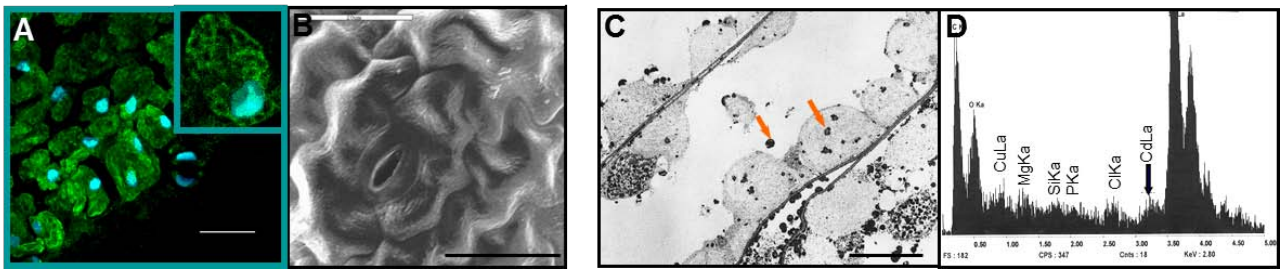

Figure 6. (A) Monitoring gene expression using *in situ hibridization* and fluorescence microscopy. (B) Micrograph of leaf surface by scanning microscopy. (C-D) Quantification and subcellular detection of metals (Cd) by X-ray microanalysis [Rodríguez-Serrano *et al*. (2009) Plant Physiol. 150: 229-243; Sandalio *et al*. (2001) J. Exp Bot. 52: 2115-2126; Romero-Puertas *et al*. (2004) Plant Cell Environ. 27: 1122-1134; Romero MC (2002) PhD thesis].

Acknowledgements. These studies have been carried out at the technical service facilities of the Universities of Granada, Jaén and Oxford Brooks and CIB-CSIC, with the aid of grants BFI2002-04440-C02-01, BIO-2005-03305, BIO2008-04067, and BIO2012-36742, co-financed by ERDF and MICINN.

Microscopy to study ion homeostasis and membrane transporters

Andrés Belver, Raquel Olías, Olivier Cagnac, Mª Nieves Aranda-Sicilia, Francisco Javier Gálvez, Ana P. Ortega, Noelia Jaime-Pérez, Ali AbouKila, Mª Isabel Gaspar, Mª Elena Sánchez, KeesVenema and Pilar Rodríguez-Rosales*

Department of Biochemistry, Cell and Molecular Biology of Plants, Estación Experimental del Zaidín, CSIC, Profesor Albareda 1, 18008 Granada, Spain

*corresponding author: pilar.rodriguez@eez.csic.es

• SlNhaD is a putative tomato Na^+/H^+ antiporter localized in plastids throughout plant tissues

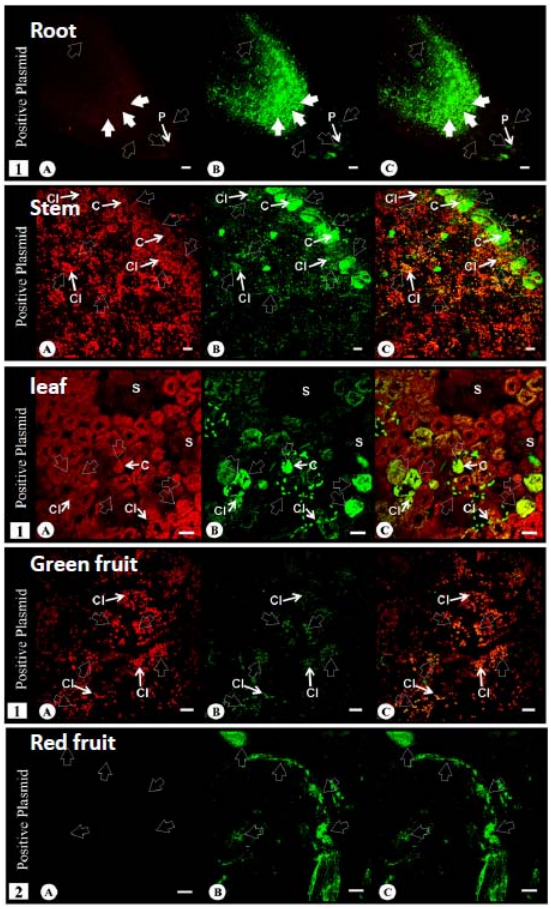

← Figure 1. Tissues from *Nicotiana benthamiana* infected with Agrobacterium transformed with a SlNhaD-GFP construct. (A) Red channel. (B) Green channel. (C) Red channel plus green channel. C, cell; Cl, chloroplast; P, plastid; S, stoma. Bars: 20 µm [Olías *et al*. (2009) Plant Abiotic Stress Tolerance Conference, Vienna, Austria].

• Phenotypic characterization of a *nhd1* Arabidopsis mutant (for the putative plastidial Na^+/H^+ antiporter, AtNHD1): chloroplast structure

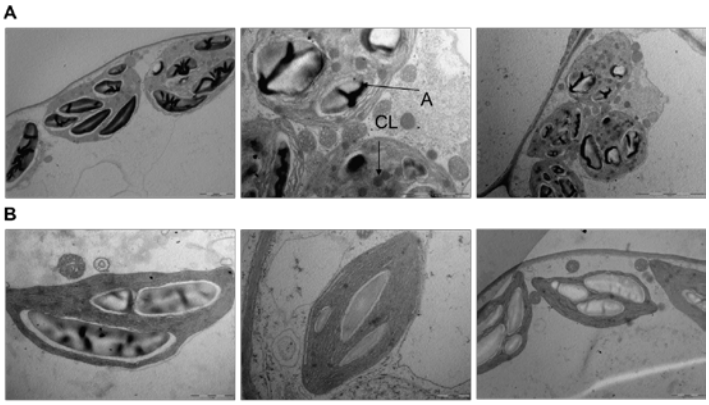

↑ Figure 2. TEM photomicrograph of chloroplasts. (A) Two weeks old WS ecotype wild type plants. (B) *atnhd1* mutant plants, lines L3, L13 and L16 [Olías and Belver, unpublished results].

• Arabidopsis KEA2 encodes a K^+/H^+ antiporter localized in chloroplast

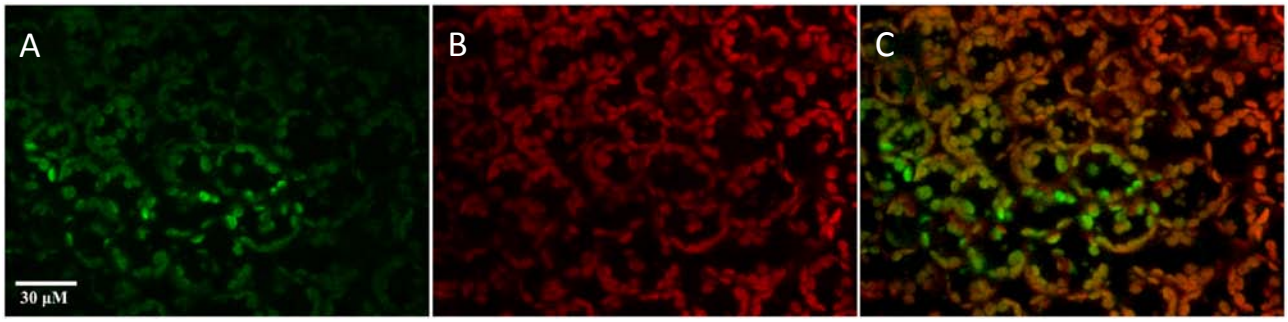

Figure 3. Localization of AtKEA2 studied by confocal microscopy. The first 300 bp of AtKEA2 fused to eGFP was transiently expressed in seedlings. (A) GFP fluorescence from a cotyledon. (B) Chlorophyll autofluorescence of the same field as (A). (C) Merged of (A) and (B) images [Aranda-Sicilia *et al*. (2012) Biochim. Biophys. Acta, Biomembranes 1818: 2362].

- **Vcx1p is a vacuolar K^+/H^+ antiporter from *Saccharomyces cerevisiae***

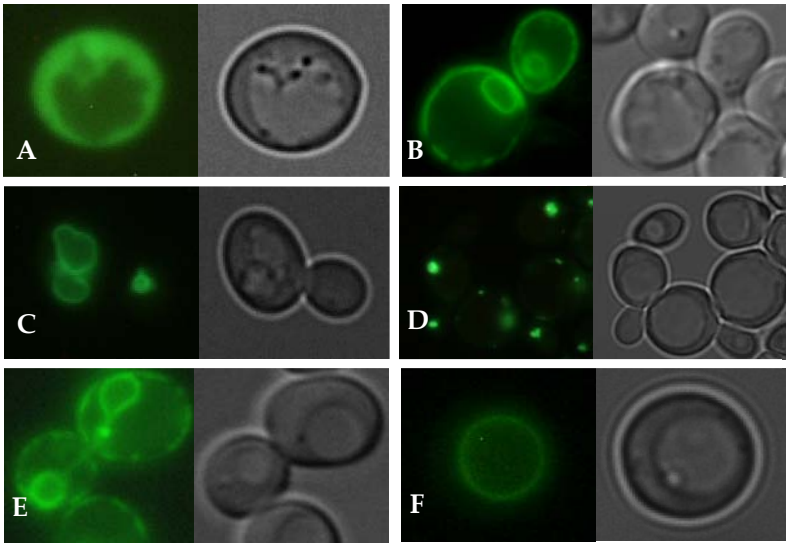

Figure 4. Vacuolar localization of Vcx1p and Vcx1p-H303A mutant. (A) Vacuolar $Ca2^+/H^+$ exchanger Vcx1p fused to GFP at the C terminus displayed a typical signal of ER localization as observed for the vacuolar Na_/H_ exchanger Vnx1p in the same conditions. When Vnx1p was fused to eYFP at the N terminus, the fluorescent signal was observed at the vacuolar membrane (B). An identical localization for Vcx1p (C) and its inactive mutant form Vcx1p-H303A (D) was observed when they were fused to eYFP at their N termini. Fluorescence was observed in the cytosol of cells expressing a free form of eYFP (E). A positive control of vacuolar membrane localization was obtained using the vacuolar ATPase Vph1p subunit fused to GFP at the C terminus (F) [Cagnac *et al*. (2010) J. Biol. Chem. 285: 33914].

- **Localization of the endosomal K^+/H^+ antiporter LeNHX2 in tomato roots**

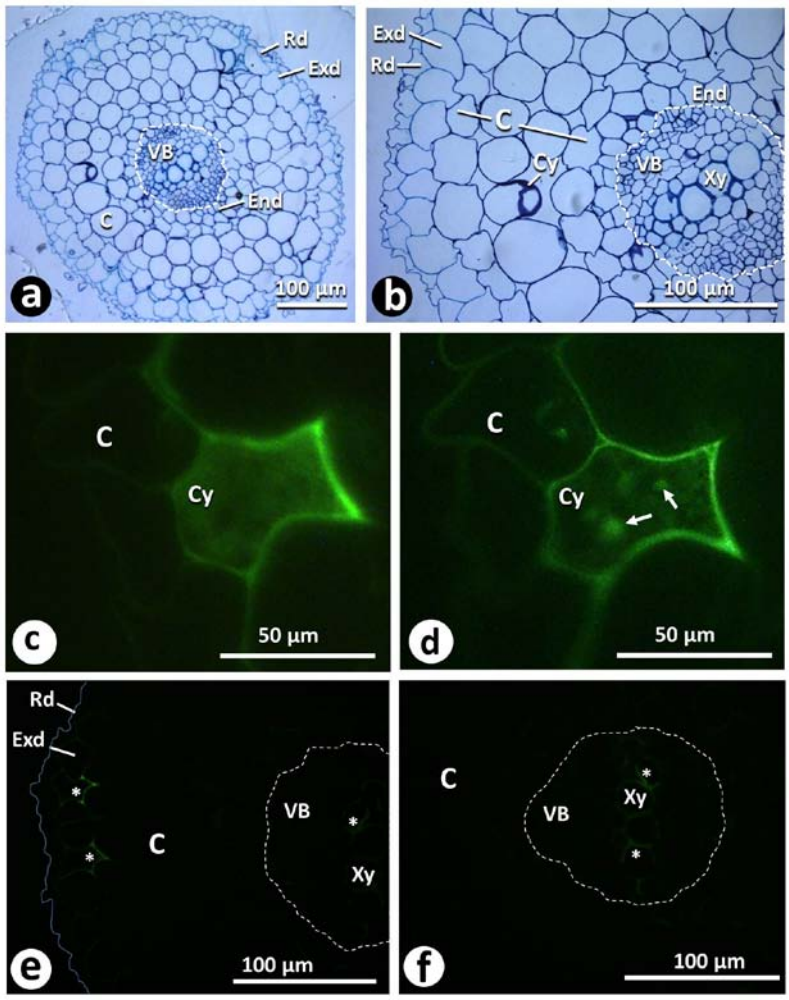

Figure 5. Fluorescence immunolocalization of the histagged LeNHX2 in roots. Transverse sections of Unicryl-embedded roots of the L-452 transgenic (A-E) and the untransformed (Control, F) plant lines, grown hydroponically in 120 mM NaCl-supplemented solution for three days. (A-B) Toluidine blue stained sections. (C-D) High magnification images of two seriate sections corresponding to a cortex cell showing intensely labeled spots after immunocyto-chemistry. (E-F) Negative controls (primary antibody omitted and untransformed plant, respectively). Arrows, expression spots; Asterisks, autofluorescence; C, cortex; Cy, cytoplasm; End, endodermis; Exd, exodermis (limits marked by solid blue line); Rd, rhizodermis; VB, vascular bundle (limits marked by dotted white line; Xy, xylem [Huertas *et al*. (2013) Plant Cell Environ., DOI: 10.1111/ pce.12109].

Acknowledgements. This work has been supported by numerous research projects. Currently active projects include ERDF co-funded grants AGL2010-17090 and BIO2012-33655 from the Spanish government, and P2011-CVI-7558 from Junta de Andalucía.

Microscopy to study plant sexual reproduction

Juan de Dios Alché*, Antonio Jesús Castro, Mª Carmen Fernández, Juan David Rejón, Krzysztof Zienkiewicz, Sonia Morales, Mohamed M´rani, José Carlos Jiménez-López, Agnieszka Zienkiewicz, José Angel Traverso, Adoración Zafra, Mª José Jiménez-Quesada, Estefanía García-Quirós, Concepción Martínez-Sierra and Mª Isabel Rodríguez-García

Department of Biochemistry, Cell and Molecular Biology of Plants, Estación Experimental del Zaidín, CSIC, Profesor Albareda 1, 18008 Granada, Spain

*corresponding author: juandedios.alche@eez.csic.es

- **Pollen development under an ultrastructural view: first TEM studies at the EEZ**

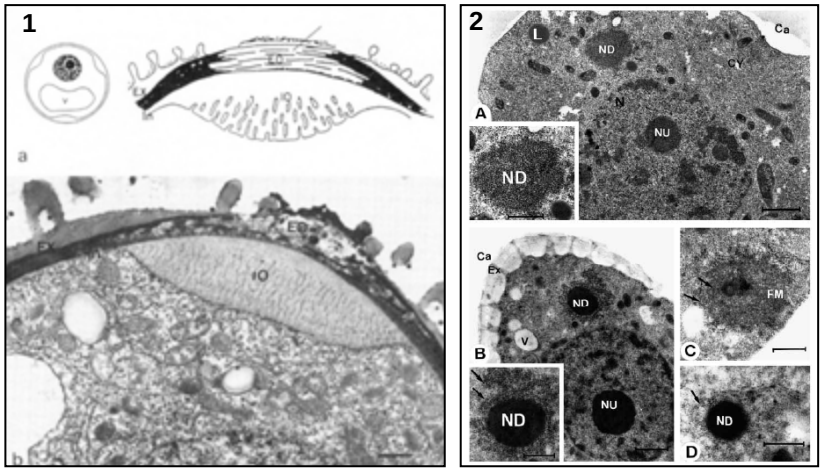

Figure 1. (A) Aperture formation in the olive pollen [Fernández and Rodríguez-García (1989) New Phytol. 111: 717]. (B) Cyto-chemical features of nucleoloids in olive microsporocites [Alché *et al*. (1994) J. Cell Sci. 107: 621].

- **Bright field and fluorescence microscopy applied to the study of pollen development**

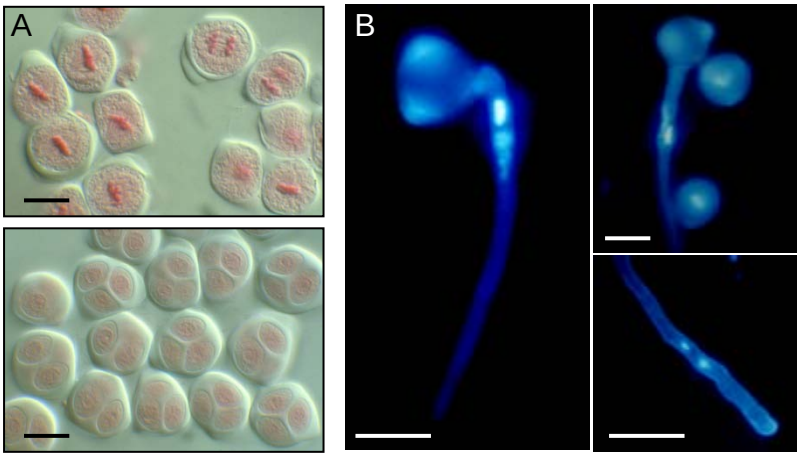

Figure 2. (A) Study of olive male meiosis by orcein staining and differential interference contrast (DIC) microscopy [Alché JD (1991) PhD thesis]. (B) Study of nuclear dynamics in the olive pollen tube by DAPI staining and fluorescence microscopy.

- **Scanning Electron Microscopy (SEM): surfing on the surface**

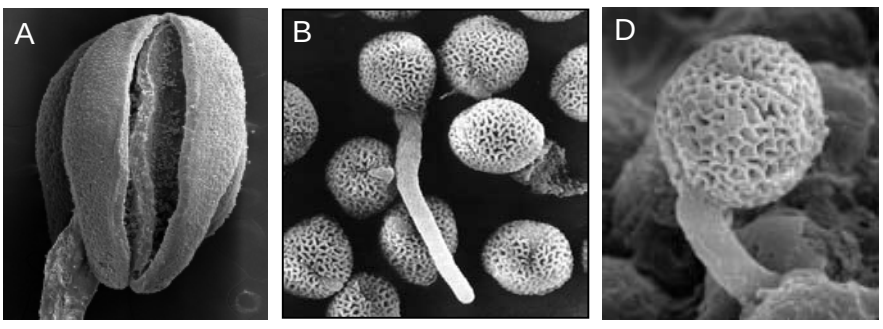

Figure 3. (A) SEM photomicrograph of an olive dehiscent anther. (B-C) SEM photomicrograph of olive pollen grains germinating *in vitro* (B) and *in vivo* through the stigmatic papillae (C).

- **Cellular localization of biological molecules: what, where and when**

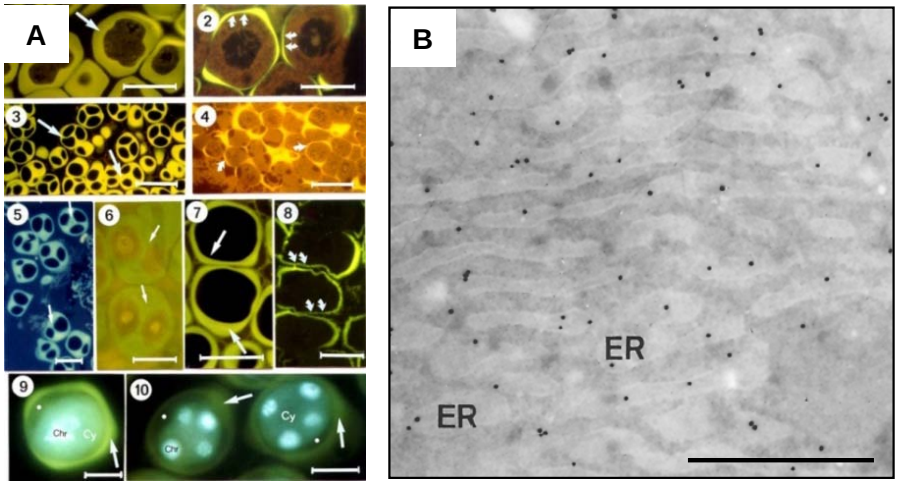

Figure 4. (A) Localization of callose by aniline blue in olive meiocytes [Alché and Rodríguez-García (1997) Biotech. Histochem. 72: 285]. (B) Immunolocalization of Ole e 1 protein in mature olive pollen grains. ER, endoplasmic reticulum [Rodríguez-García *et al*. (1995) Planta 196: 558].

- **Confocal Laser Scanning Microscopy (CLSM): deep tissue imaging and 3-D reconstruction**

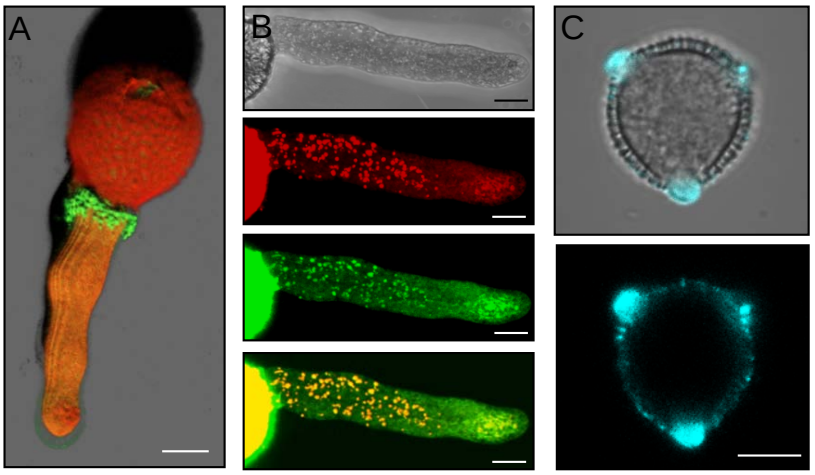

Figure 5. (A) Localization of galactans (green fluorescence) in germinating olive pollen [Castro *et al*. (2013) Ann. Bot. 112: 503]. (B) Co-localization of caleosin (green) and oil bodies (red) in olive pollen tubes [Zienkiewicz *et al*. (2010) J. Exp. Bot. 61: 1537]. (C) Localization of profilin in olive pollen [Morales *et al*. (2008) J. Microsc. 231: 332].

- **Beyond structure: microscopy and function**

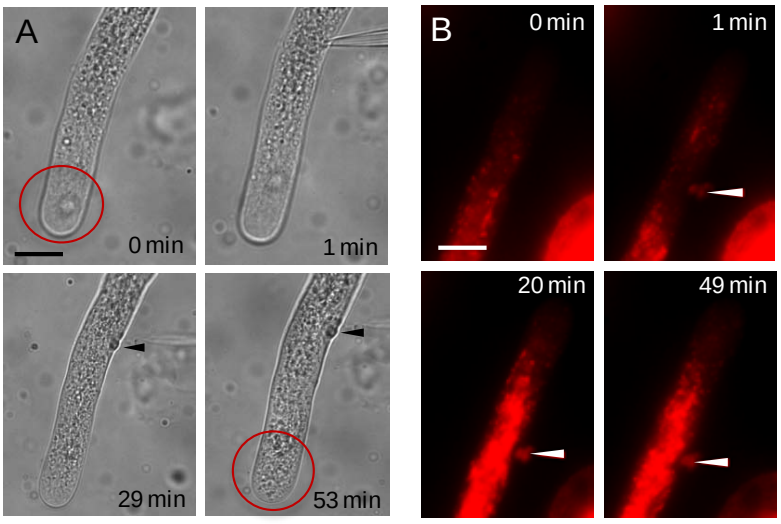

Figure 6. (A) Time course transmitting light microscopy analysis of pollen tube behaviour after antibody microinjection. After 1 h, the pollen tube growth stopped and the clear zone was not longer visible (red circle). (B) Time course fluorescence microscopy analyses of organelle distribution, motility and behavior after vital stain + antibody microinjection [Zienkiewicz *et al*. unpublished].

Acknowledgements. This work has been supported by numerous research projects. Currently active projects include EFDF co-funded grants BFU2011-22779 (Ministerio de Economía y Competitividad), P2010-CVI5767, P2010-AGR6274 and P2011-CVI7487 (Junta de Andalucía), and PEOPLE-PIOF-GA-2011-301550 (European Research Council).

SOIL MICROBIOLOGY AND SYMBIOTIC SYSTEMS

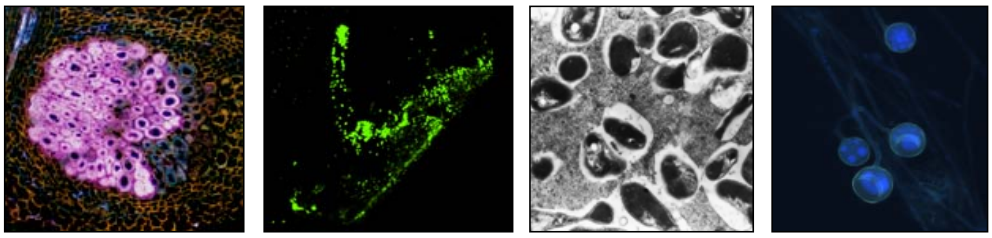

Microscopy to study PAHs caption by roots inoculated with *Rhizophagus custos*

Elisabet Aranda*, Rocio Reina, Patricia Godoy, Martin Scervino, Jose Antonio Siles, Antonio Illana, Rodolfo Torres, Tania Ho, Maria Isabel Tamayo, Julia Martín, Nuria Molinero, Jose Manuel García, Inmaculada García-Romera and Juan Antonio Ocampo-Bote

Department of Microbiology and Symbiotic System, Estación Experimental del Zaidín, CSIC, Profesor Albareda 1, 18008 Granada, Spain

*corresponding author: elisabet.aranda@eez.csic.es

- **Bright field microscopy applied to the study of hyphal length development**

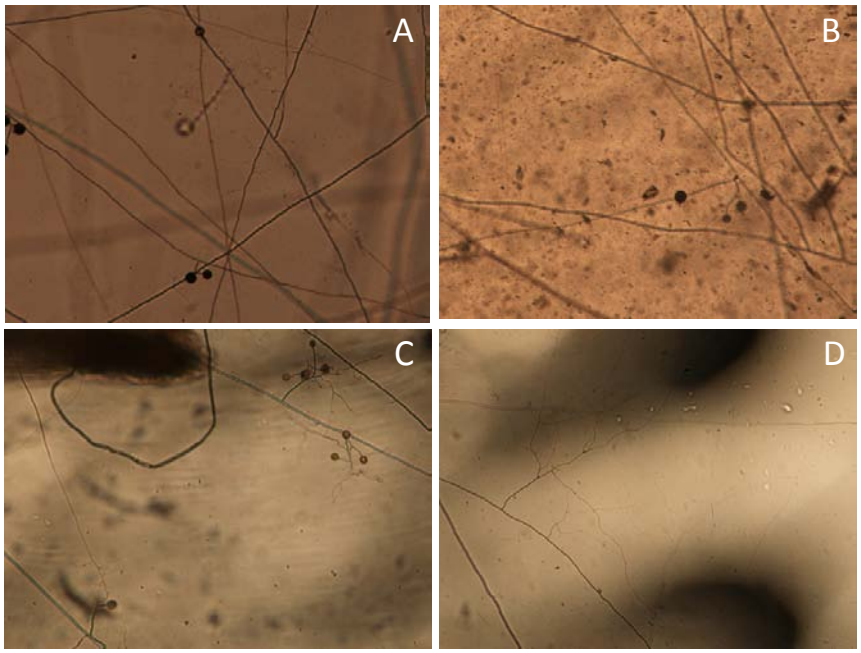

Figure 1. (A) Hyphae and spores of *R. custos* (B) Hyphae and spores of *R. custos* in presence of 280 μM of anthracene. (C) Hyphae, BAS structures and spores of *R. custos* in presence of 280 μM of anthracene. (D) Hyphae, BAS structures and spores of *R. custos* in presence of 280 μM of phenanthrene.

- **Bright field and fluorescence microscopy applied to the study of anthracene and phenanthrene absorption by mycorrhizal and non mycorrhizal roots**

1. **Absorption by the roots exudates**

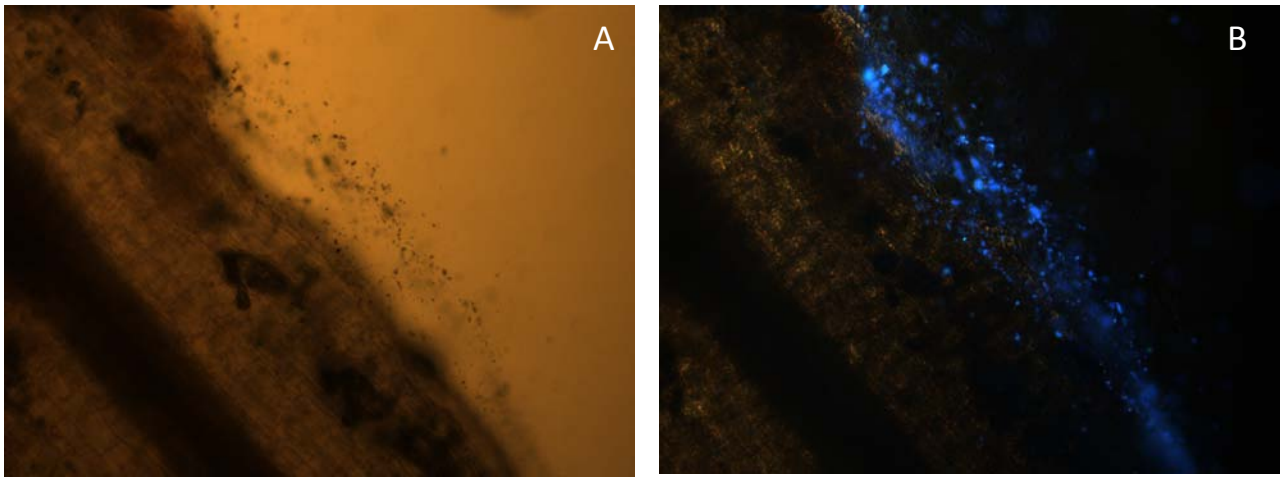

Figure 2. (A) Bright field microscopy of carrot root (*Daucus carota*). (B) Observation of anthracene bounding to root surface using fluorescence microscopy.

2. Adsorption by mycorrhizal roots and fungal structures

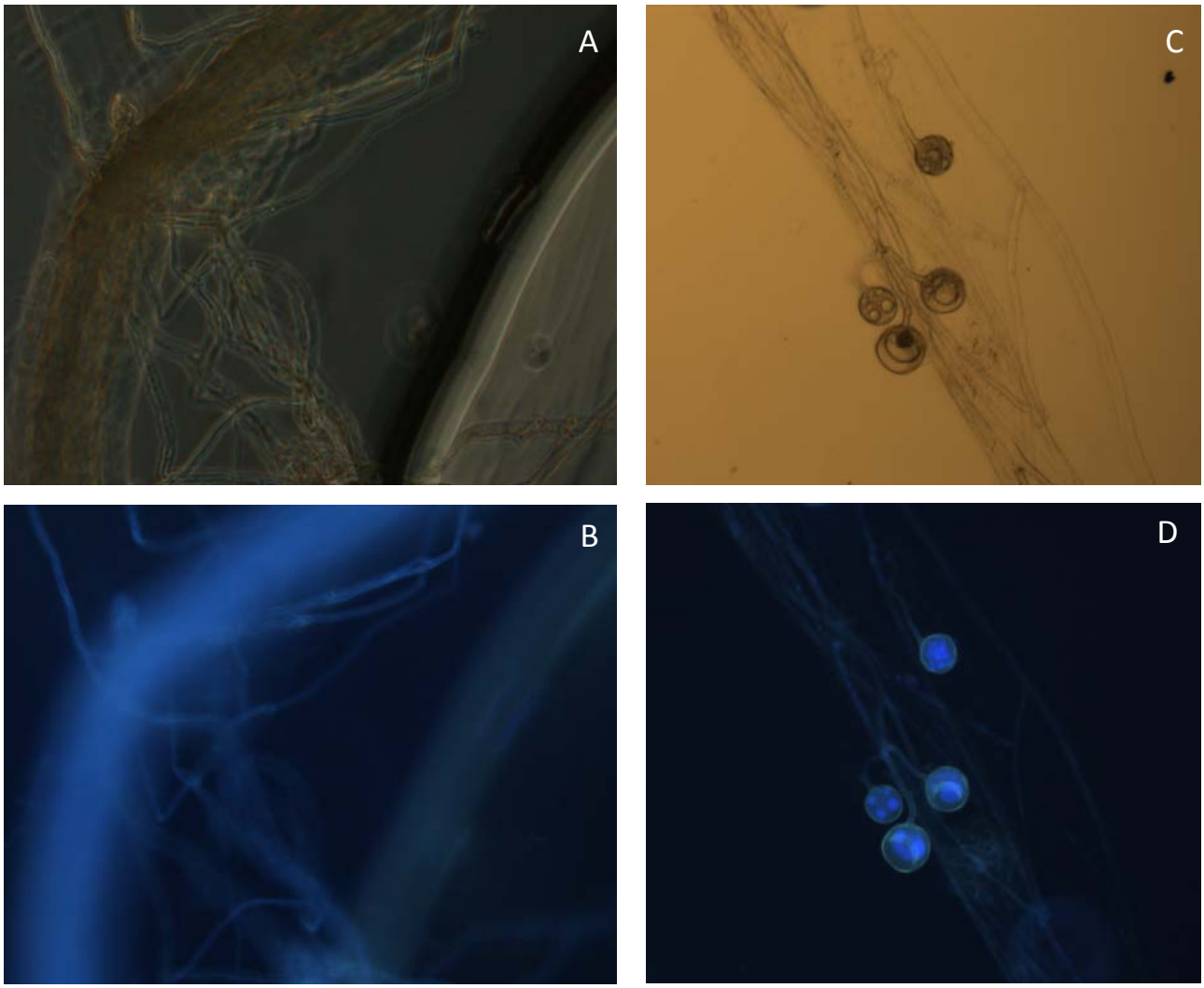

Figure 3. (A) Observation of extrarradical mycelia of *R. custos* cultured in presence of 70 µM anthracene bright field. (B) Observation of extrarradical mycelia of *R. custos* fluorescence microscopy. (C) Observation of fungal spores of *R. custos* cultured in presence of 70 µM anthracene bright field. (D) Observation of fungal spores of *R. custos* using fluorescence microscopy.

Acknowledgements. This work has been founded by the Excellence Project of the Junta de Andalucía (P09-CVI-4778).

Observation of the arbuscular mycorrhizal fungal structures in roots by microscopy-based techniques

Horst Vierheilig, Nuria Molinero, Rafael León, José Ángel Martín, Elisabet Aranda, Rocío Reina, Patricia Godoy, José Antonio Siles, Antonio Illana, Rodolfo Torres, Tania Ho, María Isabel Tamayo, Julia Martín, José Manuel García*, Inmaculada García-Romera and Juan Antonio Ocampo-Bote

Department of Microbiology and Symbiotic System, Estación Experimental del Zaidín, CSIC, Profesor Albareda 1, 18008 Granada, Spain

*corresponding author: josemanuel.garcia@eez.csic.es

- **Destructive non-vital methods to visualize Arbuscular Mycorrhizal fungus in roots**

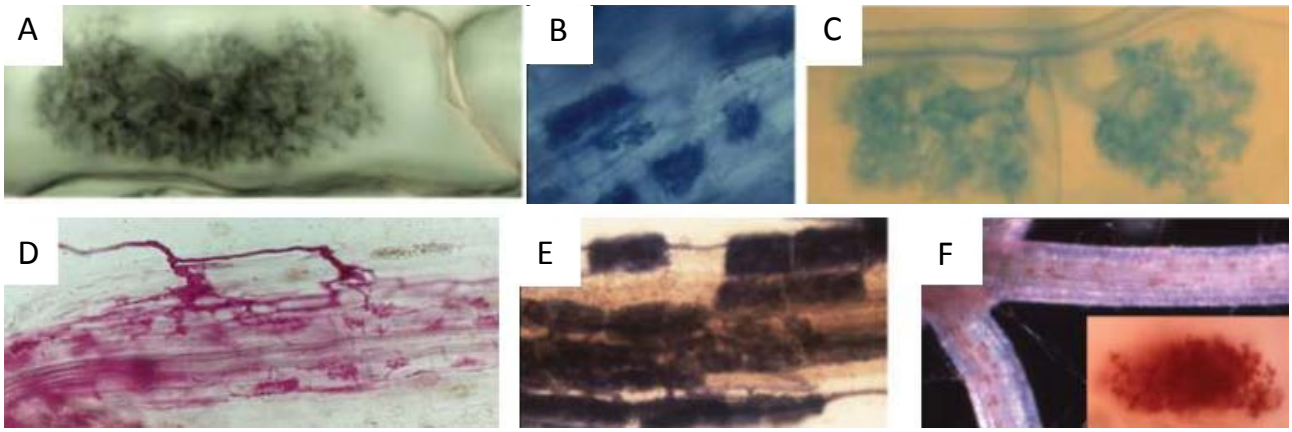

Figure 1. Observation of AM fungal structures stained by chlorazol black (A), trypan blue (B), aniline blue (C), acid fuchsin (D), ink (E) and neutral red (F) [Vierheilig *et al*. (2005) Physiol. Plant. 125: 393-404].

- **Vital stains to visualize Arbuscular Mycorrhizal fungus in roots**

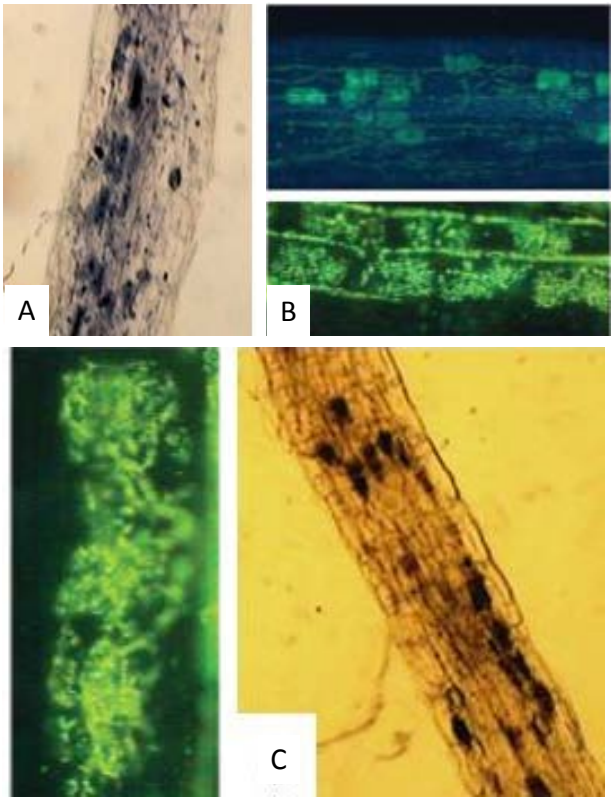

Figure 2. Vital stains of fungal succinate dehydrogenase-SDH (A) and fungal alkaline phosphatase in roots (B-C). Fluorescent staining of alkaline phosphatase activity (B), where arbuscules can be clearly distinguished under higher magnifications [Vierheilig *et al*. (2005) Physiol. Plant. 125: 393-404].

- **"*In vivo*" observation of fungal structures in roots by epifluorescence and confocal laser scanning microscopy.**

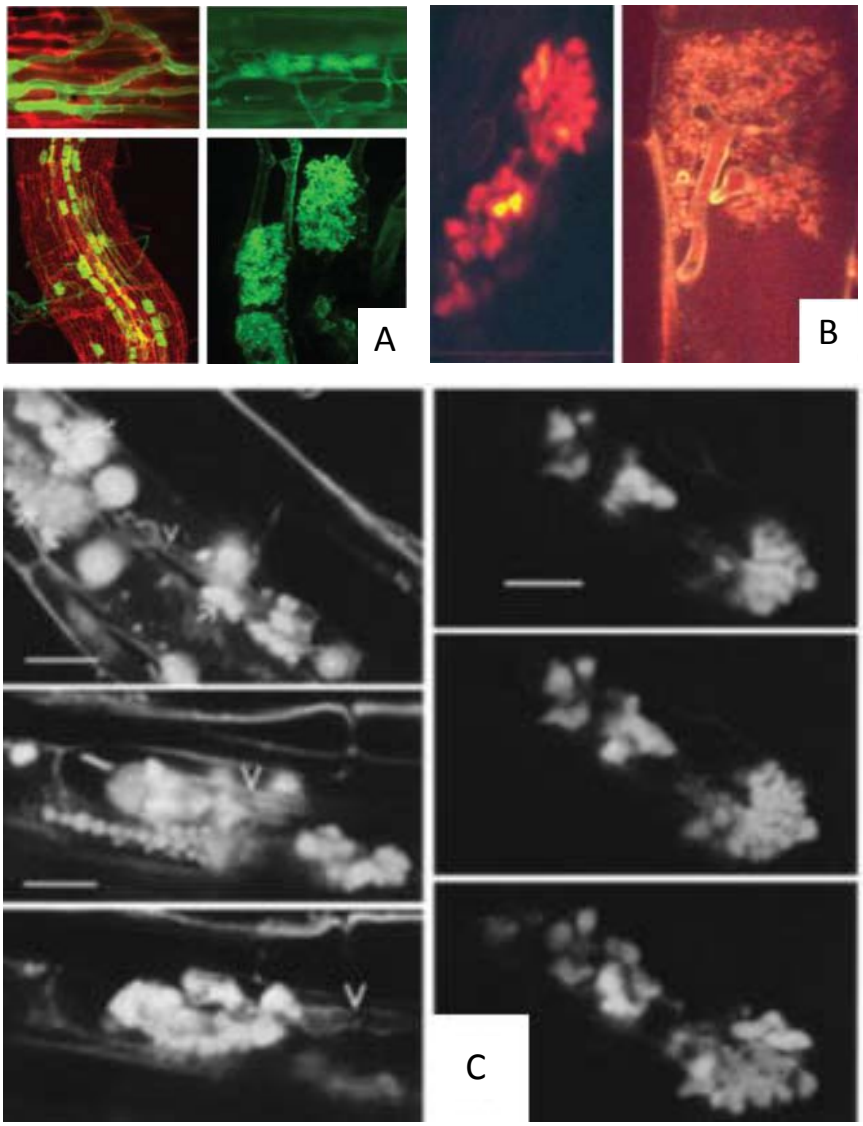

Figure 3. AM fungal structures observed by confocal laser scanning microscopy (CLSM) in sectioned roots stained for chitin with fluorescein isothiocyanate (FITC)-conjugated wheat germ agglutinin (A). Autofluorescing collapsed arbuscule observed by CLSM (B). *In vivo* observations by CLSM showing a strong autofluorescence of fungal structures. Successive layers of an arbuscule at different depths (C) [Vierheilig *et al*. (2005) Physiol. Plant. 125: 393-404; Vierheilig *et al*. (1999) Mycological Res. 103: 311-314].

Acknowledgements. Financial support has been obtained from research projects granted to the member of the group among the FEDER co-funded grants from Junta de Andalucía (CVI 260) and MINECO.

Microscopy to study plant-bacteria interaction

Eulogio J. Bedmar*, María J. Delgado and Socorro Mesa

Department of Soil Microbiology and Symbiotic Systems, Estación Experimental del Zaidín, CSIC, Profesor Albareda 1, 18008 Granada, Spain

*corresponding author: eulogio.bedmar@eez.csic.es

- **Histochemical detection of β-galactosidase activity in nodule sections**

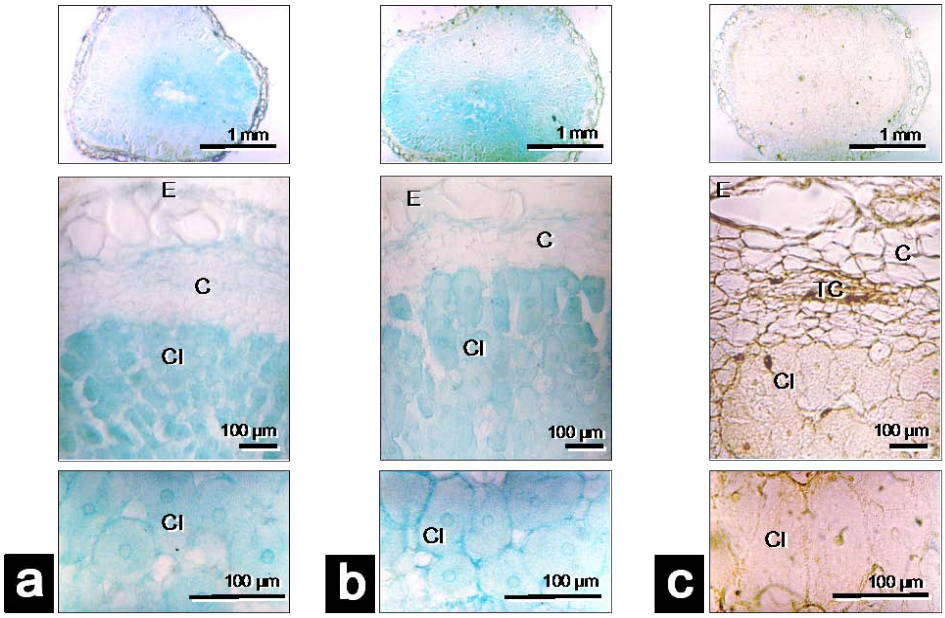

Figure 1. In situ expression of β-galactosidase activity in longitudinal sections of 35-d old soybean (*Glycine max* L., cv. Williams) nodules induced by *Bradyrhizobium japonicum* USDA110 containing a P_{nirK}-lacZ transcriptional fusion. Nodules were obtained from plants grown in the absence (A) or the presence (B) of 4 mM KNO_3. Nodule sections from nitrate-treated soybeans inoculated with *B. japonicum* USDA110 containing plasmid pMP220 were used as a control (C). Nodule sections (25 µm) were cut using a manual microtome, mounted on 3-aminopropyl triethoxy-silane (APES)-coated slides, deparaffinized with xylene and rehydrated through a graded ethanol series. Observations were made using an Axioplan microscope (Carl Zeiss Ltd, Gottingen, Germany). OC, outer cortex; IC, inner cortex; IZ, infected zone; VB, vascular bundles [(2004) Physiol. Plant. 20: 205-211].

- **Fluorescence microscopy applied to the study of *Phaseolus vulgaris* endosymbionts**

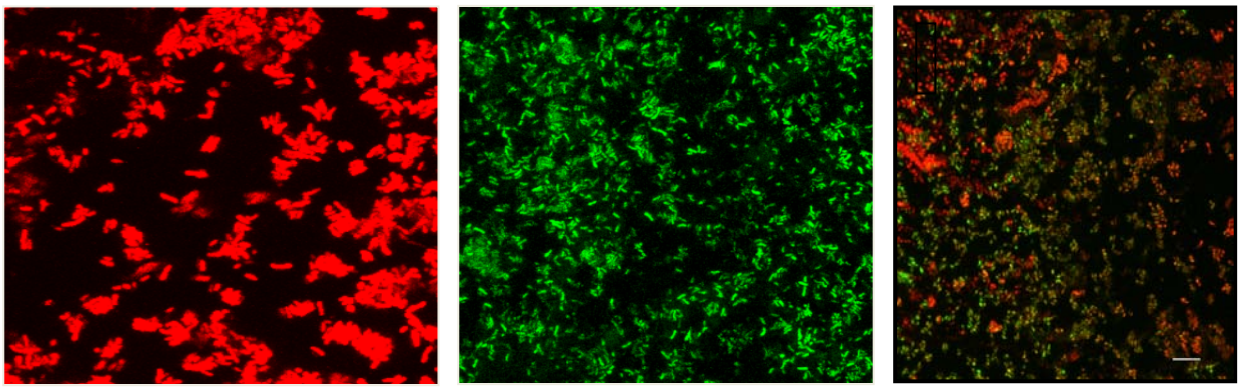

Nodules formed by *R. tropici* CIAT61

Nodules formed by *B. phymatum* GR60

Nodules co-occupied by *B. phymatum* GR60 and *R. tropici* CIAT61

Figure 2. Emission of fluorescence by nodules formed by *Burkholderia phymatum* GR60 containing plasmid miniTn7(Gm) P_{rrnB} P1-*gfp*-a and *R. tropici* CIAT61 containing plasmid miniTn7 $(Gm)_{PA1/04/03}$ *DsRedExpress*-a on roots of common bean (*Phaseolus vulgaris* L., cv. Flamingo) [Plant and Soil. DOI 10.1007/s11104-012-1499-6]. The emission of fluorescence by the nodules was inspected by confocal laser scanning microscopy (CLSM) using a Nikon C1 confocal microscope. Simultaneous excitation was performed with an Ar (50 mW) (488 nm) and a He-Ne (2 mW) (543 nm) laser.

- **Fluorescence microscopy applied to the study of the infection process of *Phaseolus vulgaris* by *R. tropici* CIAT61**

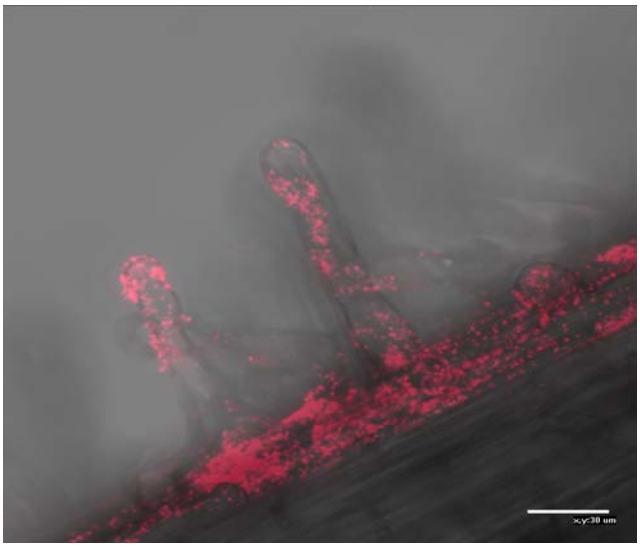

Figure 3. Attachment of *R. tropici* CIAT61 to the root cortex of *Phaseolus vulgaris* L., cv. Flamingo, and infection thread inside the root hair.

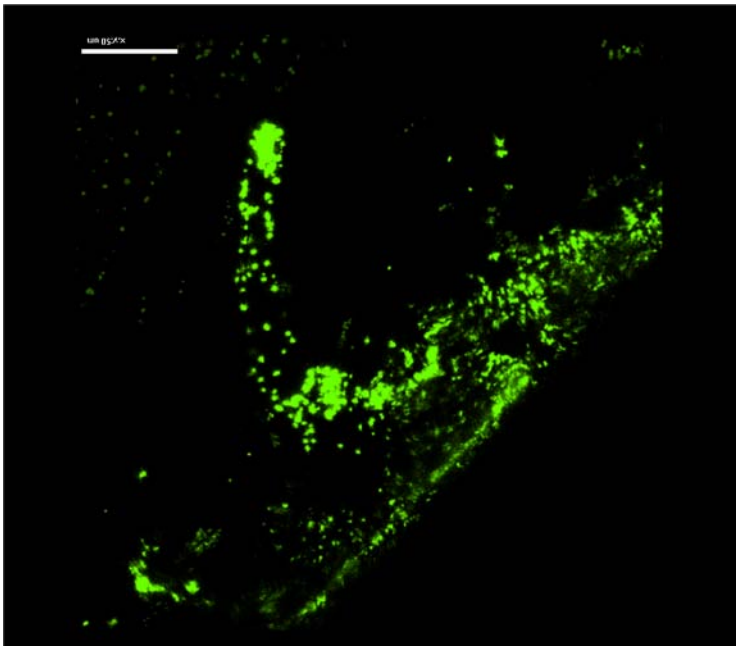

Figure 4. Infection thread formed by *B. phymatum* GR60 during infection of *Phaseolus vulgaris* L., cv. Flamingo. Cells expressing fluorescent proteins were examined using a Leica M165FC stereo microscope equipped with epifluorescence detection.

Acknowledgements. Financial support has been obtained from ERDF co-funded grants BMC2002-04126-C03-02, P07-CVI-3177, RNM-4746, AGL2010-18607 and 200940I116.

Microscopy to study structure, dynamics and function of rhizobacterial genomes

Nicolás Toro García*, José Ignacio Jiménez-Zurdo, Fernando Manuel García-Rodríguez, Omar Torres-Quesada, Francisco Martínez-Abarca, Manuel Fernández-López, Pablo José Villadas, Mª Dolores Molina-Sánchez, Rafael Nisa-Martínez, Mercedes Reinoso Colacio, Laura Martínez-Rodríguez, Antonio José Fernández-González, José Francisco Cobo, Alexandra Peregrina, Vanesa Díaz-Prado, Vicenta Millán, José Mª del Arco, and Ascensión Martos-Tejera

Department of Microbiology and Symbiotic Systems, Estación Experimental del Zaidín, CSIC, Profesor Albareda 1, 18008 Granada, Spain

*corresponding author: nicolas.toro@eez.csic.es

- **Influence of the RNA chaperone Hfq on the *Sinorhizobium meliloti*-alfalfa symbiosis**

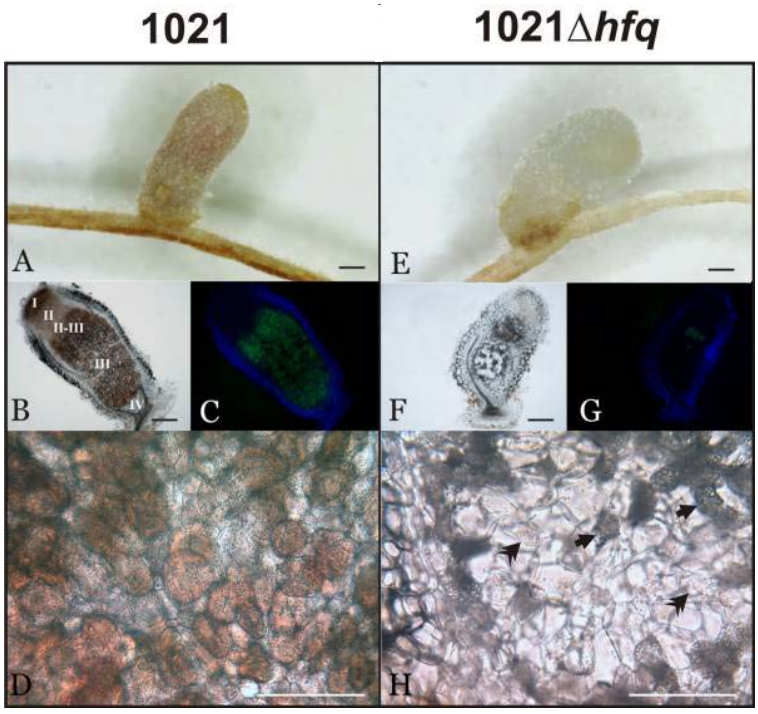

Figure 1. The 1021Δ*hfq* mutant is impaired in the survival within the nodule cells. Representative enlarged images of nodules induced in alfalfa plants by the 1021 (A) and 1021Δ*hfq* (E) strains. Bright-field microscopy of longitudinal sections of the same nodules (B, F); the zones characterizing the histology of nitrogen-fixing indeterminate nodules are indicated in (B). Merged images of the same nodule sections observed with green and blue filters (520 nm and 470 nm, respectively) (C, G). Magnification of the images of central nodule tissues (D, H); 1021Δ*hfq*-induced nodules are scarcely invaded by bacteria and show signs of premature senescence: degradation of leghemoglobin (arrows) and cell debris (double arrowheads). Bars, 250 µm [Torres-Quesada *et al*. (2010) BMC Microbiol. 10: 71].

- **Localization of *S meliloti* gene expression using reporter genes**

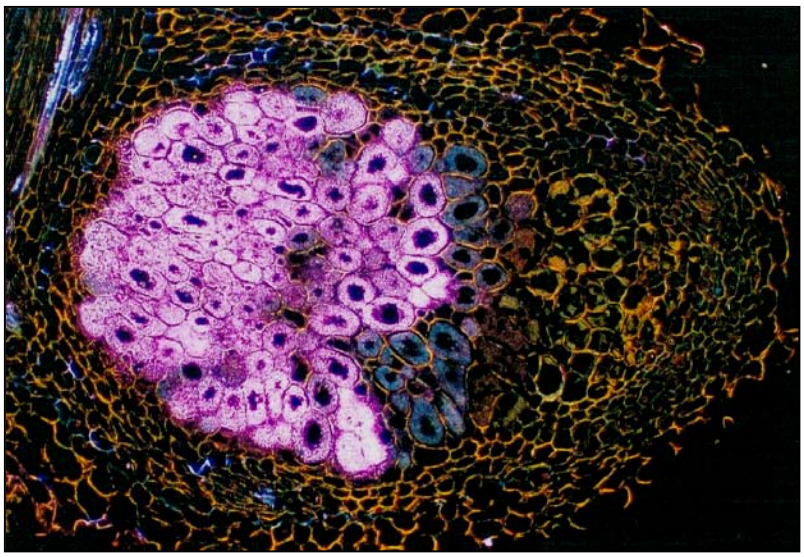

Figure 2. Histochemical localization of β-glucuronidase activity in alfalfa nodules. Dark field microscopyof 5 mm longitudinal section stained with 0.25% toulidine blue of nodules elicited by *S meliloti* strain 2011 containing transcriptional fusion of β-glucuronidase gene under the *nfeB* promoter [García-Rodríguez and Toro (2000) Mol. Plant Microbe Interact. 13: 583-591].

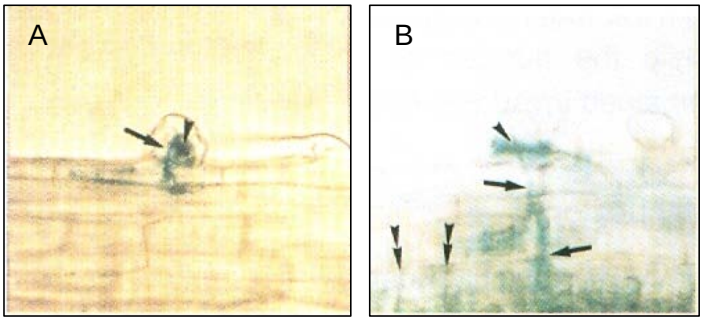

Figure 3. Histochemical localization of β-galactosidase activity in undissected and cleared alfalfa roots 3d after inoculation with *R, meliloti* strain GRM8 carrying a putA-lacZ transcriptional fusion. (A) Expression in the crook of a curled root hair (arrowhead) (Hac phenotype) and inside the infection thread developing into the root hair (arrow) (Inf phenotype). The magnification is x32. (B) Hac (arrowhead) and Inf (arrows) phenotypes. Note cortical cell division (double arrowheads) in front of advancing infection threads (arrows). The magnification is x40 [Jiménez-Zurdo *et al*. (1997) Mol. Microbiol. 23: 85-93].

- **Light microscopy applied to the study of nodule development**

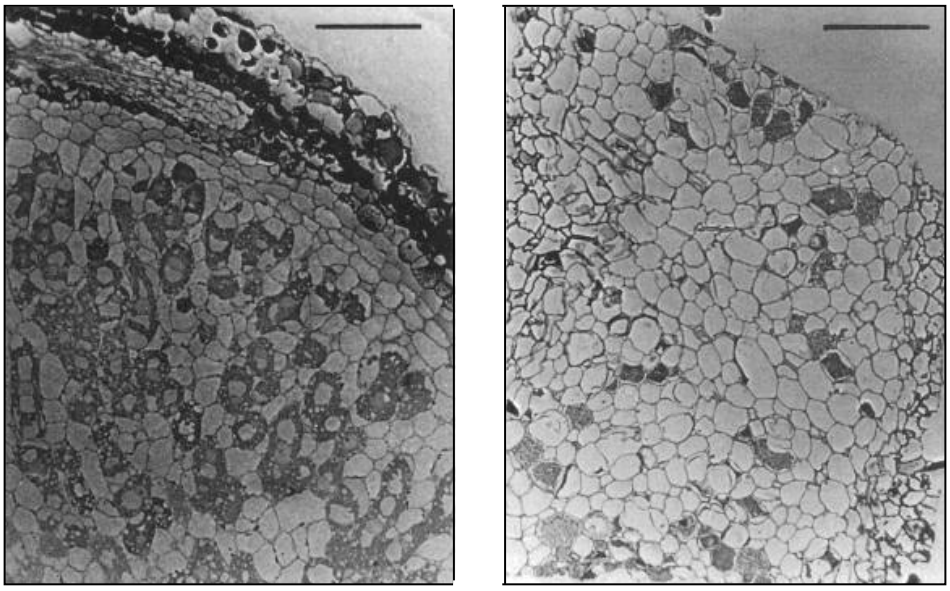

Figure 4. Light microscopy of 2 mm sections of *Acacia* root nodules elicited by wild-type GRH2 (A) and mutant GRH2-57 (B). Bars, 50 µm [López-Lara *et al*. (1995) Microbiology 141: 573-581].

- **Transmission electron microscopy applied to the study of nodule development**

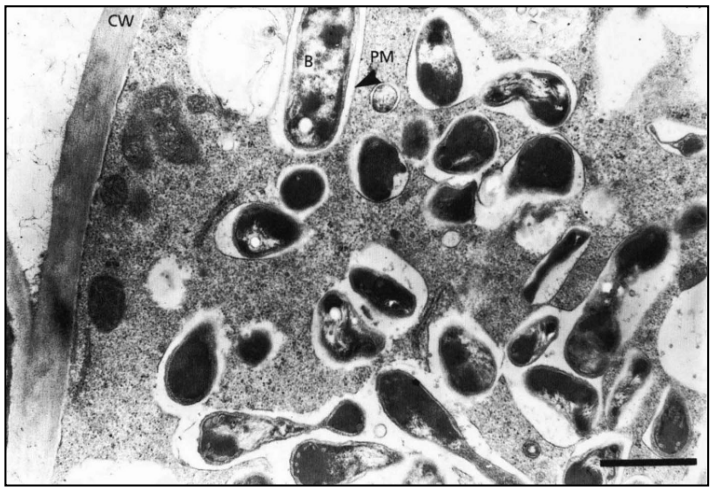

Figure 5. Transmission electron microscopy of a detailed infected cell in longitudinal sections of an effective root nodule of *Acacia cyanophylla* infected with wild type *Rhizobium* sp. (Acacia) strain GRH2. Note the numerous symbiosomes containing pleomorphic bacteroids surrounded by peribacteroid membranes. CW, cell wall; B, bacteroid; PM, peribacteroid membrane. Bar, 1 µm [López-Lara *et al*. (1995) Microbiology 141: 573-581].

Acknowledgements. This work has been supported by numerous research projects. Currently active projects include ERDF co-funded grants AGL2009-07925, P08-CVI-03549, CSD2009-0006 and BIO-2011-24401.

ANIMAL NUTRITION

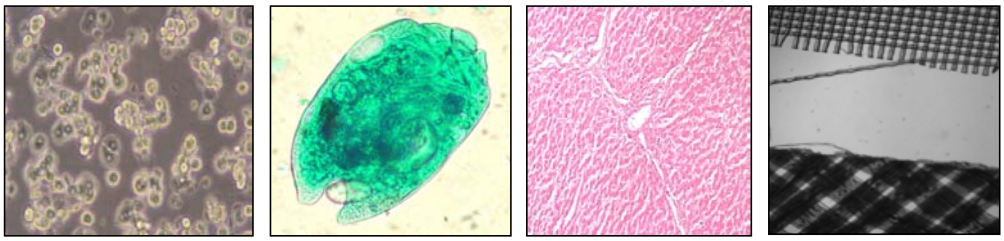

Microscopy use in ruminant nutrition

A Ignacio Martín García*, David R Yáñez Ruiz, Leticia Abecia Aliende, Ana Arco Pérez, Alejandro Muñoz Martínez and Eduarda Molina Alcaide

Institute of Animal Nutrition, Estación Experimental del Zaidín, CSIC, Camino del Jueves s/n, 18100 Armilla, Granada, Spain

*corresponding author: ignacio.martin@eez.csic.es

- **Rumen ciliate protozoa counting and identification**

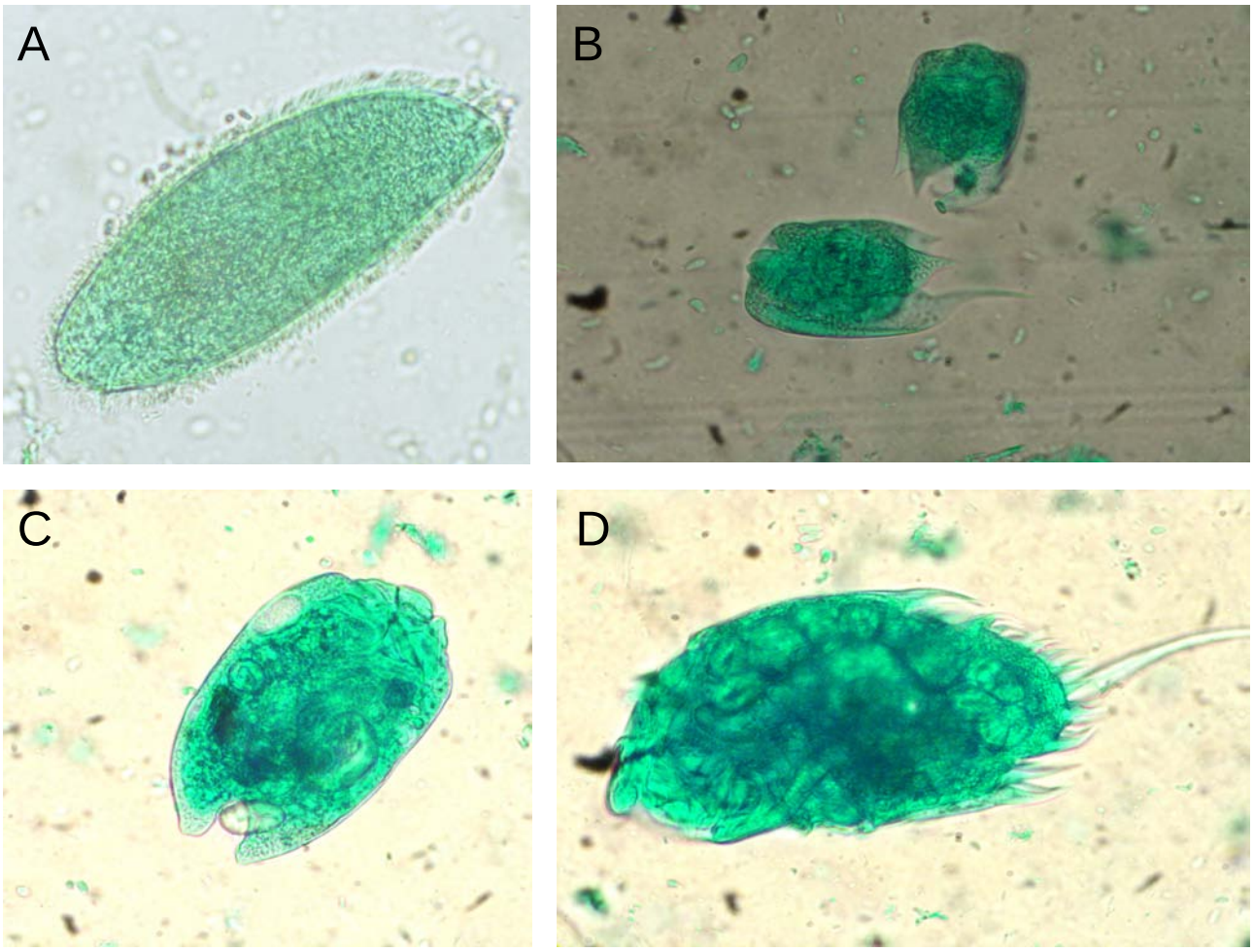

Figure 1. The identification and quantification of the numbers of rumen ciliate protozoa are conducted according to Dehority (2003, Nottingham Univ Press). Approximately 200 mL samples of rumen contents (liquid + solid) are collected manually, via rumen cannula, before the morning feeding. Then, 10 mL samples are fixed in equal volume of 18.5% formaldehyde solution, sealed and kept at room temperature. After thorough homogenization of each sample, one mL is pipetted using special wide aperture pipette and placed in a test tube. Then two drops of 2% of brilliant green solution are added and kept overnight at room temperature. Subsequent dilutions are made with 30% glycerol solution according to concentration of cell number in the sample. The following species are usually founded in the rumen of Murciano-Granadina goats: (A) *Isotricha prostoma*, (B) *Entodinium caudatum,* (C) *Diplodinium sp.* and (D) *Ophryoscolex caudatus.* The count in each sample is performed in 100 fields in Sedwidge-Rafter counting chamber in an optical microscope at magnification X 100, with eyepiece grid containing 0.5 mm^2.

- **Checking adequate tissues to be used in rumen *in situ* degradability studies**

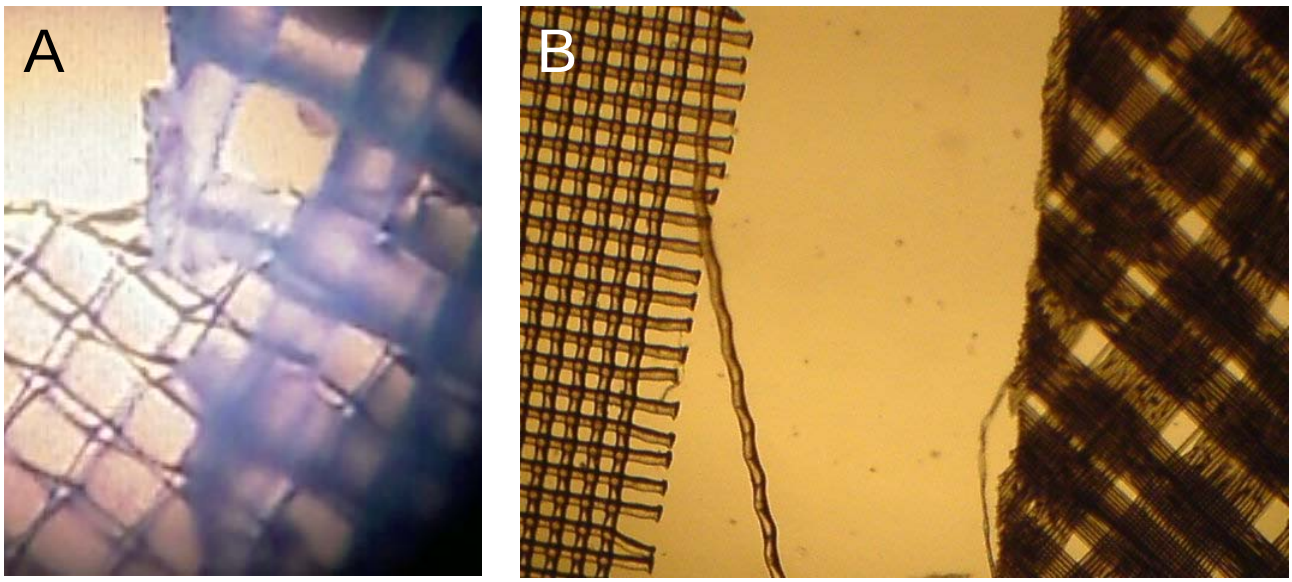

Figure 2. Different types of fabrics are used in our lab to study degradability of feeds in the rumen. (A) Standard nylon fabric for nylon bags elaboration. (B) Commercial *in situ* degradability bags from Ankom®. The choice of adequate microorganism-permeable tissues is of great importance depending on plant component and particle size to be studied.

Acknowledgements. This work has been supported by numerous research projects. Currently active projects include: AGL2011-27218, AGL2011- and FP7-SOLID, KBBE-266367.

Microscopy in primary culture of porcine hepatocytes and liver histology

Lucrecia González-Valero, José Miguel Rodríguez-López, María Luz Rojas-Cano, Aurelio Martín-Castro, Manuel Lachica and Ignacio Fernández-Fígares*

Institute of Animal Nutrition, Estación Experimental del Zaidín, CSIC, Camino del Jueves s/n, 18100 Armilla, Granada, Spain

*corresponding author: ignacio.fernandez-figares@eez.csic.es

- **Evolution over time of primary culture of porcine hepatocytes**

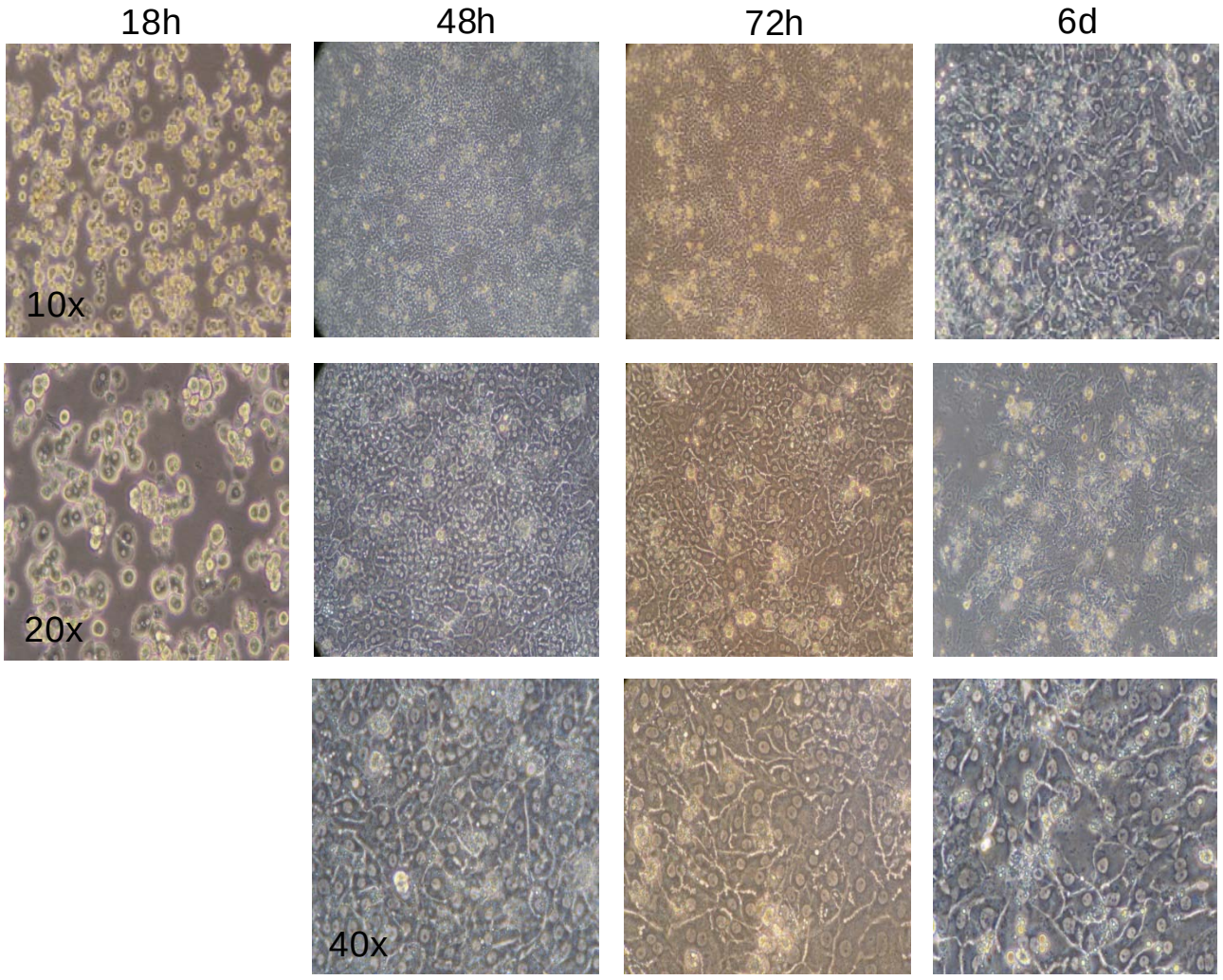

Figure 1. An inverted microscope is used at 10X, 20X or 40X to monitor the evolution of the culture over time. Hepatocytes culture is an *in vitro* technique, useful for the study of liver metabolism. Hepatocytes were isolated from young pigs by collagenase perfusion and seeded into collagen-coated T-25 flasks. Monolayers were established in medium containing fetal bovine serum for 1 day and switched to a serum-free medium for the remainder of the culture period [Fernández-Fígares *et al*. (2004) Domestic Animal Endocrinology 27: 125-140].

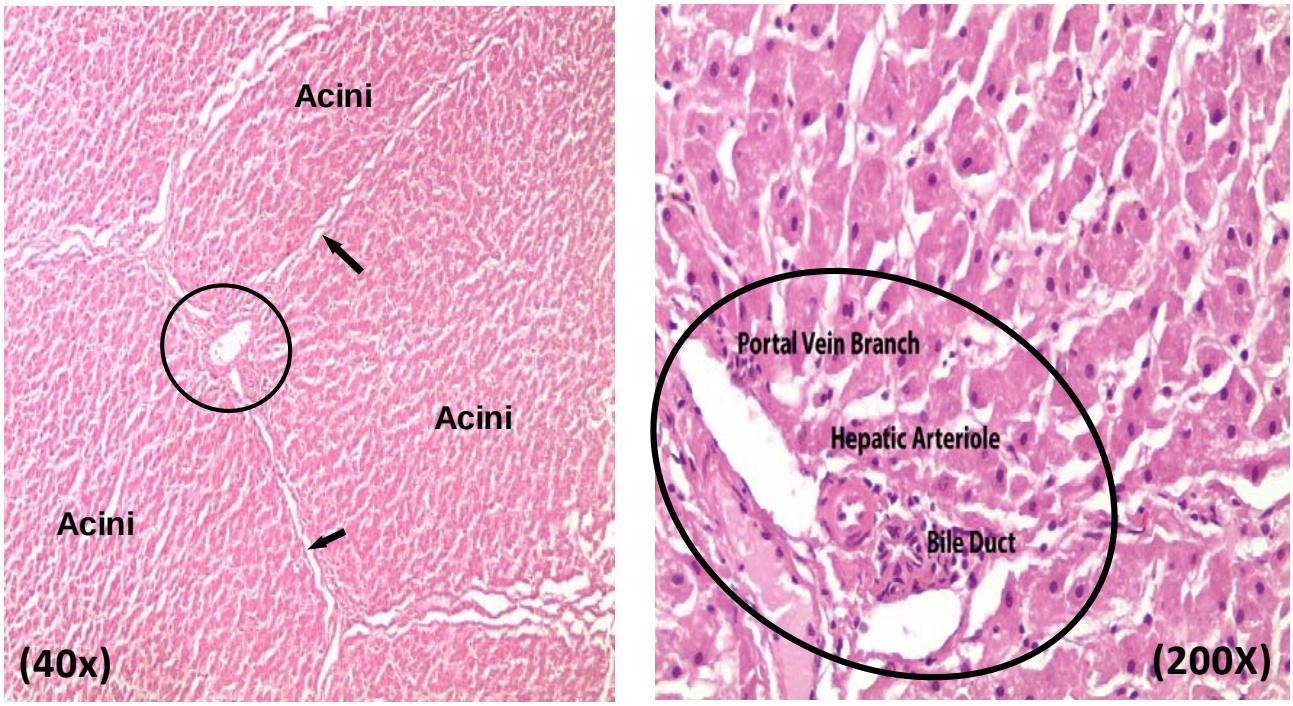

Figure 2. Photomicrographs of a histological section of the liver of pigs fed a diet supplemented with 1% of conjugated linoleic acid. The arrows show lack of widened conjunctive walls or fibrosis. The ovals mark a portal area containing the bile duct, the hepatic arteriole and the portal vein branch. Liver is divided histologically into 4 main lobules, which take the shape of irregular polygonal prisms also called acini. At the corners between adjacent lobules are the so-called portal areas. These are regions of connective tissue which include branches of the bile duct, the portal vein, and the hepatic artery. Along the central axis of each lobule runs a central vein, which is a branch of the hepatic vein. For histological analysis, the livers were thawed and cross sections of liver from each pig were excised and fixed in 10% buffered formalin fixative. After routine processing, livers were embedded in paraffin, sectioned at 5 mm and stained with haematoxylin-eosin and reticulin stain for optical examination. Micrographs of liver were taken at a final magnification of 40X or 200X using an optical microscope and a camera. In the histological study, we assessed the presence of steatosis, cytoplasmic vacuolization (glycogen or other causes) and architectural changes as fibrosis (increase in conjunctive tissue), inflammation (portal and/or lobular), necrotic or neoplastic changes and deposits (iron, bilirubin and glycogen). No anatomo-pathological changes were observed in livers of pigs fed conjugated linoleic acid compared to control pigs [Fernández-Fígares *et al*. (2012) Animal 6: 1058-1067].

Acknowledgements. This work has been supported by research projects AGL2006-05937 and AGL2009-08916.

ENVIRONMENTAL GEOCHEMISTRY

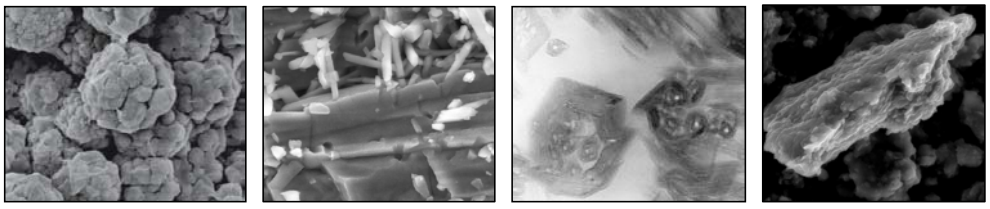

Electron microscopy in mineralogy and material science

F. Javier Huertas*, Javier Cuadros, Saverio Fiore, P. Ignacio Iriarte, Sandra de la Fuente, Marisa Rozalén, Chiara Cappelli, Peter C. Ryan, Francisco Huertas and José Linares

Department of Low Temperature Mineral Process, Instituto Andaluz de Ciencias de la Tierra, CSIC, Avda. de las Palmeras 4, 18100, Granada, Spain
Formerly Department of Environmental Geochemistry, Estación Experimental del Zaidín, CSIC, Profesor Albareda 1, 18008, Spain

*corresponding author: javier.huertas@eez.csic.es

- **Scanning electron microscopy (SEM) studies of alteration, genesis and evolution of natural and synthetic minerals**

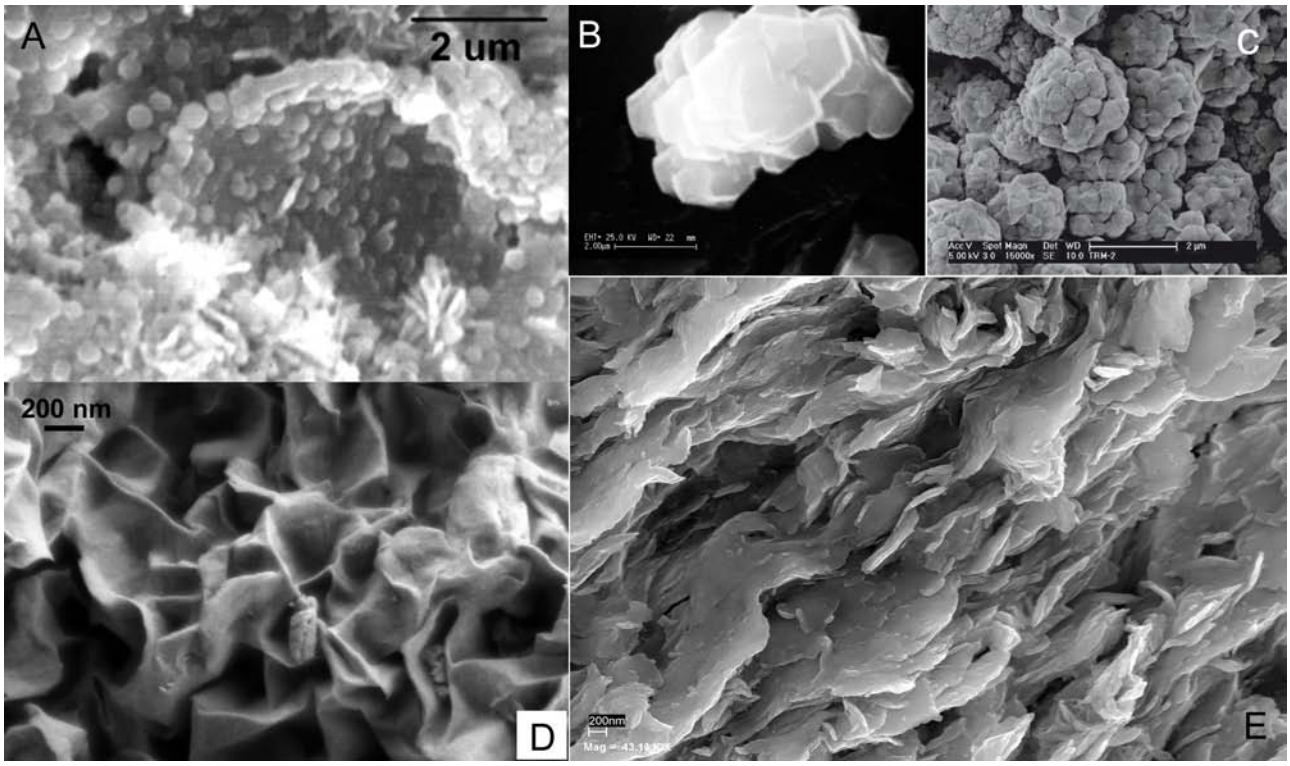

Figure 1. (A) Spherical kaolinite growing from the gel surface [Fiore *et al*. (1985) Clays Clay Min. 43: 353]. (B) Kaolinite crystals obtained by hydrothermal synthesis. (C) Kaolinite-smectite ball-like structures [Dudek *et al*. (2007) Am. Mineralog. 92: 179]. (D) High resolution image of a Fe-rich synthetic kaolinite [Iriarte *et al*. (2005) Clays Clay Min. 53: 1]. (E) High resolution image of smectite flakes after alkaline alteration.

- **Scanning electron microscopy (SEM) applied to asbestos and fibrous silicates studies**

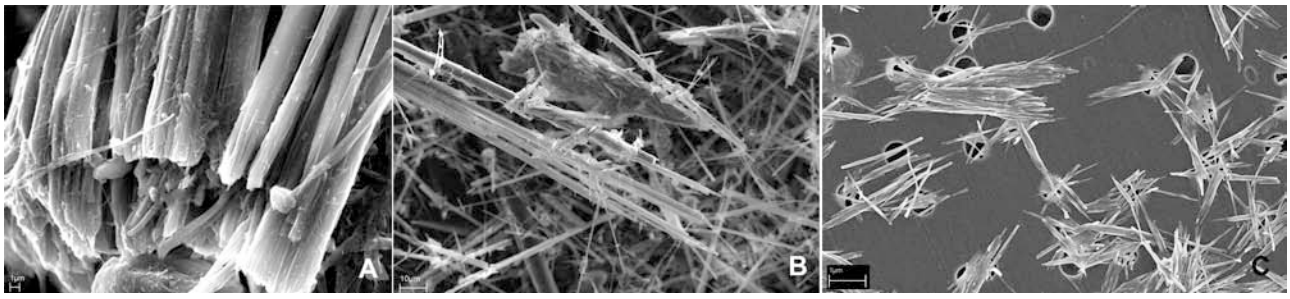

Figure 2. (A) Termination of a fiber bundle of antophylite asbestos (Goliamo Kameniane, Bulgaria). (B) Bundle of chrysotile asbestos (Mina Laurel, Ojén, Málaga). In both plates, see de presence of small fibers with a high length:diameter ratio, hazardous by inhalation. (C) Individual crystals of palygorskite.

- **Analytical electron microscope (AEM): TEM as a nanoprobe for nanominerals**

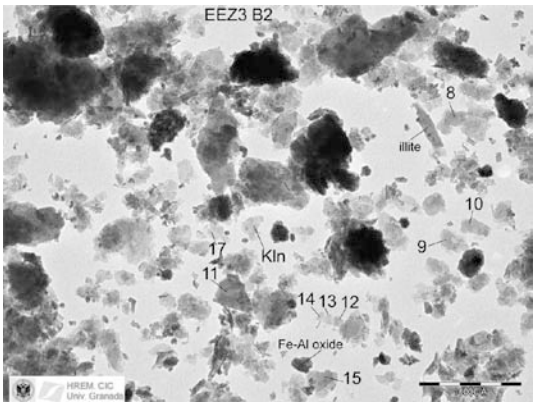

Figure 3. TEM images of single crystals—note platy morphology with some curled edges. Spot AEM compositional analyses are indicated by numerals and correspond to illite, kaolinite and Fe-Al oxy(hydroxi)des, and mixed layers kaolinite/smectite (K-S) with different ratio of K and S in soils of a terrace chronosequence in moist tropics of Costa Rica [values in Table 2, Ryan & Huertas (2009) Geoderma 151: 1]. The lone illite crystal in Qt2-B2 is likely aeolian in origin.

- **The structure and order-disorder in silicates by High resolution (HR)TEM**

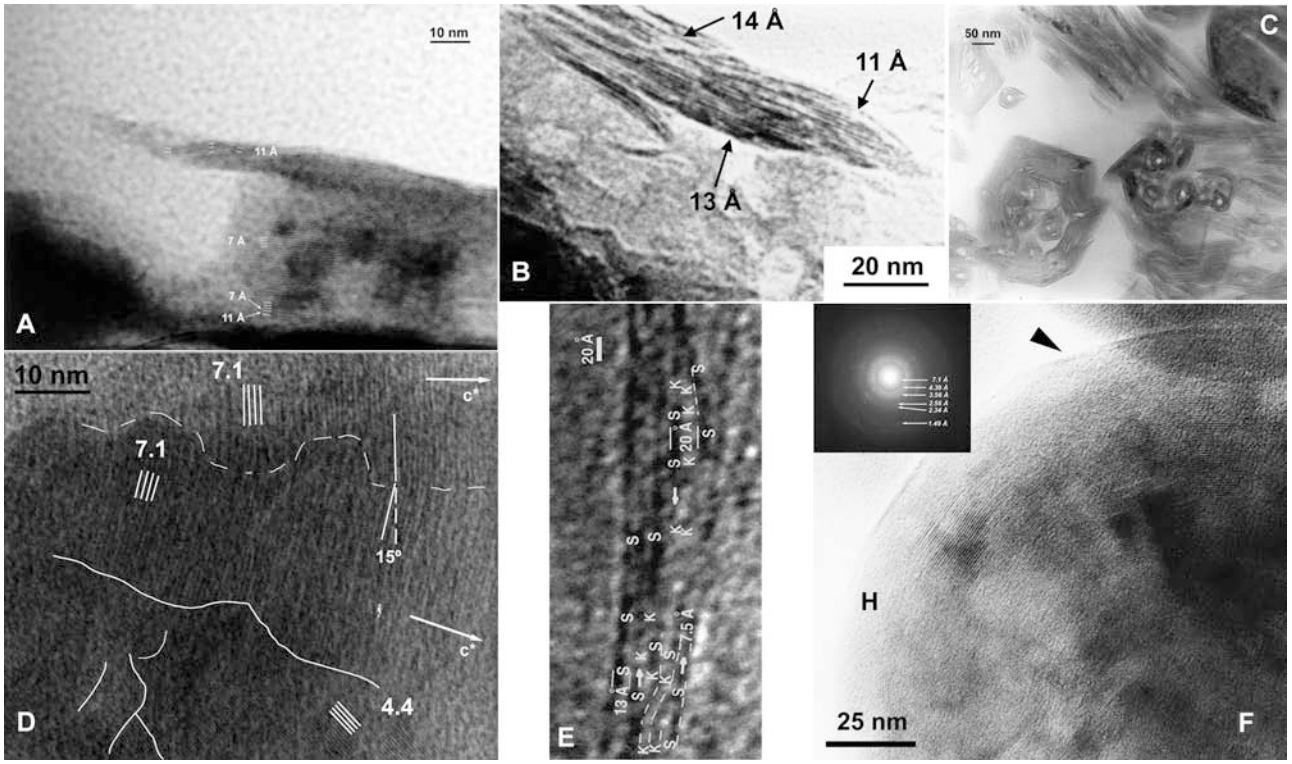

Figure 4. (A) Latice fringe image showing a kaolinite crystal (7 Å) and a smectite particle (11 Å) in contact with it; in lower part of the kaolinite crystal there is one smectite layer with a 11 Å spacing [Huertas *et al*. (2000) Am. J. Sci. 300: 504]. (B) Lattice fringe image of a smectite particle showing variable spacings. (C) Lattice fringe images of halloysite particles in pyroclastic deposits (Mt. Vulcano, Aeolian Islands, Italy). (D) Details of the joint of two radial crystals of kaolinite. The upper crystal shows (001) layers in direct contact with amorphous material. Several types of crystal joins are observed. The lower crystal shows fringes at 4.4 Å corresponding to (020) planes [Huertas *et al*. (2004) Clay Min. 39: 423]. (E) Lattice fringe images of representative interstratified kaolinite–smectites. The lateral transition from S to K is indicated by arrows. Note 20 Å spacing for KS packets and 27 Å spacing for KKS packets [Ryan & Huertas (2009) Geoderma 151: 1]. (F) Details of the internal structure of a spherical particle of kaolinite, showing radiating crystals with 7.1 Å spacing characteristic of (001) layers are elongated in the c* direction and arranged around a protocrystalline core (C) and covered by a smooth halo (H) The inset shows a SAED pattern of a spherical particle, exhibiting concentric halos with individual spots [Huertas *et al*. (2004) Clay Min. 39: 423].

Acknowledgements. This work has been supported by a number of research projects from EU, Ministries of Education, Science and Technology, Innovation and Economy and Competitiveness, and Junta de Andalucía, as contracts with ENRESA. Microscope observations were performed at University of Bari, CIC-University of Granada and IMAA-CNR.

Observation of the thermal decomposition of calcite by heating and the process of hydration in bentonites by environmental scanning electron microscopy (ESEM)

Concepción Jiménez de Cisneros* and Emilia Caballero

Department of Low Temperature Mineral Process. Instituto Andaluz de Ciencias de la Tierra, CSIC, Avda. de las Palmeras 4, 18100 Armilla Granada, Spain

Formerly Department of Environmental Geochemistry, Estación Experimental del Zaidín, CSIC, Profesor Albareda 1, 18008, Granada, Spain

*corresponding author: concepcion.cisneros@iact.ugr-csic.es

- **Thermal decomposition of calcite**

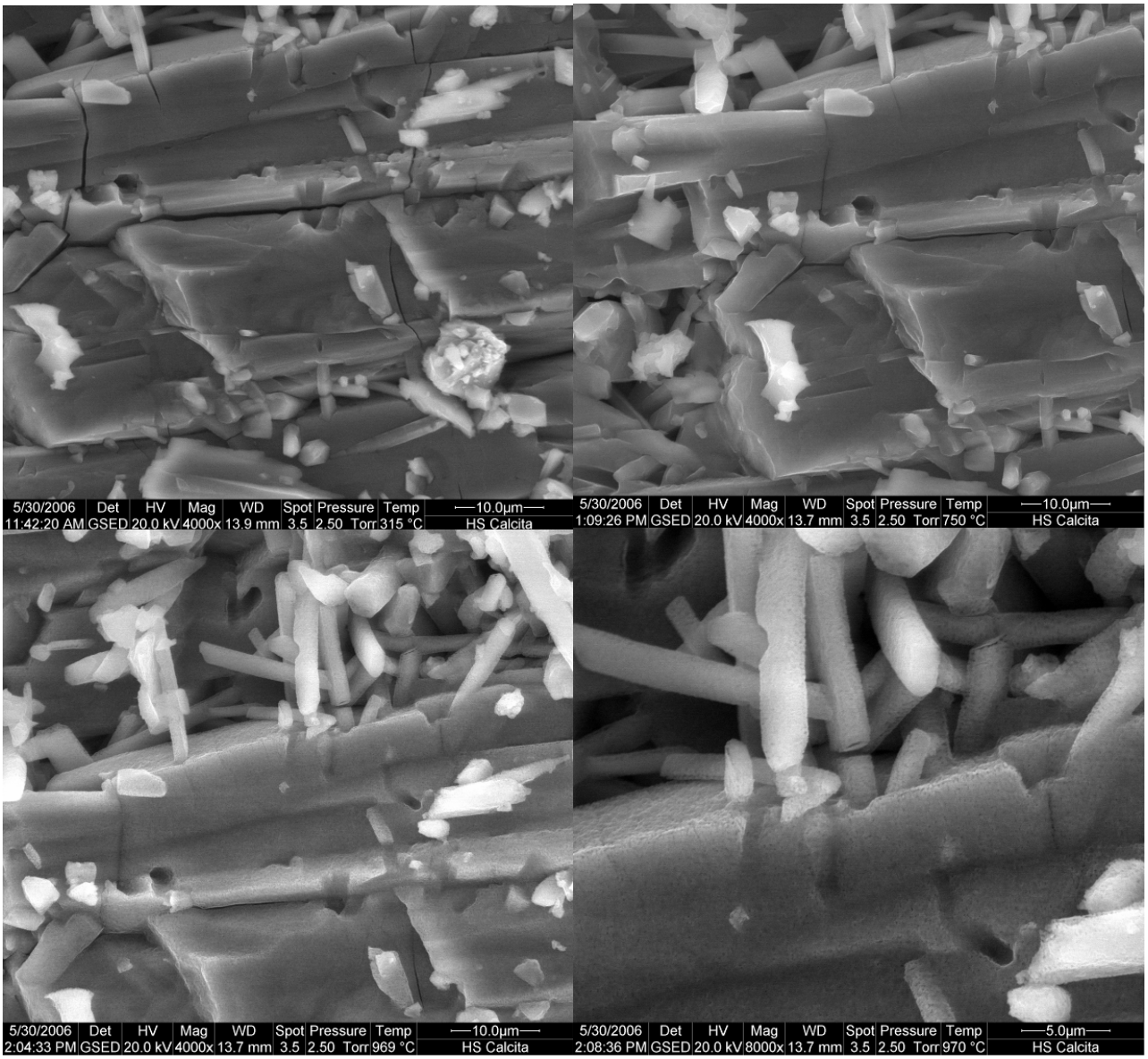

Figure 1. Environmental SEM sequences obtained by the heating process of carbonated samples.

- **Process of hydration in bentonites**

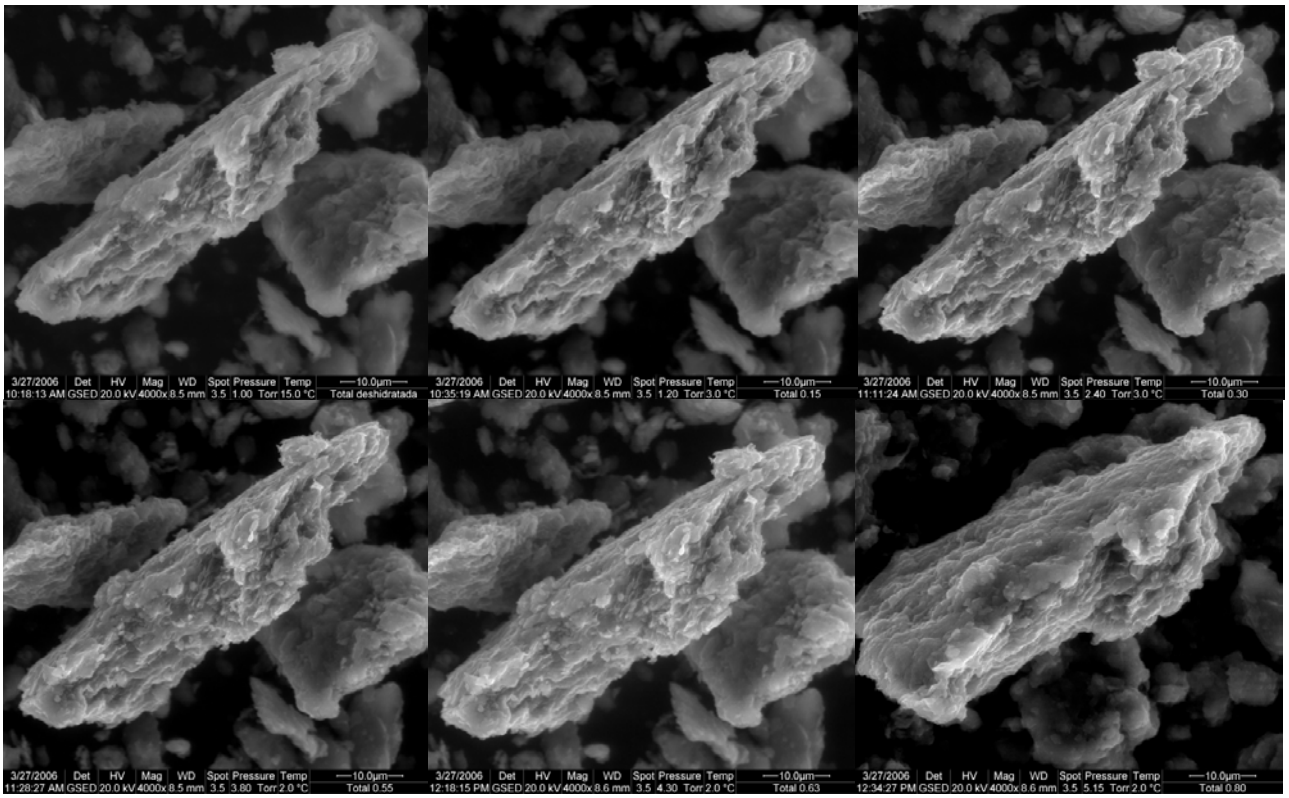

Figure 2. Bentonite hydration sequence observed by environmental SEM (upper panels, from left to right, dehydrated and relative humidities of 0.15 and 0.30, respectively; lower panels, from left to right, relative humidities of 0.55, 0.63 and 0.80, respectively).

Acknowledgements. This work has been supported by research projects CGL2004-01651 and CGL2007-61876.

PHOTOMICROGRAPHY CONTEST

1st Prize to the best scientific photomicrograph

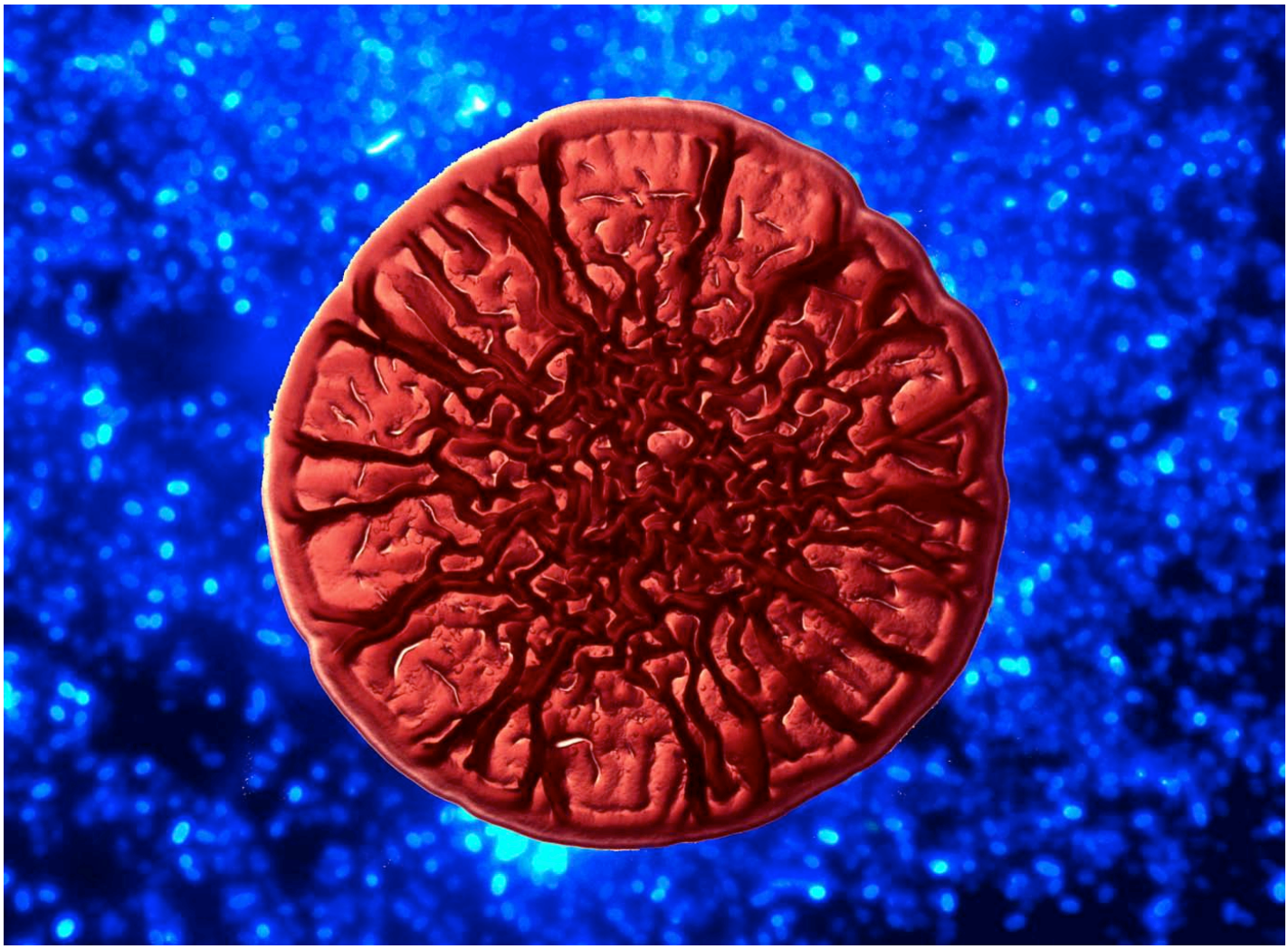

FORMAS Y COLORES

Altos niveles del segundo mensajero bacteriano di-GMP cíclico causan la sobre-producción de exopolisacáridos como la celulosa (imagen de fondo, microscopía de fluorescencia tras tinción con calcofluor). En *Pseudomonas*, esto da lugar a colonias con aspecto rugoso y mayor unión del colorante Rojo Congo (imagen frontal, tomada con un estereomicroscopio).

AUTORES: MARTA MARTÍNEZ-GIL, MARÍA ISABEL SORIANO, MARÍA ISABEL RAMOS-GONZÁLEZ Y MANUEL ESPINOSA-URGEL

2nd Prize to the best scientific photomicrograph

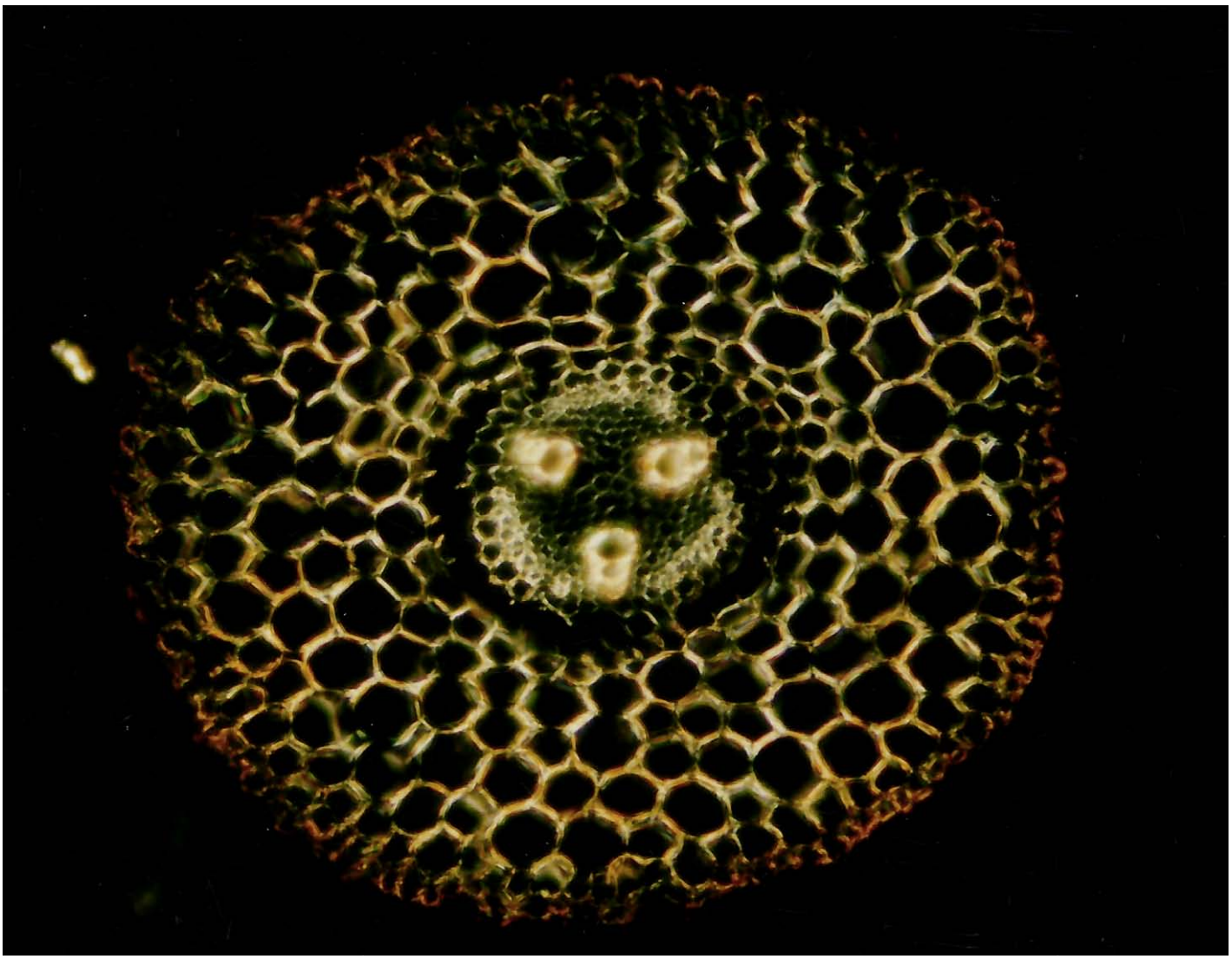

MANDALA TRIARCA

Visualización *in vivo* de pared celular en cortes transversales de raíz secundaria de guisante mediante microscopía óptica con luz polarizada

AUTORES: MARÍA RODRÍGUEZ SERRANO Y LUISA M. SANDALIO

3rd Prize to the best scientific photomicrograph

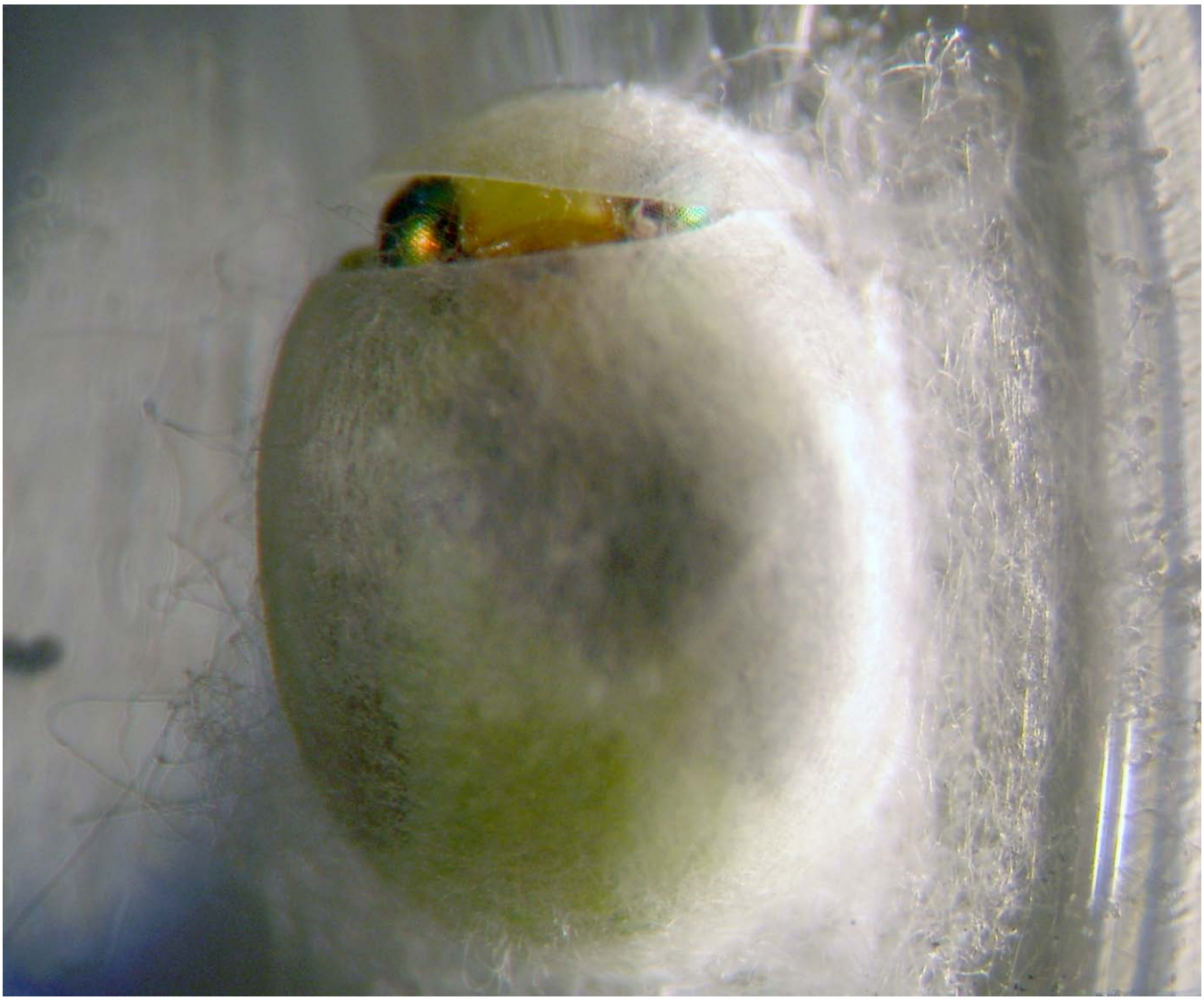

!HOLA!

En la imagen se muestra una adulto de crisopa (*Chrysoperla carnea*) en el momento en el que comienza a salir del capullo, en cuyo interior se produce la metamorfosis, es decir, la transformación de la larva en adulto. Para la realización de la fotografía se utilizó un estereomicroscopio Nikon SMZ7800 al que se le adaptó una cámara Nikon COOLPIX S520

AUTORES: MARÍA LUISA FERNÁNDEZ SIERRA

4th Prize to the best scientific photomicrograph

INFECTION OF ROOT PARASITIC PLANTS IN TOMATO

Infection initial phase of root parasitic plant *Phelipanche ramosa* in tomato observed with stereoscopic microscopy

AUTOR: ROCÍO TORRES VELA

Prize to the most original photomicrograph

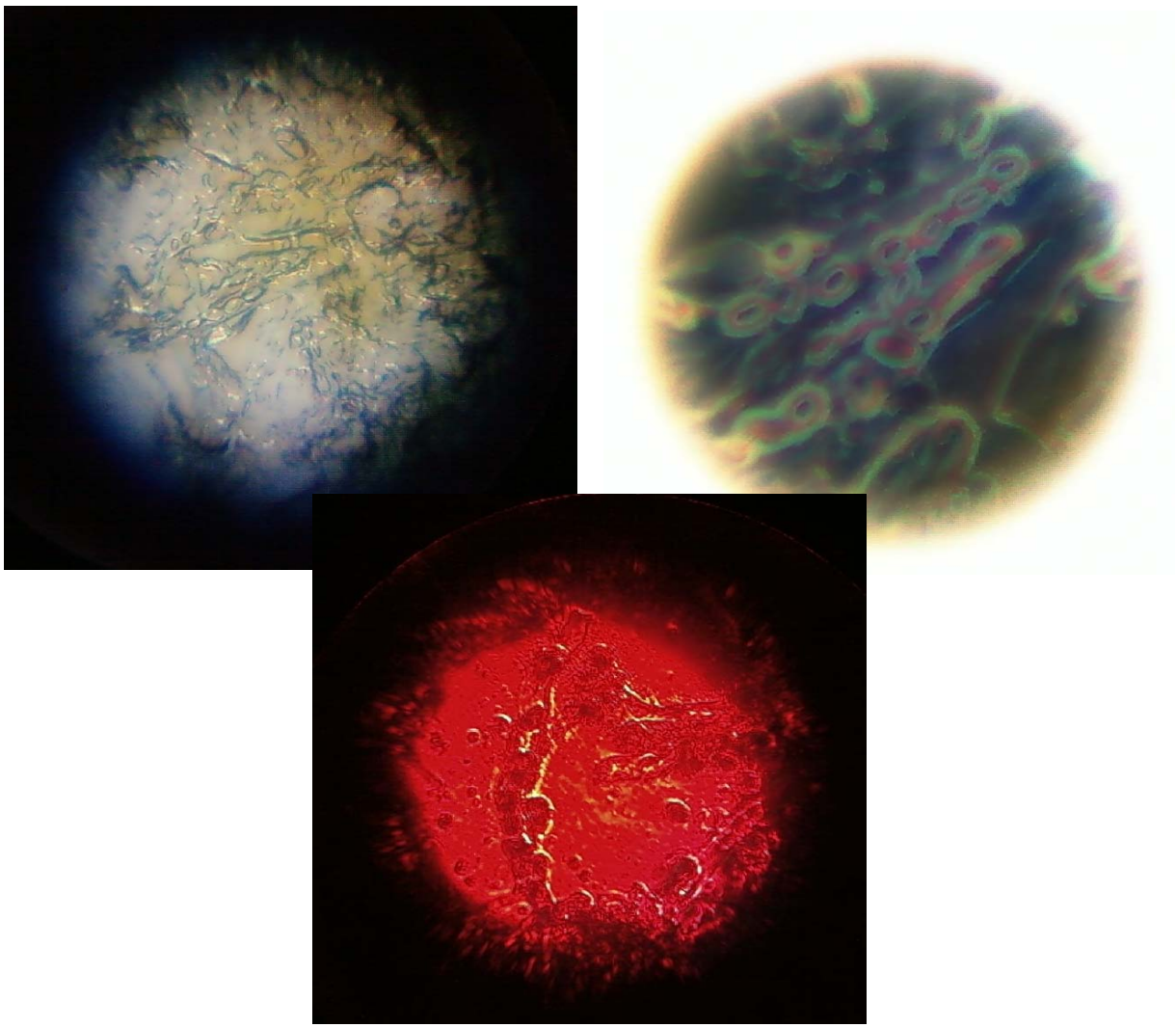

"ESPOROMOVIL"

Fotografías de esporas de *Morchella cónica* tomadas con la cámara de un móvil Samsung SGH -L760 de 2 megapíxeles a una resolución de 1600x1200 y 1280x960 sobre el ocular de un microscopio óptico escolar con luz a través de espejo modelo Vixen SE-800 (50X-800X). La primera foto (arriba, izq.) fue realizada con luz artificial blanca procedente de una lámpara de bajo consumo. La segunda (arriba, der.) corresponde a una imagen en negativo. La tercera (abajo) fue realizada con luz procedente de un LED rojo. Las muestras se colocaron sobre un portaobjeto de plástico transparente procedente de embalajes de juguetes.

AUTOR: PEDRO PALOMARES

Other contestant photomicrographs

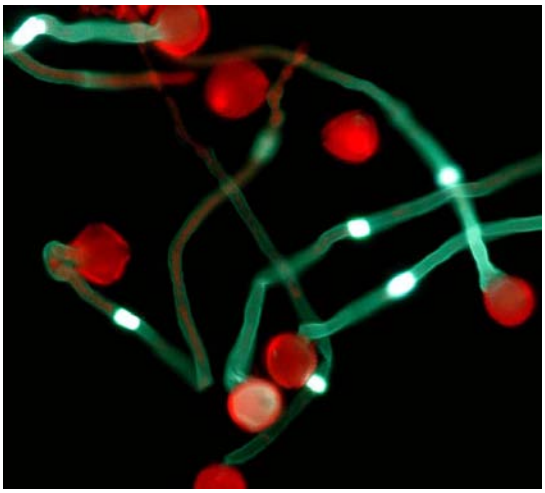

CEREZAS

Granos de polen de olivo germinando in vitro y teñidos con sirofluor: un fluorocromo específico para calosa (beta 1-3 glucanos). Microscopía de epifluorescencia. Luz de excitación azul. Captura con cámara Nikon doméstica a través de los oculares

AUTOR: Juan de Dios Alché

¿A QUÉ NO SABES DONDE TENGO MIS NÚCLEOS?

Granos de polen de olivo sobre la superficie del estigma. Tinción con DAPI. Microscopía de epifluorescencia. Captura digital con cámara analógica.

AUTOR: Juan de Dios Alché

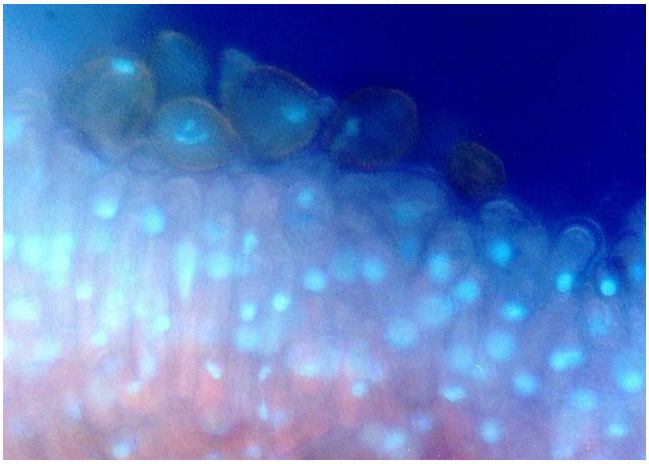

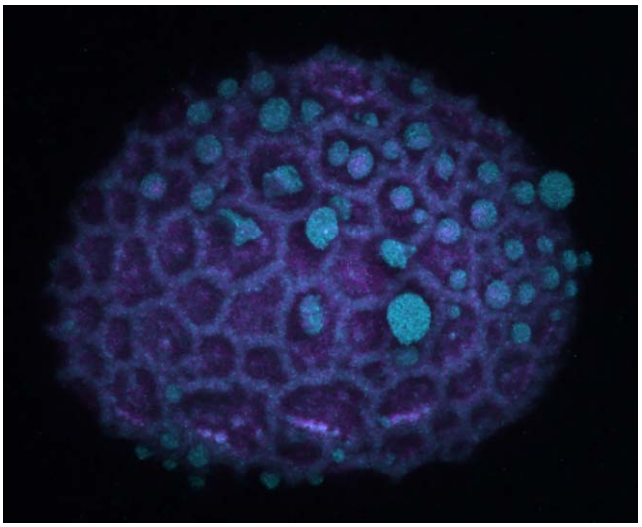

LO QUE NO SE VÉ EN LOS RAMOS DE NOVIA

Grano de polen de *Lilium*. Ornamentación de la pared y material del "pollen coat" observado con autofluorescencia a múltiples longitudes de onda. Microscopía confocal: proyección de un z-stack

AUTOR: Juan de Dios Alché

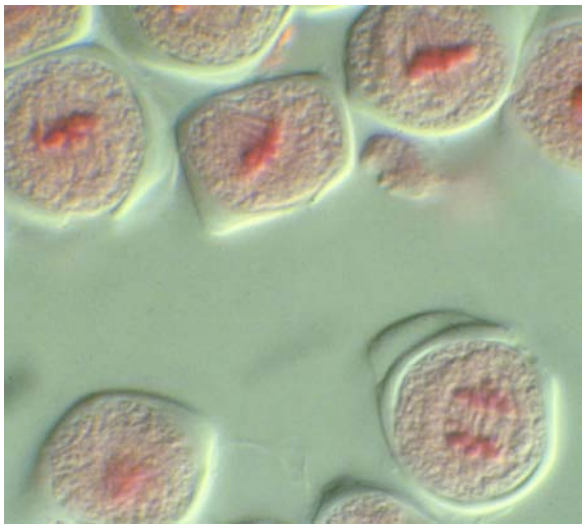

PASTELITOS DE OLIVO

Células madres de polen de olivo durante la primera división meiótica. Estadios de metafase I-anafase. Microscopía de campo claro con contraste interferencial diferencial (DIC). Tinción con orceína acética. Captura con cámara analógica.

AUTOR: Juan de Dios Alché

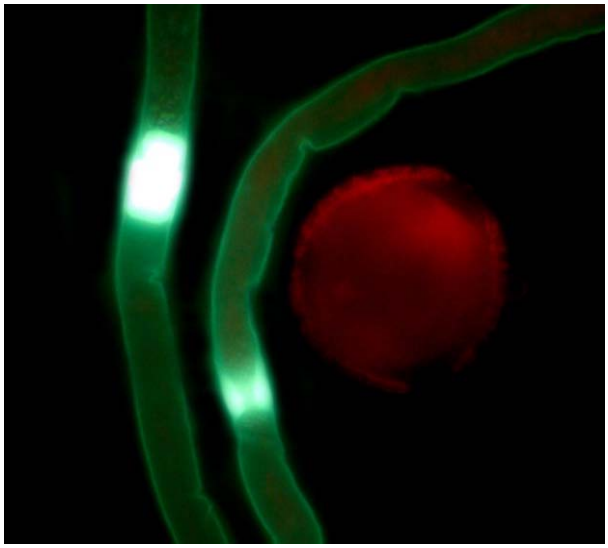

CEREZAS

Granos de polen de olivo germinando *in vitro* y teñidos con sirofluor: un fluorocromo específico para calosa. Microscopía de epifluorescencia. Luz de excitación azul. Captura con cámara Nikon doméstica a través de los oculares

AUTOR: Juan de Dios Alché

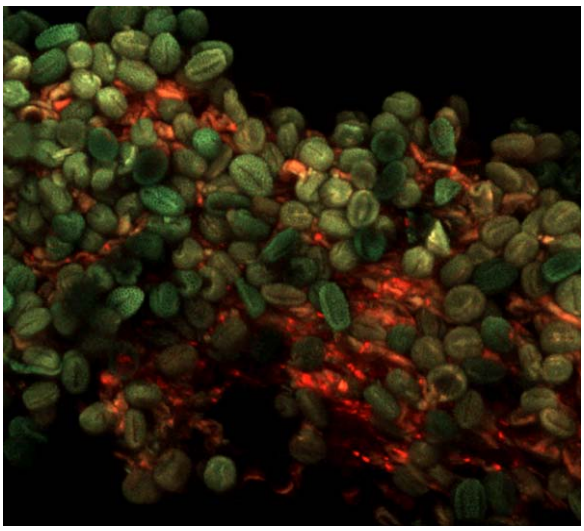

A POR UNA BUENA COSECHA

Granos de polen de olivo sobre la superficie estigmática. Marcado de ROS y NO. Microscopía confocal: proyección de un z-stack

AUTORES: Dori Zafra & Juan de Dios Alché

PASTELITOS DE OLIVO

Células madres de polen de olivo durante la primera división meiótica. Estadios de metafase I-anafase. Microscopía de campo claro con contraste interferencial diferencial (DIC). Tinción con orceína acética. Captura con cámara analógica.

AUTOR: Juan de Dios Alché

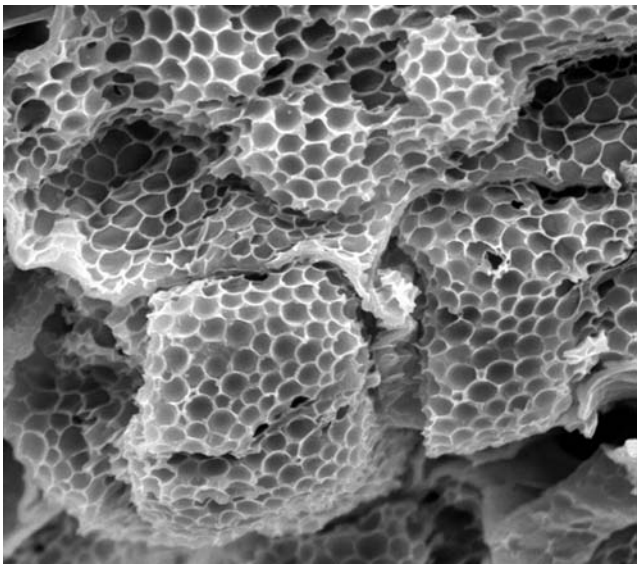

RICO PANAL DE MIEL

Semilla de olivo. Microscopía electrónica de barrido

AUTORES: José Carlos Jiménez, María Isabel Rodríguez García & Juan de Dios Alché

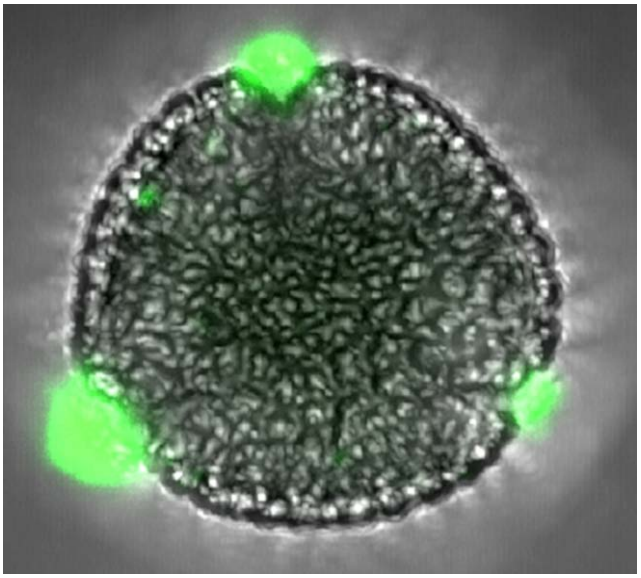

¡OS VAIS A ENTERAR!

Grano de polen de olivo. Inmunolocalización de proteínas alergénicas (señal verde) durante su elución al medio de cultivo a través de las aperturas. Anticuerpo secundario marcado con DyLight 488. Microscopía confocal: sección óptica y luz transmitida.

AUTORES: Sonia Morales & Juan de Dios Alché

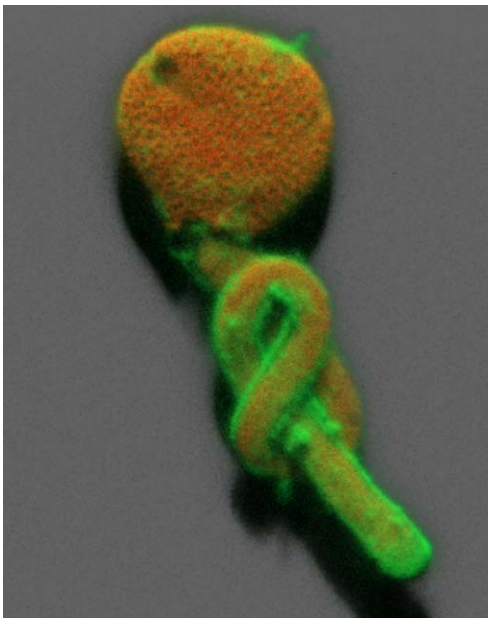

¡REALMENTE ME HE HECHO UN LÍO!

Grano de polen de olivo germinando *in vitro.* Inmunolocalización de AGPs con un anticuerpo primario y un anticuerpo secundario conjugado con Alexa-488. Microscopía confocal: proyección de un z-stack y sombreado 3-D con Imaris

AUTORES: Cynthia Suárez & Juan de Dios Alché

PASTELITOS DE OLIVO

Tétradas de microsporas de olivo. Microscopía de campo claro con contraste interferencial diferencial (DIC). Tinción con orceína acética. Captura con cámara analógica

AUTOR: Juan de Dios Alché

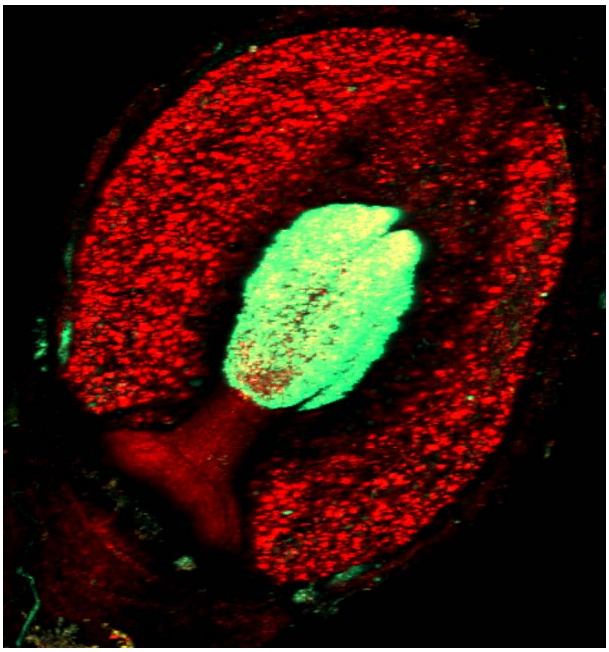

¡A VER QUIEN ME ATACA DE ESTA GUISA!

Flor de olivo marcada para la detección de ROS. La intensa señal verde sobre el estigma probable-mente corresponde a acumulación de ROS con fines defensivos frente a hongos y bacterias. Mi-croscopía confocal: proyección de un z-stack

AUTORES: Dori Zafra & Juan de Dios Alché

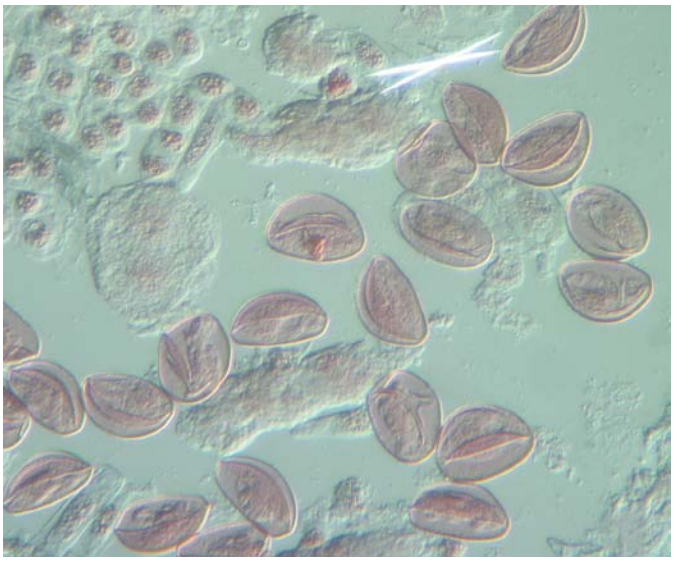

SUAVE QUE ME ESTÁS MATANDO

Granos de polen de ciprés. Microscopía de campo claro con contraste interferencial diferencial (DIC). Tinción con orceína acética. Captura con cámara analógica.

AUTOR: Juan de Dios Alché

Y YO CON ESTOS PELOS...

Sección transversal de hoja mostrando la distribución del aparato fotosintético (cloroplastos en azul, haces vasculares en verde). Autofluorescencia (excitación 488) y luz transmitida. Microscopía confocal: proyección de un z-stack

AUTOR: Juan de Dios Alché

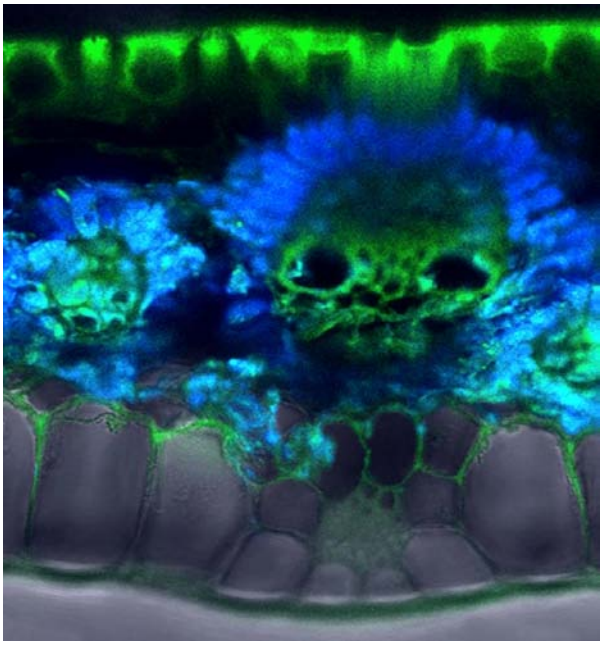

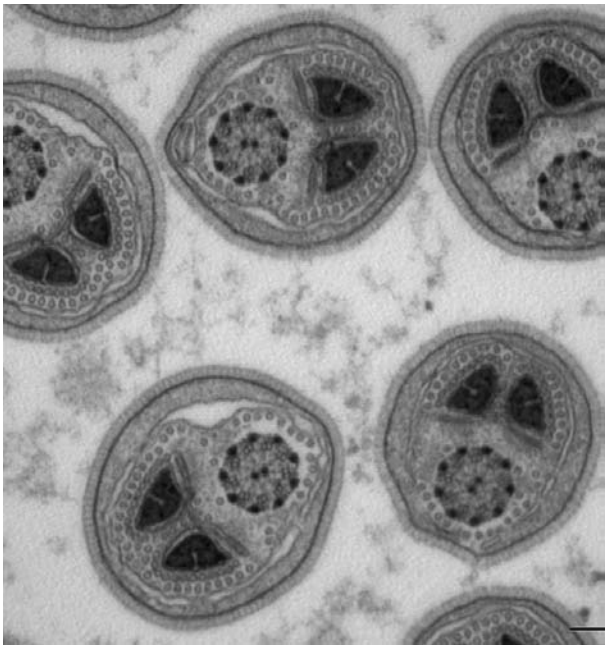

EL GRITO DEL HOMÚNCULO...

En los siglos XVII y XVIII, los preformacionistas creyeron ver un hombre en miniatura en los espermatozoides humanos, al que denominaron "homúnculo". La fotografía fue realizada con un microscopio electrónico de transmisión JEOL TEM-1011, y muestra varias secciones transversales correspondientes a la pieza media de espermátidas del saltamontes *Eyprepocnemis plorans*

AUTORES: Juan Pedro Martínez Camacho & Juan de Dios Alché

¡Y NO ES SIERRA NEVADA!

Flor de olivo. La intensa señal verde sobre el estigma corresponde a acumulación de NO. Microscopía confocal: proyección de un z-stack

AUTORES: Dori Zafra & Juande Alché

BURBUJAS

Cuerpos lipídicos aislados de semillas de olivo teñidos con el rojo Nilo. Microscopía de epifluorescencia. Luz de excitación azul.

AUTOR: Agnieszka Zienkiewicz

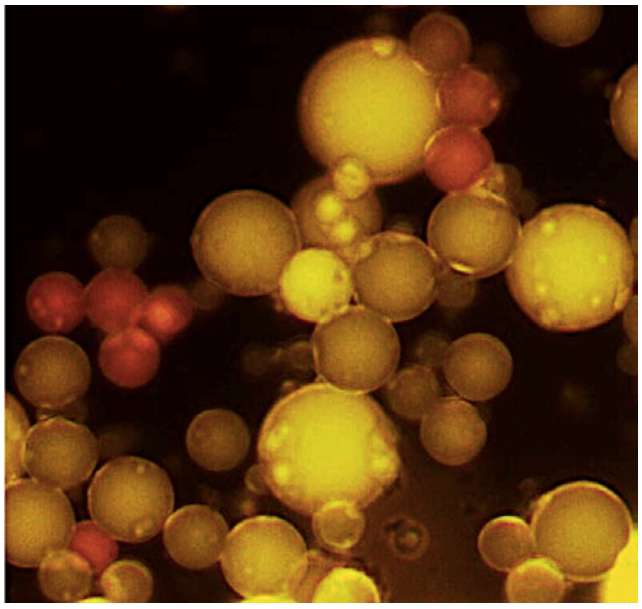

¡CON LO A GUSTITO QUE ESTÁBAMOS EN EL AGUA!

Algas verdes de las lagunas de Sierra Nevada. Microscopía electrónica de transmisión, microscopio JEOL 1011

AUTORES: Pedro Sánchez & Juan de Dios Alché

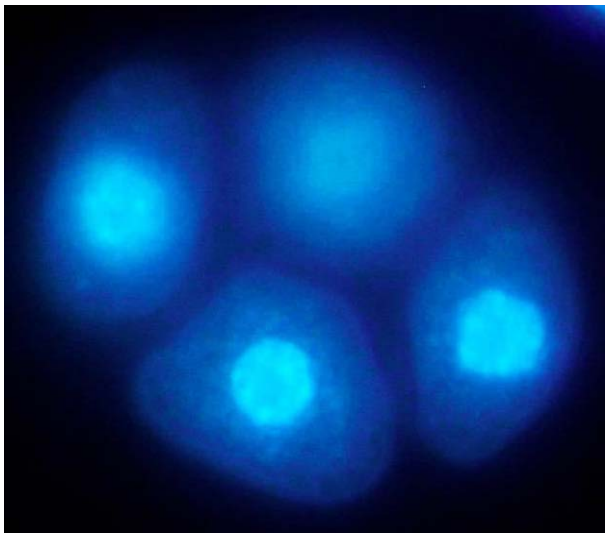

LOS OJOS AZULES

Polen de olivo en estadio de tetrada. Los núcleos teñidos con DAPI. Microscopía de epifluorescencia. Luz de excitación ultravioleta.

AUTOR: Agnieszka Zienkiewicz

¿DÓNDE ESTÁN ESOS ALÉRGENOS?

Grano de polen de olivo. Doble marcado inmunocitoquímico de proteínas alergénicas con partículas de oro de dos tamaños diferentes. Las proteínas alergénicas se acumulan en cisternas del retículo endoplásmico. Microscopía Electrónica de Transmisión, microscopio JEOL 1011

AUTORES: Sonia Morales & Juan de Dios Alché

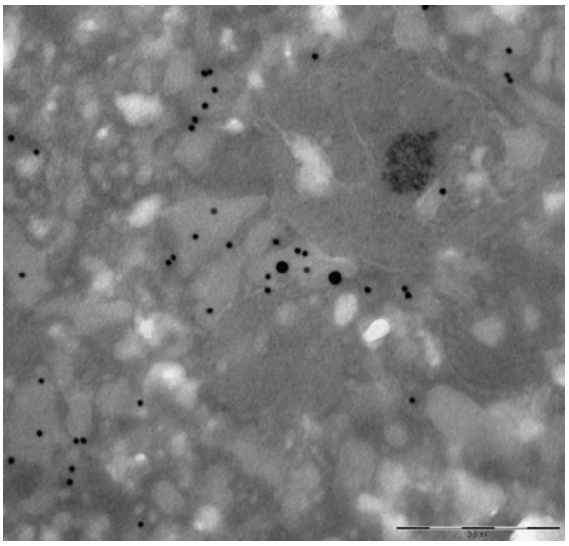

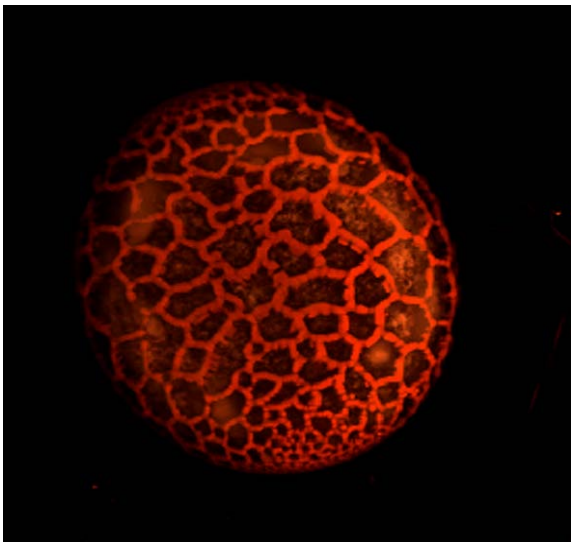

¿MARTE O POLLEN DE LILIUM?

Grano de polen de *Lilium*. Autofluorescencia (excitación 546 nm) Microscopía confocal: projección de un z-stack

AUTOR: Krzysztof Zienkiewicz

LOS DEDITOS

Papilas de *Hyacinthus orientalis*. Los núcleos teñidos con DAPI. Microscopía de epifluorescencia

AUTOR: Agnieszka Zienkiewicz

GEOMETRÍA PEROXISOMAL

Micrografías de frutos de pimiento en las que destaca la estructura interna de los cuerpos cristalinos de los peroxisomas- Microscopía electrónica de transmisión (TEM)

AUTOR: José Manuel Palma

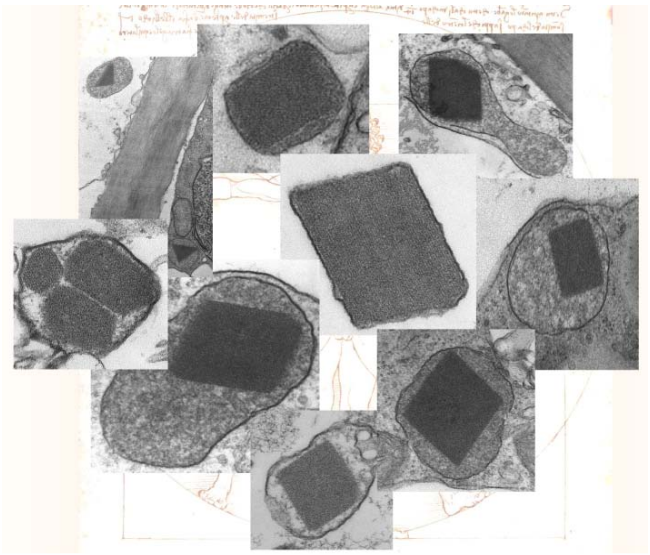

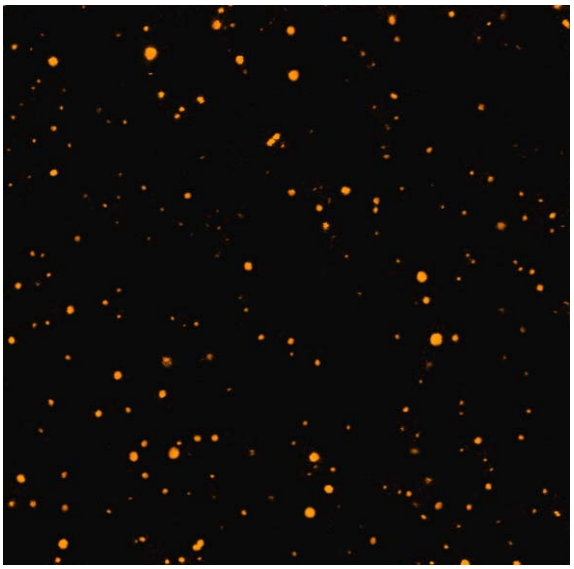

CIELO ESTRELLADO

Cuerpos lipídicos aislados de polen maduro de olivo. Microscopía de fluorescencia. Tinción con rojo Nilo.

AUTORES: Krzysztof Zienkiewicz & Antonio J. Castro

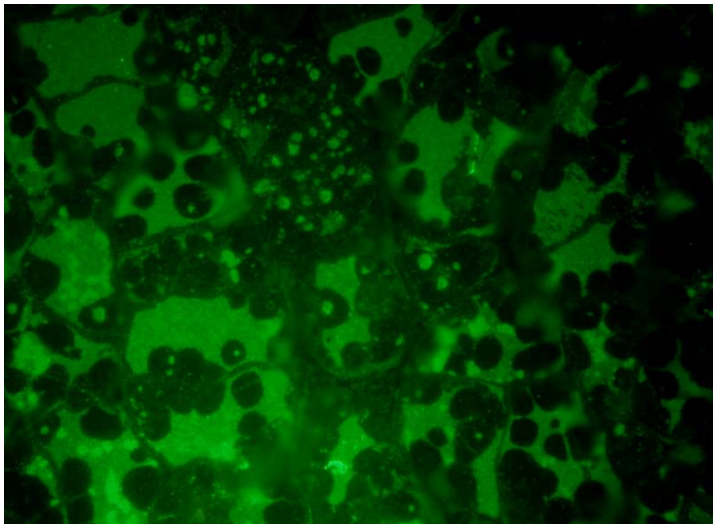

GRUYERE

Immunolocalization of the 11S-type globulins in olive cotyledons during *in vitro* seed germination. Epifluorescence Microscopy

AUTOR: José Carlos Jiménez López

¡QUE TE PILLO!

Tubo polínico de olivo en el que se observan los dos núcleos espermáticos y el núcleo vegetativo. Microscopía de fluorescencia. Tinción con DAPI.

AUTOR: Antonio J. Castro

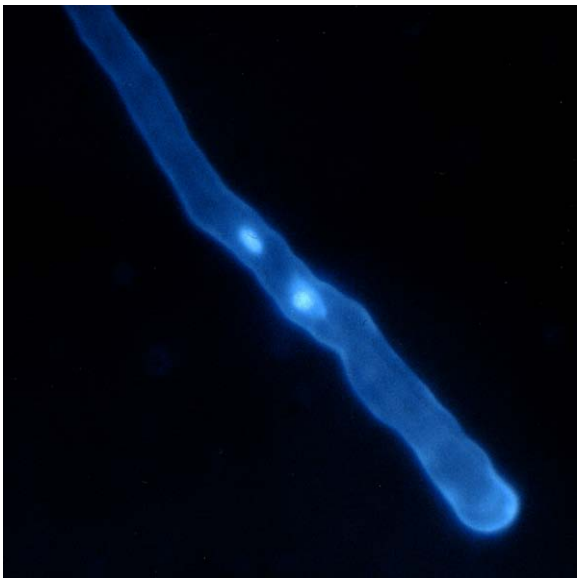

POLINIZANDO

Flor de olivo en plena polinización en la que se observan los granos de polen sobre el estigma. Estereomicroscopía.

AUTORES: Juan David Rejón & Antonio J. Castro

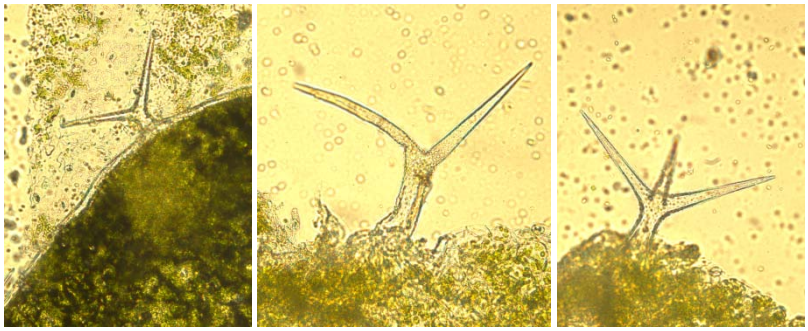

TRICOMA

Microscopio invertido de epifluorescencia

AUTORES: Carmelo Ruiz & Marina Leterrier

NO TE CORTES NI UN PELO

Cuchilla de diamante para la obtención de cortes histológicos y detalle del filo. Fotografía obtenida en un estereomicroscopio Leica M165FC

AUTORES: Alicia Rodríguez & Mª Carmen Perálvarez

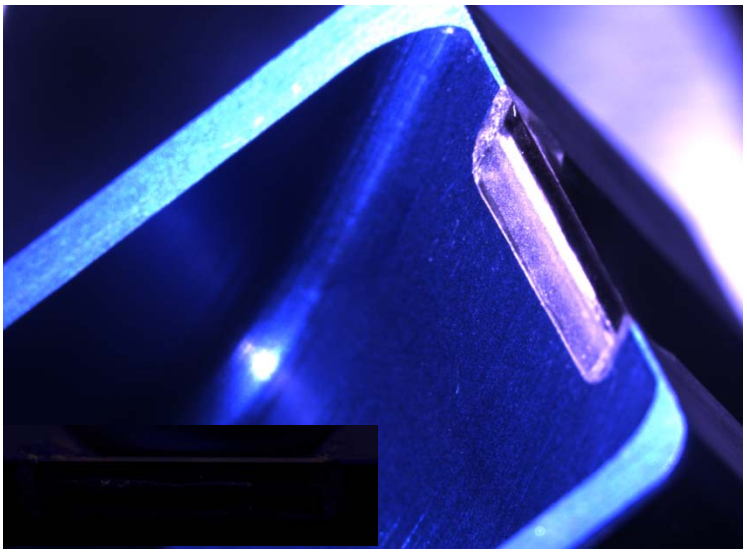

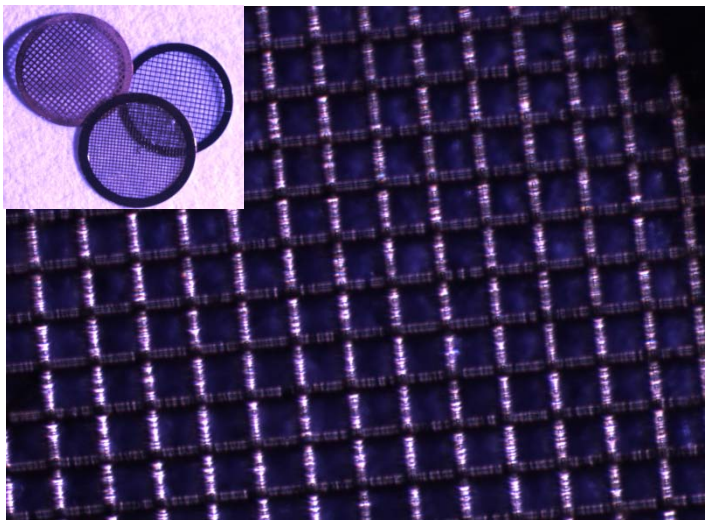

A LA PARRILLA SALEN MEJOR

Rejillas de 3.05 mm de diversos materiales (Cu, Ni, Au) para microscopía electrónica de transmisión. Fotomicrografías obtenidas en un estereomicroscopio Leica M165FC

AUTORES: Alicia Rodríguez & Mª Carmen Perálvarez

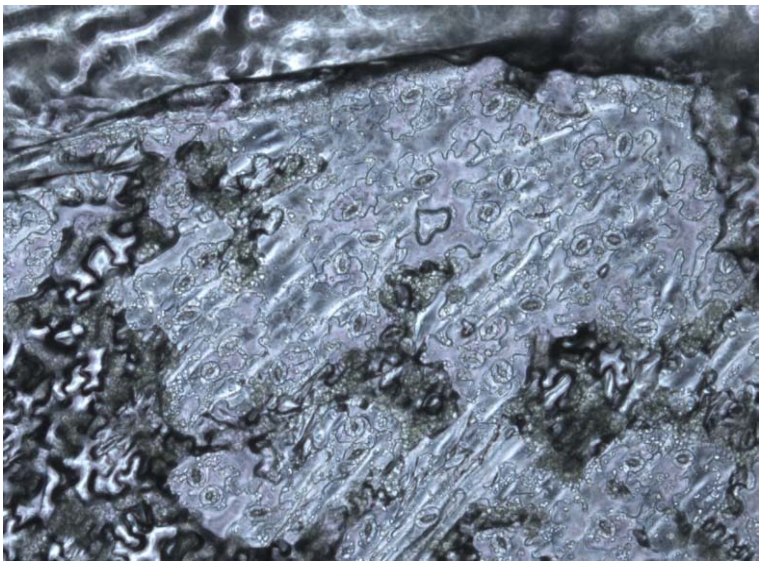

CREPÚSCULO

Estomas. Microscopio invertido de epifluorescencia

AUTORES: Carmelo Ruiz & Marina Leterrier

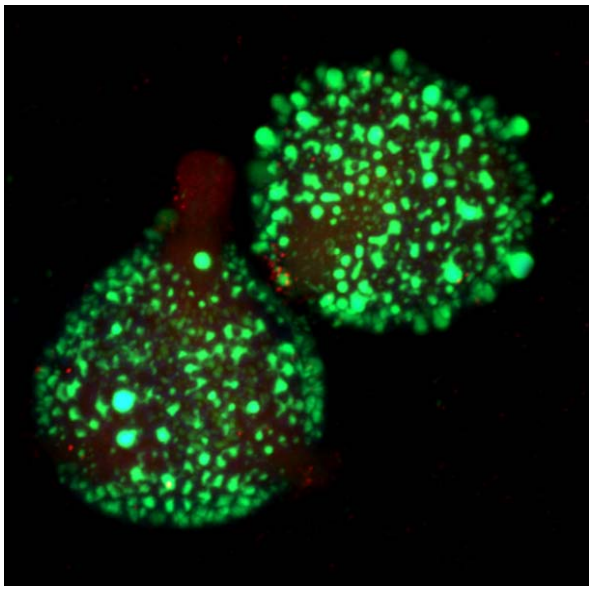

PSICODÉLICO

Polen maduro de olivo. Detección de lípidos y caleosina. Microscopía confo-cal. Tinción con rojo Nilo.

AUTORES: Krzysztof Zienkiewicz & Antonio J. Castro

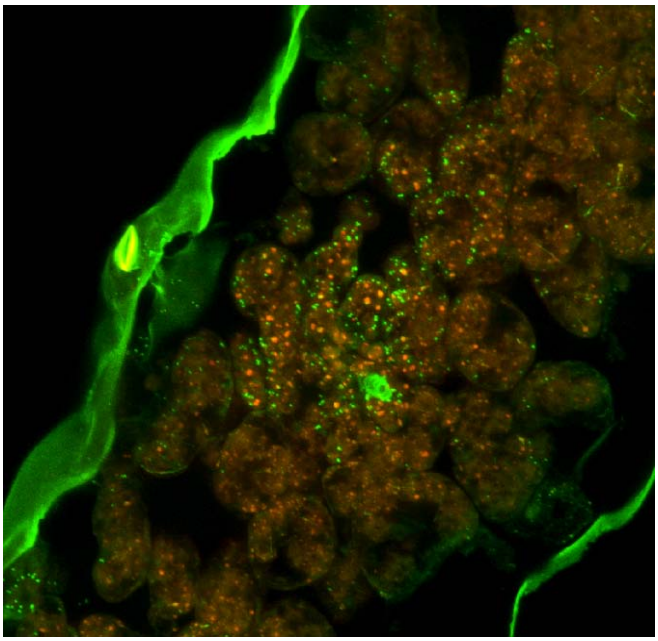

CONSTELACIÓN TISULAR

Visualización in vivo de la producción de radicales superóxido (O2.-) en sección transversal de hoja utilizando dihidroetidio y microscopía láser confocal

AUTORES: Diana M. Pazmiño, Nieves de la Casa & Luisa M. Sandali

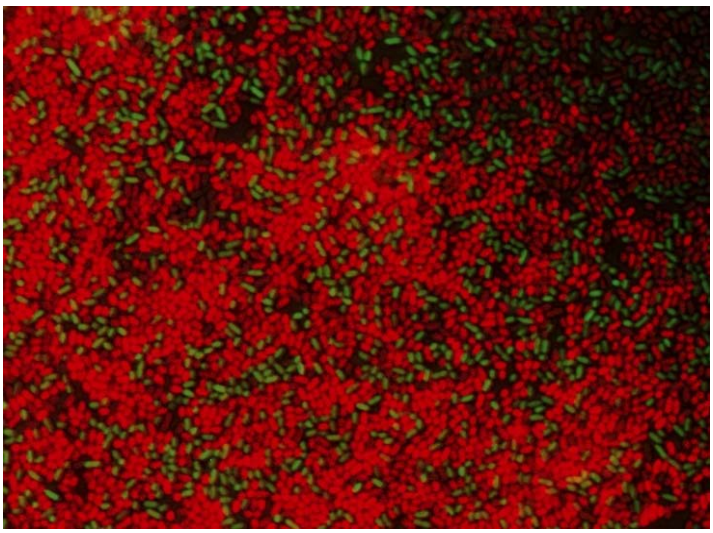

PUNTILLISMO BACTERIANO

Biofilm mixto de dos cepas de *Pseudomonas putida* marcadas con dsRed y gfp. La cepa silvestre (rojo) puede formar microcolonias mientras que un mutante deficiente en la adhesina LapF (verde), sólo puede asociarse al biofilm de la cepa silvestre. Superposición de imágenes de fluorescencia obtenidas con un microscopio Zeiss Axioscope

AUTORES: Marta Martínez-Gil, María Isabel Soriano & Manuel Espinosa-Urgel

DEPREDACIÓN

En la imagen se muestra una larva de crisopa (*Chrysoperla carnea*) depredando una pupa de mosca del olivo (*Bactrocera oleae*). Para la realización de la fotografía se ha empleado un estereomicroscopio Nikon SMZ7800 al que se le ha adaptado una cámara Nikon COOLPIX S520

AUTOR: M. Luisa Fernández Sierra

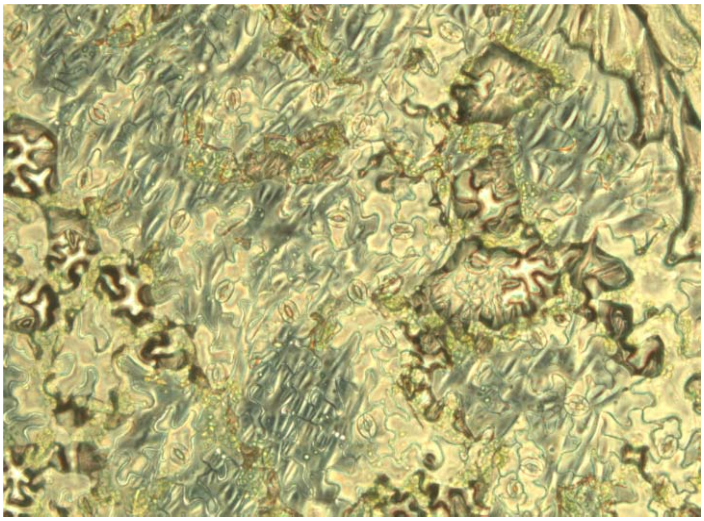

ESTOMA-R

Estomas. Microscopio invertido de epi-fluorescencia

AUTORES: Carmelo Ruiz & Marina Leterrier

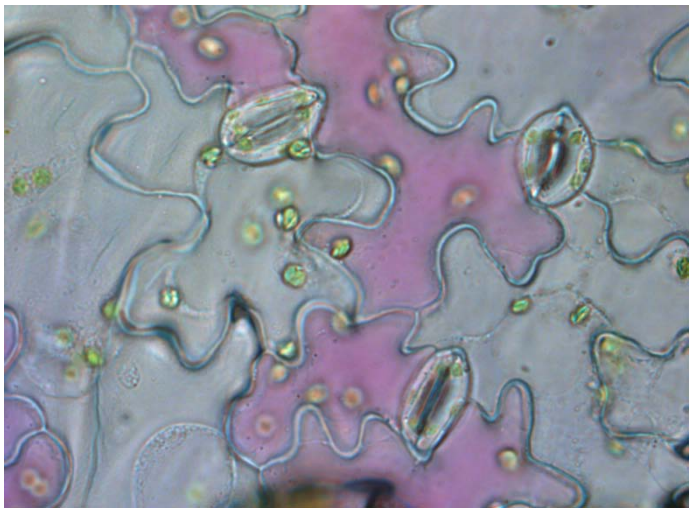

¡VAMOS DE FIESTA (I)!

Estomas. Microscopio invertido de epi-fluorescencia

AUTORES: Carmelo Ruiz & Marina Leterrier

EYECCIÓN

Microscopio invertido de epifluorescencia

AUTORES: Carmelo Ruiz & Marina Leterrier

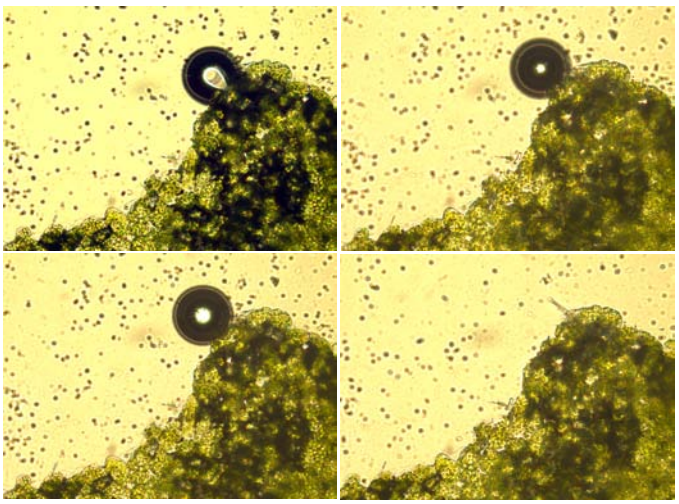

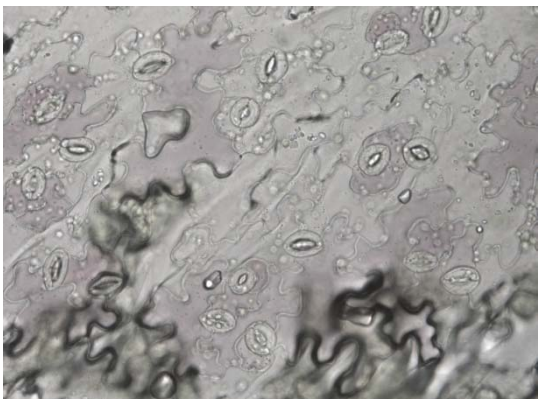

¡VAMOS DE FIESTA (II y III)!

Estomas. Microscopio invertido de epi-fluorescencia

AUTORES: Carmelo Ruiz & Marina Leterrier

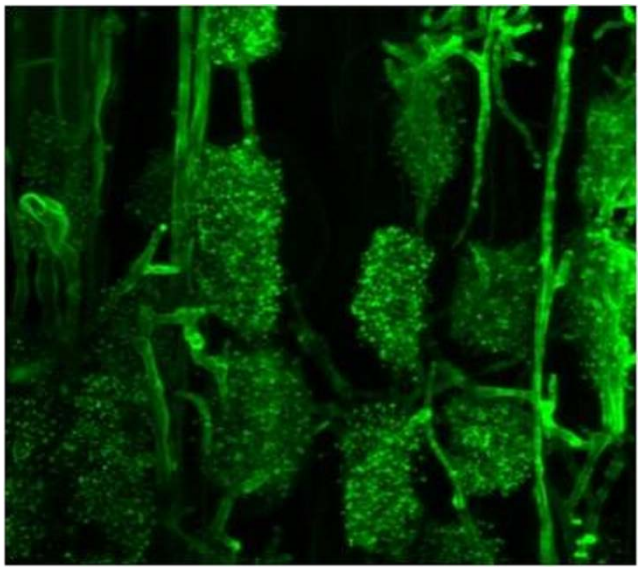

ARBUSCULAR MYCORRHIZAL FUNGI

Arbuscule of mycorrhizal fungi (*Glomus intraradices*) stained with WGA-Alexa Fluor 488 in tomato root and observed with confocal laser scanning microscopy (CLSM), 3-D image

AUTOR: Rocío Torres Vera

INFECTION OF ROOT PARASITIC PLANT IN TOMATO

Initial phase of root parasitic plant (*Phelipanche ramosa*) infection in tomato observed with a stereo-microscope. The parasite contacts the host root

AUTOR: Rocío Torres Vera

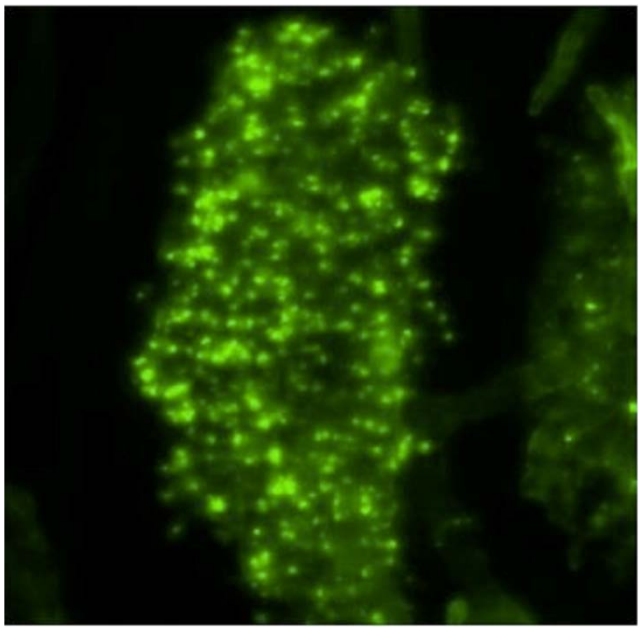

MYCORRHIZAL ARBUSCULE

Arbuscule of mycorrhizal fungi (*Glomus intraradices*) stained with WGA-Alexa Fluor 488 in tomato root and observed with confocal laser scanning microscopy (CLSM), 3-D image

AUTOR: Rocío Torres Vera

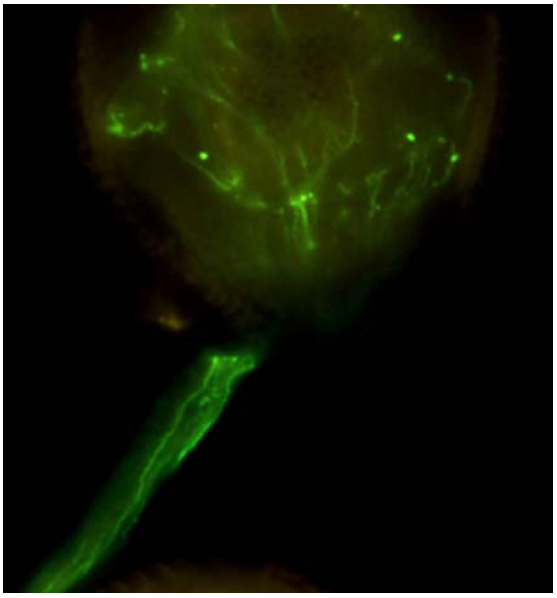

VIAS DE TRANSPORTE RÁPIDO

Visualización de la red de microtúbulos del grano polen germinado de olivo en un microscopio de fluorescencia mediante un anticuerpo antitubulina.

AUTOR: María Isabel Rodríguez García

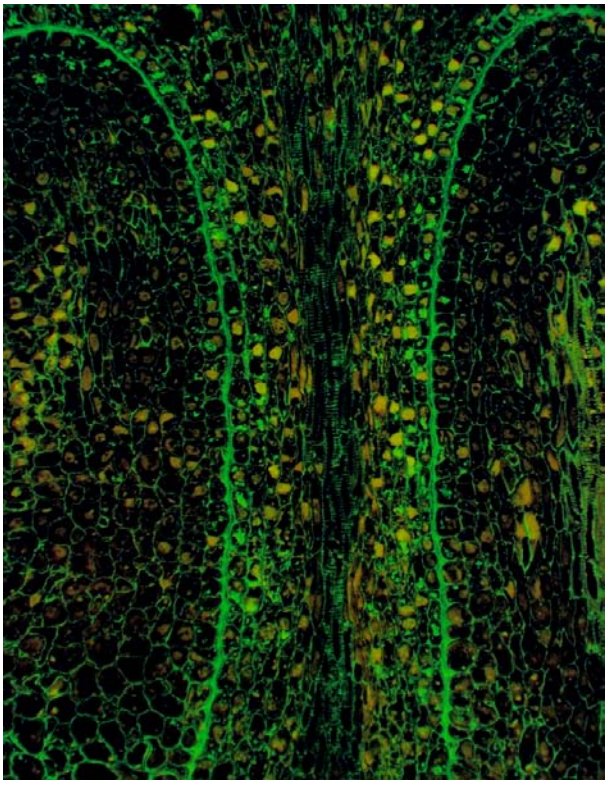

EMPEDRADO VERDE

Inmunolocalización de pectinas ácidas esterificadas en las paredes celulares del ovario (fluorescencia verde) mediante el anticuerpo JIM7

AUTORES: Cynthia Suarez, Anna Majewska-Sawka & María Isabel Rodríguez García

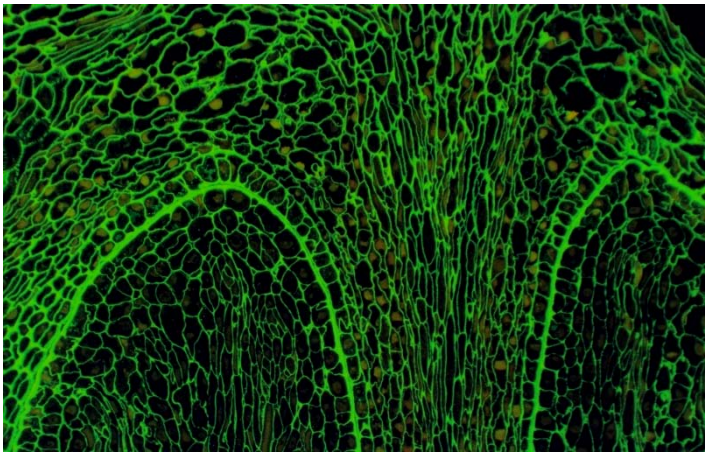

LA CATEDRAL

Inmunolocalización de pectinas ácidas esterificadas en las paredes celulares del ovario en las paredes celulares del ovario de olivo (fluorescencia verde) mediante el anticuerpo JIM7

AUTORES: Cynthia Suarez, Anna Majewska-Sawka & María Isabel Rodríguez García

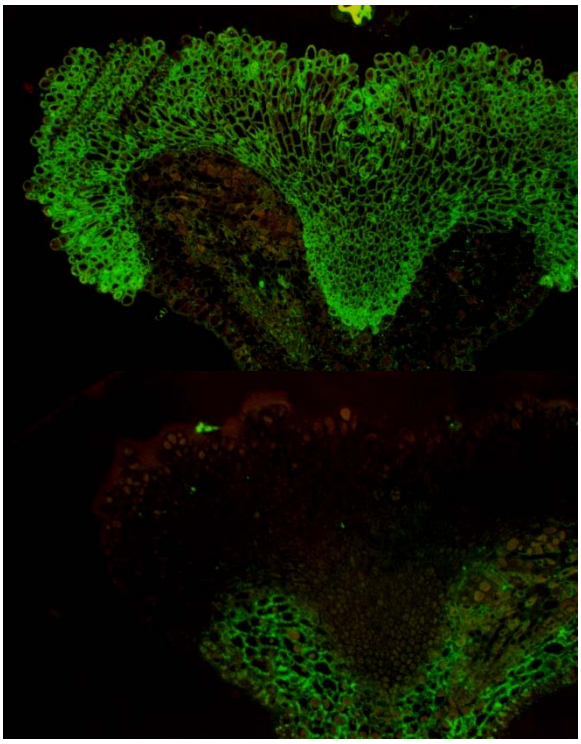

CARA Y CRUZ DE UNA MISMA MONEDA

Estigma de olivo. Imagen de arriba: inmunolocalización de AGPs en el pistilo de olivo (fluorescencia verde) mediante el anticuerpo JIM13. Imagen de abajo: inmunolocalización de pectinas ácidas esterificadas en las paredes celulares del pistilo de olivo (fluorescencia verde) mediante el anticuerpo JIM7

AUTORES: Cynthia Suárez, Anna Majewska-Sawka & María Isabel Rodríguez-García

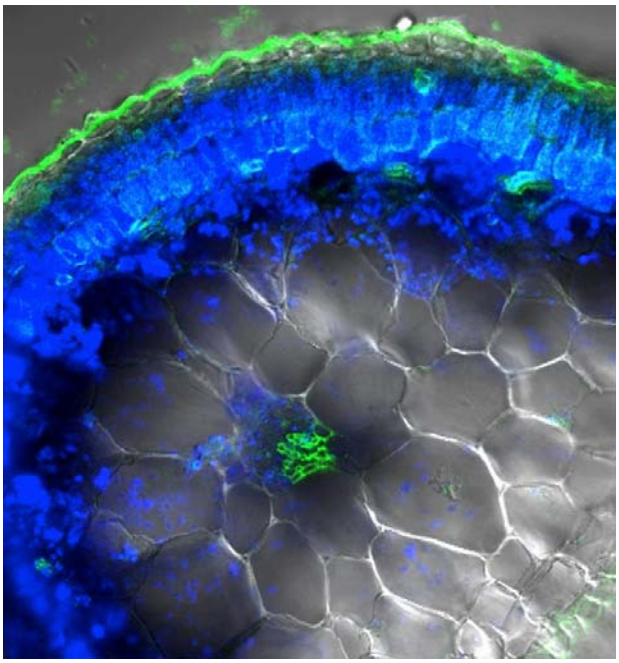

Y YO CON ESTOS PELOS...

Sección transversal de hoja mostrando la distribución del aparato fotosintético (cloroplastos en azul, haces vasculares en verde). Autofluorescencia (excitación 488) y luz transmitida. Microscopía confocal: proyección de un z-stack

AUTOR: Juan de Dios Alché

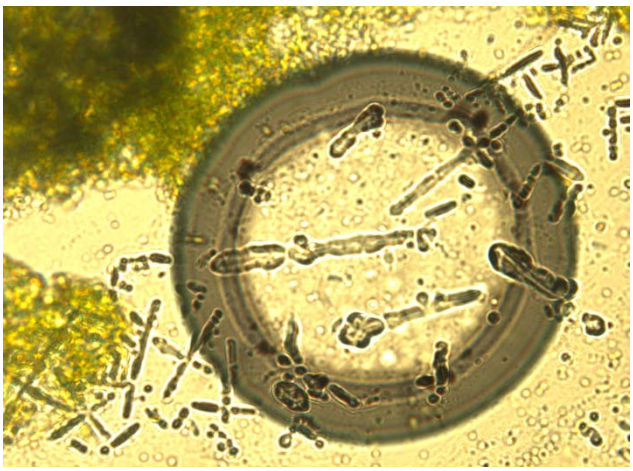

INVITACIÓN

Microscopio invertido de epifluorescencia

AUTORES: Carmelo Ruiz & Marina Leterrier

Author index

A

Page

Abecia, L. 29
Aboukila, A. 13
Alché, J.D. 15
Aranda, E. 19, 21
Aranda, M.N. 13
Arco, A. 29

B

Bedmar, E.J. 23
Belver, A. 13

C

Caballero, E. 37
Cabeza, I. 29
Cagnac, O. 13
Campos, M. 3
Cappelli, C. 35
Cárdenas, K. 11
Castro, A.J. 15
Cobo, J.F. 25
Corpas, F.J. 9
Cuadros, J. 35

D

De la Fuente, S. 35
Del Arco, J.M. 25
Delgado, M.J. 23
Del Río, L.A. 9
Díaz, V. 25

E

Espinosa, M. 5

F

Fernández, A.J. 25
Fernández, M. 25
Fernández, M.C. 15
Fernández, M.L. 3
Fernández, R. 5
Fernández-Fígares, I. 31
Fiore, S. 35

G

Gálvez, F.J. 13
García, E. 15
García, F. 25
García, I. 19, 21
García, J.M. 19, 21

Gaspar, M.I. 13
Godoy, P. 19, 21
González, L. 31

H

Ho, T. 19, 21
Huertas, F. 35
Huertas, F.J. 35
Huertas, O. 5

I

Illana, A. 19, 21
Iriarte, PI. 35

J

Jaime, N. 13
Jiménez , J.C. 15
Jiménez , J.I. 25
Jiménez , M.J. 15
Jiménez de Cisneros 37

L

Lachica, M. 31
León, R. 21
Linares, J. 35
López, E. 9

M

Martín, J. 19, 21
Martín, J.A. 21
Martín, A. 31
Martín, A.I. 29
Martínez, C. 15
Martínez, G. 29
Martínez, L. 25
Martínez, M. 5
Martínez-Abarca, F. 25
Martos, A. 25
Matilla, M.A. 5
Mesa, S. 23
Millán, V. 25
Molina, E. 29
Molina, M.D. 25
Molinero, N. 19, 21
Morales, S. 15
M´rani, M. 15
Muñoz, A. 29

N

Nisa, R. 25

O

Ocampo, J.A. 19, 21
Olías, R. 13
Olmedilla, A. 11
Ortega, A.P. 13

P

Palma, J.M. 9
Paredes, D. 3
Pazmiño, D.M. 11
Peregrina, A. 25

Q

Quesada, J.M. 5

R

Ramos, E. 29
Ramos, M.I. 5
Reina, R. 19, 21
Reinoso, M. 25
Rejón, J.D. 15
Rodríguez, J.M. 31
Rodríguez, M. 11
Rodríguez, M.I. 15
Rodríguez, P. 13
Rojas, M.L. 31
Romero, M.C. 11
Rozalén, M. 35
Ryan, P.C. 35

S

Salmerón, C.M.
Sánchez, M.E. 13
Sandalio, L.M. 11
Santamaría, S 5
Sanz, M. 11
Scervino, M. 19
Serrano, I. 11
Siles, J.A. 19, 21
Soriano, M.I.
Suárez, C.

T

Tamayo, M.I. 19, 21
Toro, N. 25
Torres, O. 25

Torres, R. 19, 21
Traverso, J.A. 15
Travieso, M.L. 5

V

Venema, K. 13
Vierheilig, H. 21
Villadas, P.J. 25

Y

Yáñez, D.R. 29
Yousef, F. 5

Z

Zafra, A. 15
Zienkiewicz, A. 15
Zienkiewicz, K. 15

We make it visible.